2016

PHILEX MINING CORPORATION

Technical Report on the Bumolo Porphyry Copper-Gold Deposit in Tuba, Benguet, Philippines

Authors:

Noel C. Oliveros

Victor B. Maglambayan

Roy Ronald C. Luis

Maria Lourdes M. Faustino

Mark Adrian M. La Rosa

Raymond G. Aldea Genesis D. Cellona

Kryztal Irish N. Irorita Adrian T. Pascual

Benix M. Masangcay Randie P. Nicanor

Gemma G. Francisco Jesse P. Segura

FEBRUARY 2016

Table of Contents

List of Figures

List of Tables

List of Photos

Executive Summary

Philex Mining Corporation (Philex) is currently undertaking a Resource definition drilling program on the Bumolo porphyry copper-gold deposit at the Bumolo Project of Philex. The Bumolo Project lies within the MPSA 156-2000 CAR of Philex.

As part of this work, Philex has incorporated the result of the on-going drilling program as of February 2016 into a maiden Mineral Resource estimate (MRE) for Bumolo Project. Philex has completed the Bumolo MRE in accordance with the requirements and guidelines of the Philippine Mineral Reporting Code (PMRC). Philex has assigned Noel C. Oliveros as the Competent Person (CP) for this February 2016 Bumolo MRE and to prepare the Technical Report for the Bumolo Project.

The Inferred MRE, are reported at a cut-off of 0.274%CuEq. The copper equivalent calculation derived by Padcal Mine for the Bumolo MRE are CuEq = %Cu + 0.693 x g/tAu based on Padcal Mine's estimated copper price of US$ 2.35/lb and gold price of US$ 1,145/oz and metal recoveries of 82% for copper and 80% for gold based on the average result from Padcal Mine operations as of October 2015.

Bumolo MRE at 0.274% CuEq						
Classification	**MT**	**% Cu**	**g/t Au**	**Cu Mlb**	**Au Moz**	**% CuEq**
Inferred	21.7	0.20	0.30	95.7	0.21	0.41

The maiden Bumolo MRE is based on drilling data and initial geological information interpreted by Philex geologists as of February 2016. A total of 30 diamond drill holes totaling 11,382 meters drilled in the deposit and specific gravity of 2.7 were used in the resource estimation. Drill hole spacing for assayed holes varies from around 80 by 80 meters and locally closer in central portions to around 125 by 125 meters in peripheral zones and is classified as Inferred Resources.

The Bumolo Project exploration program is professionally managed and the database is acceptable for use in mineral resource estimation. Preliminary but robust geological and resource domains of the Bumolo deposit are defined and found suitable for the maiden mineral resource estimate. There is continuity for both the copper and gold grades within the established domains with low nugget effects and large ranges. The QA-QC programs and core logging procedures follow the best industry practice and generally exceed commonly accepted standards. The copper and gold grades are estimated using Ordinary Kriging interpolation method as the mineralization is relatively homogenous. The Competent Person believes that the methodology used in the MRE is appropriate and that the result will have accuracy suitable for the intended mining method.

Philex consider Bumolo as a priority exploration project as it is seen to provide a potential additional mill feed for its Padcal operation considering the proximity and the similar nature of mineralization. The mineralization is mainly hosted by dioritic stocks characterized by sulfidic (pyrite+magnetite+chalcopyrite±bornite) quartz stockwork and disseminations confirmed by the previous underground drilling campaigns in 2001 and 2010. The present drilling campaign which commenced in 2015 has confirmed the near surface potential extent of mineralization and partially defined the lateral and vertical extent of mineralization towards the southeast. Early mineralization quartz diorite porphyry hosting the main mineralization has undergone texturally destructive potassic alteration characterized by biotite, actinolite and magnetite alteration. Disseminated chalcopyrite is closely associated with magnetite and also occurs as coarser grains in a dense stockwork of quartz and quartz-magnetite veinlets that overprinted biotite and actinolite alteration. Primary copper mineralization (chalcopyrite ± bornite) is hosted in the Clear Diorite and High-grade

Hydrothermal Breccia. Present drilling results also indicated mineralization in the adjacent wall rocks and hydrothermal breccias. Supergene copper sulfide enrichment (chalcocite ± malachite ± native copper) was observed in two adjacent holes and extends from surface to about 80m depth. Gold grade appears to be associated with copper sulfides with Cu-Au ratio ranging from 1:1 to 1:2.

The assaying of samples were commissioned to two laboratories with initial assay run conducted in Philex' Padcal Assay Laboratory and a parallel run submitted to Intertek Testing Services, Inc. (Intertek) in Manila. Both laboratories assaying protocols are to industry standard. Assay results are guaranteed by continuous and regular monitoring of the laboratory QA/QC sample insertions.

Further advanced geological studies such as geotechnical, mineragraphic and metallurgical studies will be conducted in the final stage of the resource definition drilling to support project feasibility.

1. INTRODUCTION

Philex Mining Corporation (Philex) is currently undertaking a Resource definition drilling program on the Bumolo porphyry copper-gold deposit at the Bumolo Project which is located in the Baguio Mineral District approximately 250 kms north of Manila. The Bumolo deposit is only 1.5 kms to the northeast of the Sto. Tomas II deposit of Padcal Mine of Philex. The Bumolo Project lies within the MPSA 156-2000 CAR of Philex that covers approximately 3,848 hectares.

As part of this work, Philex has incorporated the result of the on-going drilling program into a maiden Mineral Resource estimate (MRE) for Bumolo Project. Philex has completed the Bumolo MRE in accordance with the requirements and guidelines of the Philippine Mineral Reporting Code (PMRC).

This report details the exploration of the Bumolo porphyry copper-gold deposit and the data and methodology in the estimation of the Bumolo Inferred MRE.

Drilling activities at Bumolo started in 2001 with two drillholes completed from the initial drilling campaign. Another drilling campaign was launched in 2010 with eight (8) drillholes completed. Due to restricted surface access during these times, drilling was collared underground through the Shimada Tunnel.

In 2014, a review of geological data including re-logging of Bumolo drill cores from the 2010-2011 scout drilling campaign refined the lithologies and determined the spatial distribution of Cu-Au mineralization. In March 2015, surface access has been granted and the third drilling campaign commenced. Initial scout drillholes intersected significant Cu-Au mineralization which later advanced to resource definition drilling in October 2015.

Resource definition drilling is in progress with 30 drillholes completed as of February 1, 2016. The available drill core assays were included in the MRE which translated to 11,382 combined drilled meterage.

The members of the study team listed below are all current employees of Philex or have contributed to the exploration activities of the Project. The geologists involved in the project are registered professionals with the Philippine Regulations Commission.

- Noel C. Oliveros – Division Manager, Resource Management
- Victor B. Maglambayan – Division Manager, Exploration
- Reynaldo C. Estacio – Group Manager (up to 01/2016)
- Roy Ronald C. Luis – Senior Geologist and Group Exploration Manager
- Maria Lourdes M. Faustino - Geologist
- Mark Adrian M. La Rosa – Geologist
- Raymond G. Aldea – Geologist
- Genesis D. Cellona – Geologist
- Randie P. Nicanor – Geologist
- Kryztal Irish N. Irorita - Geologist
- Adrian T. Pascual – Geologist
- Benix Stephen M. Masangcay - Geologist
- Jesse P. Segura – Geologist
- Gemma G. Francisco – Geologic Database Head

This report has been prepared in accordance with the guidelines set by PMRC and therefore valid for filing with the Philippine Stocks Exchange (PSE).

1.1 Report Commission

The management of Philex has authorized the undersigned, Mr. Noel Oliveros, Competent Person in Geology, to prepare a technical report compliant with the Philippine Mineral Reporting Code ("PMRC") on the Bumolo Project in Tuba, Benguet, Philippines; where Philex has a 100% interest. This report is to be submitted to Philex, and subsequently to the Philippine Stock Exchange ("PSE") for purposes stated below.

1.2 Purpose of Report

The purpose of this technical report is to disclose the exploration results and to present the MRE for the Bumolo Project. The disclosure of the mineral resources of the Bumolo Project requires the preparation and filing of this technical report with the PSE.

1.3 Scope of Work and Terms of Reference

This report has been prepared in accordance with the guidelines set by PMRC-IRR. The legal, environmental, political, surface rights, water rights or other non-technical issues which might indirectly relate to this report are not included as Philex has its legal counsel and other experts for these other areas of concern. The scope of work undertaken in this report includes compilation of exploration results, geological modeling and PMRC-compliant MRE based on drill core assays and relevant information made available to the project as of February 01, 2016.

1.4 Compliance of Report with the Philippine Mineral Reporting Code

This report fully adheres with all the requirements of the PMRC.

1.5 Units and Currency

Throughout this report, the common measurements used are in metric units. Tonnages are shown as tonnes (1,000 kg), and million tonnes ("Mt"); other weights are in grams ("g"). Linear measurements are in meters ("m") or kilometers ("km"). Metal contents are given as parts per million ("ppm") or in percent ("%"); precious metal value (gold as grams per tonne ("g/t Au"). Areas are reported in hectares ("has"). This report also uses measurements in units that are commonly used in the industry such as ounces (oz) of gold and pounds of copper. Currency amounts are given in United States dollars ("US$"). All financial data are quoted in US$.

1.6 Qualifications

Mr. Noel C. Oliveros, Exploration Division Manager and Head of the Exploration and Resource Estimation Group of Philex, has extensive knowledge of the Bumolo deposit, having been involved in the project since its beginning. Mr. Oliveros has over 10 years of experience relevant experience in resource evaluation relevant to the style of mineralization in the Baguio Mineral District. Mr. Oliveros is a registered geologist with PRC License No. 1285 and a Competent Person (CP) for exploration and mineral resource estimation as defined under the PMRC with accreditation No. Geology CP-07-08-07 and accredited by the Geological Society of the Philippines (GSP).

2. RELIANCE ON OTHER EXPERTS AND COMPETENT PERSONS

The Philex exploration team solely studied and reviewed the geology and exploration information provided herein and has found the information to be significant. The information, interpretation, conclusions, and recommendations are based on exploration data available within the reporting cut-off date.

Philex did not rely on other experts in the preparation of this report, however wishes to appreciate the support and guidance of Redempta P. Baluda, VP for Exploration of Philex.

3. TENEMENT AND MINERAL RIGHTS

The tenement rights of Philex within the province of Benguet include three Mineral Production Sharing Agreements (MPSA) and two Exploration Permit Applications (ExPA). These are located adjacent to one another (Figure 1) along with two Applications for Mineral Production Agreements (APSA) under agreements with Philex. The total land area covered by these tenements is 11,934 has.

MPSA-276-2009-CAR encloses the Sto. Tomas II deposit where the Padcal mine currently operates. The heirs of Baldomero Nevada Sr. granted a deed of assignment for the mining rights of Philex over this area with Royalty Agreement.

Bumolo Project is within MPSA-156-2000-CAR with a total area of 3,848 has situated near the boundary with MPSA-276-2009-CAR. MPSA-157-2000-CAR on the other hand covers an area of 2,958 has at the south of MPSA-156-2000-CAR. Both MPSAs were approved on April 10, 2000.

The summary of tenement details and their respective agreements are outlined in Table 1 while Table 2 is the technical description of MPSA 156-2000-CAR which covers the Bumolo Project.

Table 1. List of mining claims maintained by Philex

Tenement	Date Approved	Area (Ha)	Claim owner	Type of Agreement	Date of Agreement
MPSA-276-2009-CAR	19-Jan-09	80.67	Heirs of Baldomero Nevada Sr.	Royalty Agreement	29-Aug-55
MPSA-156-2000-CAR	10-Apr-00	3,848.03	Philex Mining Corp.		
MPSA-157-2000-CAR	10-Apr-00	2,958.14	Philex Mining Corp.		
ExPA No. 075	20-Oct-97	486.00	Philex Mining Corp.		
ExPA No. 078	2-Sep-97	4,561.00	Philex Mining Corp.		

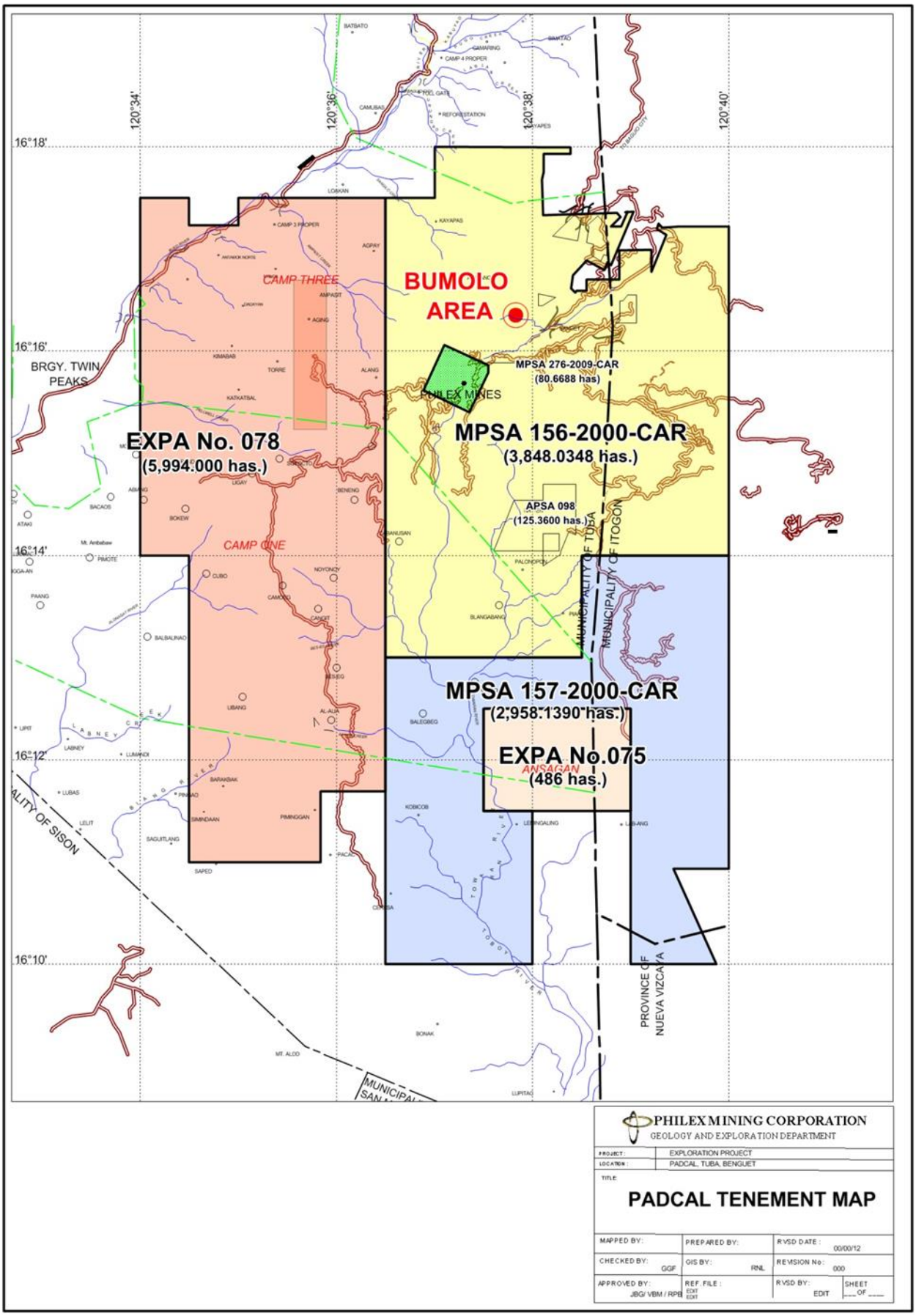

Figure 1. Padcal and Vicinity Tenement Map

Table 2. Technical Descriptions of MPSA 156-2000-CAR

Corner No.	Latitude	Longitude
1	16°13'00"	120°36'30"
2	16°17'30"	120°36'30"
3	16°17'30"	120°37'00"
4	16°18'00"	120°37'00"
5	16°18'00"	120°38'30"
6	16°17'30"	120°38'30"
7	16°17'30"	120°40'00"
8	16°14'00"	120°40'00"
9	16°14'00"	120°38'30"
10	16°13'00"	120°38'30"

4. GEOGRAPHIC FEATURES

3.1 Location and Accessibility

Bumolo is a porphyry copper-gold deposit located approximately 1.5 km northeast of Philex currently operating mine Sto. Tomas II orebody. It is situated within the southern part of the Luzon Central Cordillera mountain range which traverses the northwestern section of Luzon in a north-south direction. The nearest urban center is Baguio City, situated 206 aerial km north of Manila and is accessible via the NLEX, SCTEX, TPLEX, McArthur and Marcos Highways. From Baguio City, Bumolo can be reached going south via the paved 28 km long Philex-Kias Road (Figures 2 and 3).

Figure 2. Map of Northern Luzon with locations of Manila, Baguio, and Philex (image from Google Maps©)

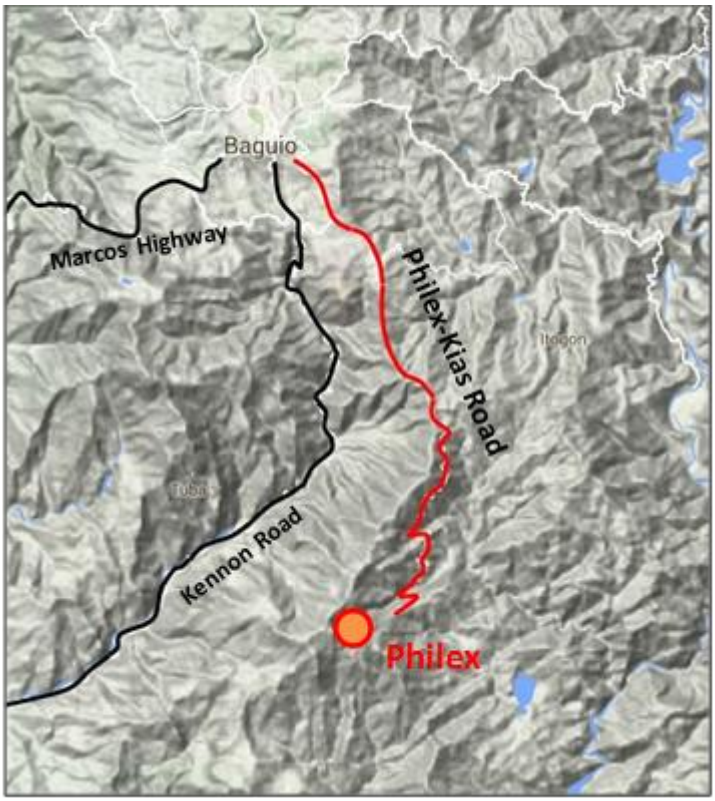

Figure 3. Location Map of Philex and Baguio showing major road network

3.2 Environmental Features, Physiography, Drainage and Vegetation

The terrain of the Luzon Central Cordillera in the vicinity of Bumolo is generally rugged with high relief. The underlying geology significantly influenced the topographic characteristics of the area. Peak elevation values are around 1,600 to 1,800 m above sea level (asl) notably along a northeast trending ridge with drainage systems of the Agno River to the east and the Bued River drainage system to the west. The elevation range in Bumolo area is approximately 1,200 to > 1,400 m asl on the southeast flank of the northeast trending ridge (Figure 4).

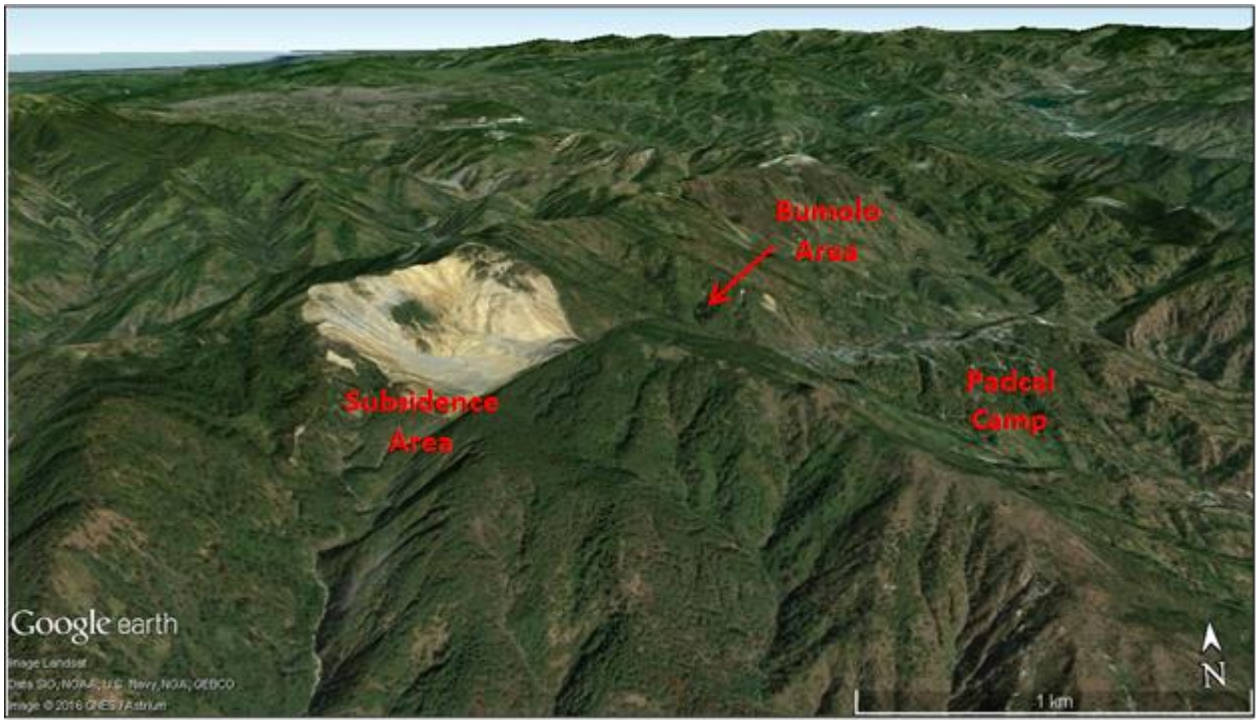

Figure 4. 3-D view of the Philex mine site and vicinity looking north showing the rugged terrain and existing vegetative cover.

The main streams within the vicinity are the Albian, Sal-angan and Balog Creeks all of which drain eastward towards the Agno River, one of the major drainage systems in the southern part of the Luzon Central Cordillera. Drainage patterns reflect the underlying geology and geologic structures present in the vicinity. The Bumolo area is situated within a drainage basin emptying onto the Albian Creek.

Various vegetation growth types are present in the area which is between 800 to 2,000 m above sea level. The area is dominated by pines, grassland and secondary growth trees. Pine stands are abundant in the upper portions and grassland in the lower portions. Two strata of pine forest are observed, namely:

a) Pine layer – pine trees dominated by Benguet Pine scientifically known as *Pinus kesiya* Royle ex-Gordon.
b) Herbacious layer – blacken ferns (higher elevations) and Rono grass, *Eulalia trispicata* and *Themeda triandra* at higher and lower elevations respectively.

3.3 Climate

Two pronounced climate conditions are observed in the area: the dry and wet seasons. The dry season occurs during the months of November to April while the wet season occurs from May to October. Average annual rainfall is about 5,000mm, with the months of July and August usually recording the heaviest rainfall.

Annual mean temperature range in the area is 12°C to 16°C and also varies with elevation, with higher elevations recording lower temperatures. Cooler temperatures persist during the months of December to February. Higher elevations have higher humidity with an average relative humidity value of 84%.

3.4 Land Use, Socio-Economic Environment and Population

The land within the vicinity of the mine site and Bumolo area consists of forest areas, plantation and pasture lands of local residents, as well as the industrial and residential facilities of the mine site. Approximately 500 has are designated as reforestation areas within the watersheds and the surroundings of the industrial and residential zones.

Two municipalities of Benguet straddle the area: Tuba to the west and Itogon to the east. Both municipalities are Ibaloi and Kankana-ey communities with the presence of various other ethno-linguistic groups brought upon by the employment opportunities from the mining activities. Much of the population in the mine area is centered within the Padcal camp located proximally to the Padcal mine. The camp (see Photo 1) and the outlying communities have a population of approximately 6,500 individuals which includes approximately 1,900 regular employees of Philex. Aside from the mine offices and facilities, the camp is also comprised of employees' housing, hospital, primary and secondary educational facilities, places of worship and local business establishments.

The main livelihood within the area is focused on mining (both small-scale and commercial) and agriculture. Majority of the population is engaged in mining related activities either as employees of Philex or as small-scale miners in the vicinity. Several livelihood projects for the benefit of the local residents were also started by Philex and are still continuing. The nearest economic center of Baguio City also provides employment opportunities to the other residents of the mine site and surrounding areas.

Photo 1. View of Padcal camp with the open pit in the background.

5. PREVIOUS WORKS

Philex has previously identified several mineral prospects within its tenements in the Baguio Mineral District. One of the significant findings is the recognition of the then Bumolo porphyry copper prospect. Further exploration upon agreement with Philex, was done by Anglo American Exploration (Philippines) Inc. from 1998 to 1999 as part of its geological and geochemical survey of the district. In Bumolo, an area of 73.56 was covered for detailed mapping and various geochemical sampling. Rock chip samples were collected from both outcrop and floats while ridge and spur soil samples were collected by auger drill. Stream sediment sampling used -40mesh for bulk leach extractable gold (BLEG) analysis and -80mesh for fire assay and AAS analysis. The samples for assays were dispatched to Intertek Testing Laboratory Services in Manila, Amdel Laboratories Ltd. in Perth, Australia and Bondar Clegg in Canada. Laboratory quality checks were included in most of the dispatches.

Anglo American delineated a 300 x 400 m stock comprising of six stages of intrusions, alteration and mineralization in the Bumolo porphyry Cu-Au deposit. Geochemistry showed highly anomalous Cu values ranging from 0.136 to 0.219 % Cu at the southern portion of the stock. On the other hand, Au values were less notable with the highest concentrations in the same area only at 0.194 to 0.599 g/t Au.

Philex attempted to conduct surface drilling, however, equipment mobilization was hampered by surface access and partly by steep slopes. The company then opted to drilling underground along the Shimada Tunnel. Drilling activities started in 2001 with two drillholes completed in 2002 and 2003. Additional 5 holes were completed in 2010 and another 3 in 2011.

Field mapping and stream sediment/rock chip sampling were later conducted in 2010. These focused on the intrusive body, both the main body and a smaller one to the southwest, which were earlier subjected to soil geochemical analysis. Stream sediments' assay results show Cu grades of 0.15% in the south-central and 0.24% in the southeastern parts of the intrusive, adjacent to soil sampling sites. Rock chip assays also confirm Cu grades of 0.123% in the southeastern portions of the intrusive. Abundant quartz veining was also observed on surface outcrops.

The drilling activities identified five types of intrusions in the Bumolo porphyry with mineralization concentrated on the upper northern portion of the stock and at the contact with the country rock at southwestern portion.

6. REGIONAL AND DISTRICT GEOLOGY

5.1 Regional Geologic Setting

The Bumolo deposit is located at the southern portion of the Baguio Mineral District. The Baguio Mineral District lies in the Central Cordillera of Luzon within the western Luzon arc. It is part of the magmatic arc associated with present day eastward-directed subduction of the South China Sea plate beneath the Philippines and Taiwan (Figure 5). It records the evolution from Cretaceous-Eocene marginal basin sedimentation and volcanism, to shallow marine sedimentation, followed by construction of a calc-alkaline magmatic arc above the Manila Trench in the Middle Miocene. The basement of northern Luzon is made up of ophiolitic and metamorphic complexes overlain by Late Cretaceous to Quaternary volcanic arcs have shown that ophiolite sequences that form the basement in northern Luzon display geochemical signatures of oceanic lithosphere formed in a suprasubduction zone setting.

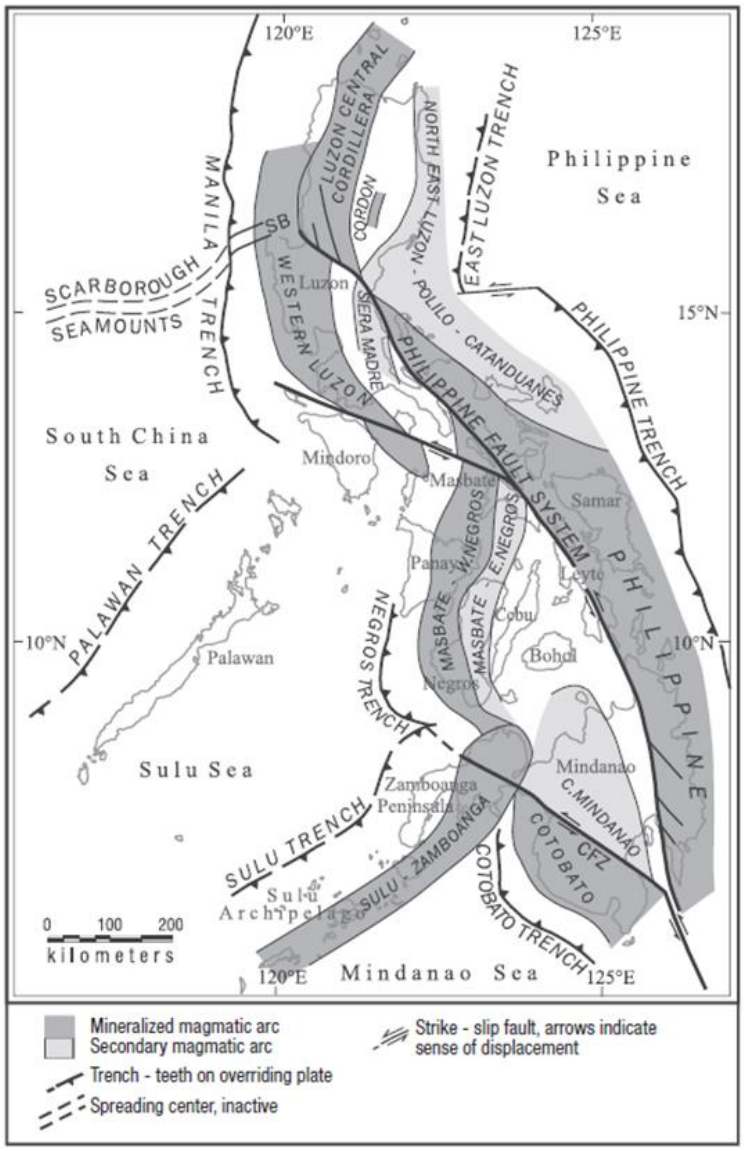

Figure 5. Cenozoic magmatic arcs and major tectonic elements of the Philippines (modified after Garwin et. al. 2005).

5.2 Stratigraphy

The ophiolithic basement is overlain by the Eocene Pugo metavolcanics, which consists of basalts, volcanic breccias, pyroclastic rocks, sandstones and mudstones (Figure 6). It is approximately more than 1,000 m in thickness and is also present in the Baguio District, Mankayan and Itogon, Benguet. It is locally metamorphosed in exposures along Ambalanga and Agno Rivers, Itogon, Benguet. This is also equivalent to the Lepanto Metavolcanics.

The Central Cordillera Diorite Complex later intruded into this formation. These Late Oligocene intrusions comprise of hornblende quartz diorites, tonalities, granodiorites, quartz monzonites and hornblende diorites. This complex has previously been known as the Agno Batholith.

Unconformably overlying the Pugo Formation is the Late Oligocene to Early Miocene Zigzag Formation which consists of conglomerates, sandstones, shales and minor limestones and volcanic flows. This sequence is about 1,700 m thick and extends from the Baguio District to Cervantes-Bontoc area. The Zigzag Formation is unconformably overlain by the late Early Miocene to early

Middle Miocene Kennon Limestone characterized as massive biothermal limestone. It is around 190 m thick and is exposed at the Baguio District, Mankayan and Itogon, Benguet.

Conformably overlying the Kennon Limestone is the Klondyke Formation with polymictic conglomerates, sandstones, mudstones and shales as members. This late Middle Miocene to early Late Miocene formation measures up to 2,820 m in thickness at its type locality along Kennon Road.

The Pliocene to Pleistocene intrusives have high potassium calc-alkaline affinities and represent a second phase of magmatism in the Central Cordillera Diorite Complex. The Lucluban Gabbro (7.5 Ma) and the Virac Granodiorite (5.2-2.4 Ma) were emplaced near the Acupan Mine. Minor andesitic and dacitic porphyries, plugs and diatremes have intruded into or peripheral to the Virac granodiorite. These include the Sto. Tomas II Dacite Porphyry (3.8 Ma), Ampucao Dacite Porphyry (2.4 Ma), Kelly Diorite (5.2 Ma), Hartwell Plug (5.2-1.0 Ma) and Balatoc Diatreme (1.5-0.8 Ma).

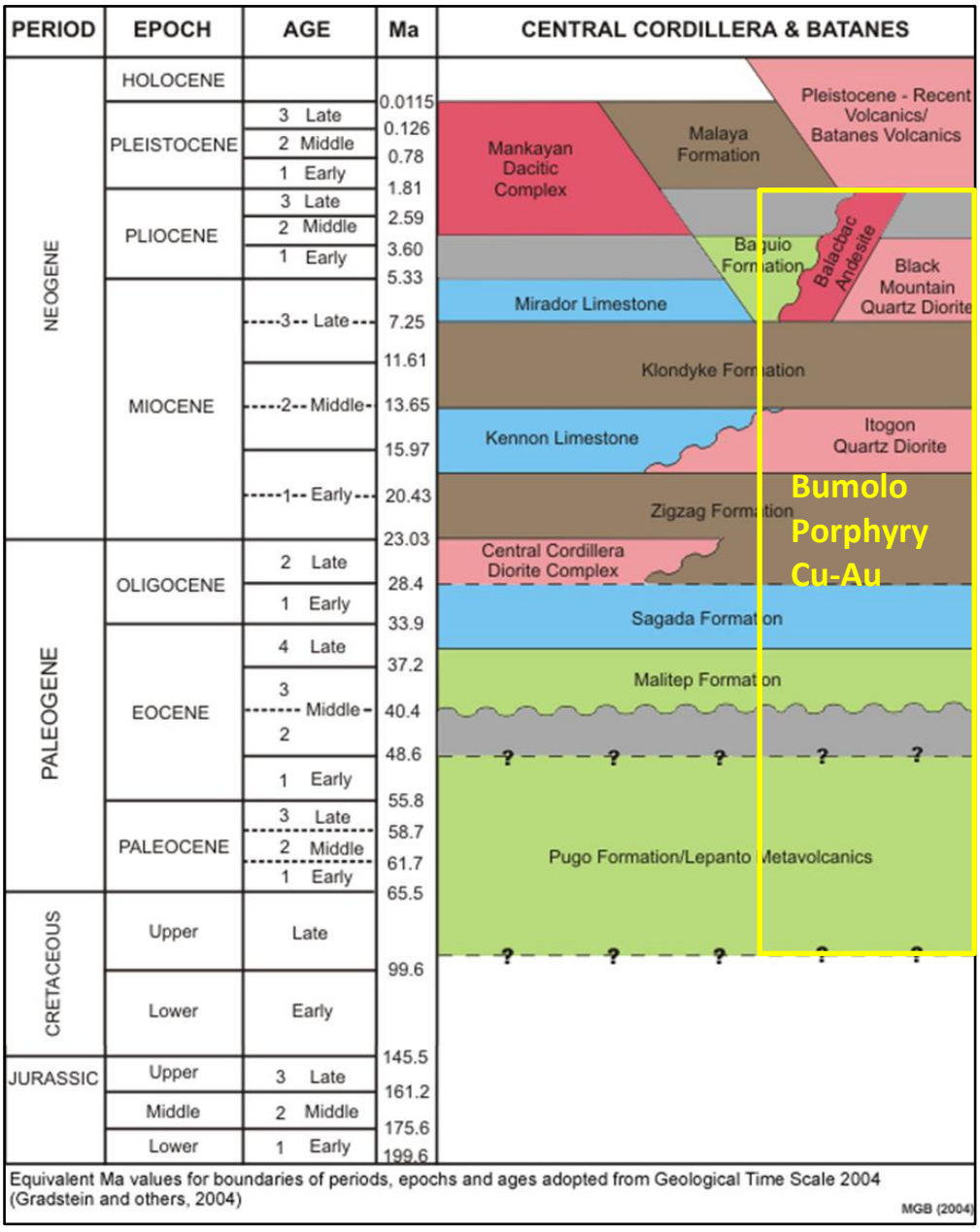

Figure 6. Stratigraphic Column of Central Cordillera

5.3 Structural Geology

Lineaments and faults in the district display two major trends, northeast and northwest (Figure 7). The northwest structures are splays of the Philippine Fault which the porphyry Cu-Au mineralization in the district is associated. The presence of orebodies (Black Mountain) and prospects (Bumolo, Camp 4 and Tapaya) exemplify this along the northwest trending Tapaya-Black Mountain Fault. This feature is parallel to the Tebbo Fault, east of the district. Interaction of these structures forms a dilational jog (NE, ENE and E-W Faults) where the epithermal and mesothermal veins occur.

The other major structures in the area are the northeast-trending Sta. Fe and Albian Faults. Both are right-lateral strike-slip faults which are steeply-dipping towards the southeast. The Sta. Fe Fault has been traced in Philex at Sto. Tomas II underground with strike of N060° and dip at 54°SE. It is believed to have been activated at the last stages of mineralization of the Sto. Tomas II orebody. On the other hand, the Albian Fault trends N035° and dips 50°-80° SE along the Albian Creek situated northeast of the Sto. Tomas II ore body.

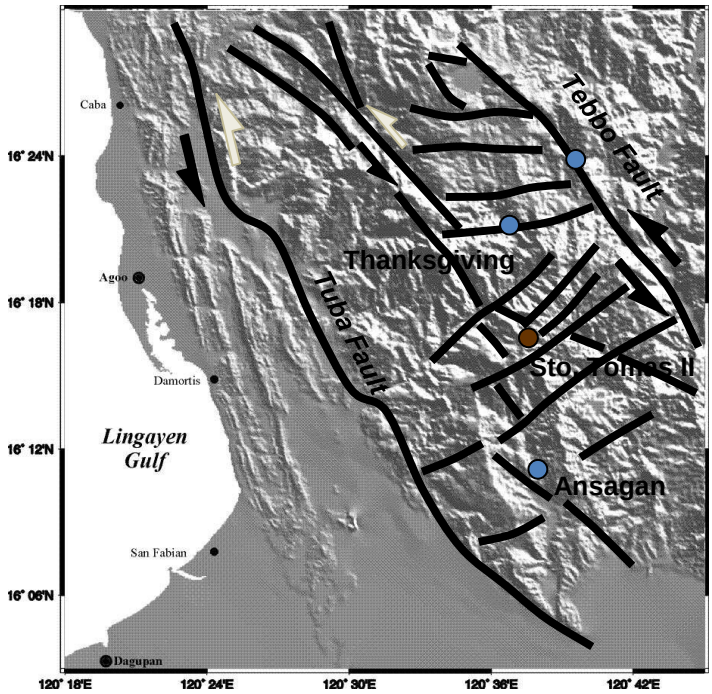

Figure 7. Structural regime in the South Central Cordillera district (after Aurelio, 2006)

7. MINERAL PROPERTY GEOLOGY

Bumolo is a porphyry copper deposit hosted in and around a multiphase, episodic diorite complex. Main-stage Cu-Au mineralization and pervasive potassic alteration (i.e., secondary biotite and magnetite) are associated with the Clear Diorite (CD) and hence considered as the progenitor intrusion. Late-stage diorite porphyries resulted to the truncation and reduction in volume of main-stage Clear Diorite porphyry. The late suite has intense veining stock works but weakly altered (i.e., phyllic-propylitic alteration) and weakly mineralized. In terms of geometry, the core of intrusive complex is dominated by the late diorite porphyries, including inter-mineral and post-mineral phases. A 3-D geology model of Bumolo showing lithologies intersected during drilling is shown in Figure 8 below.

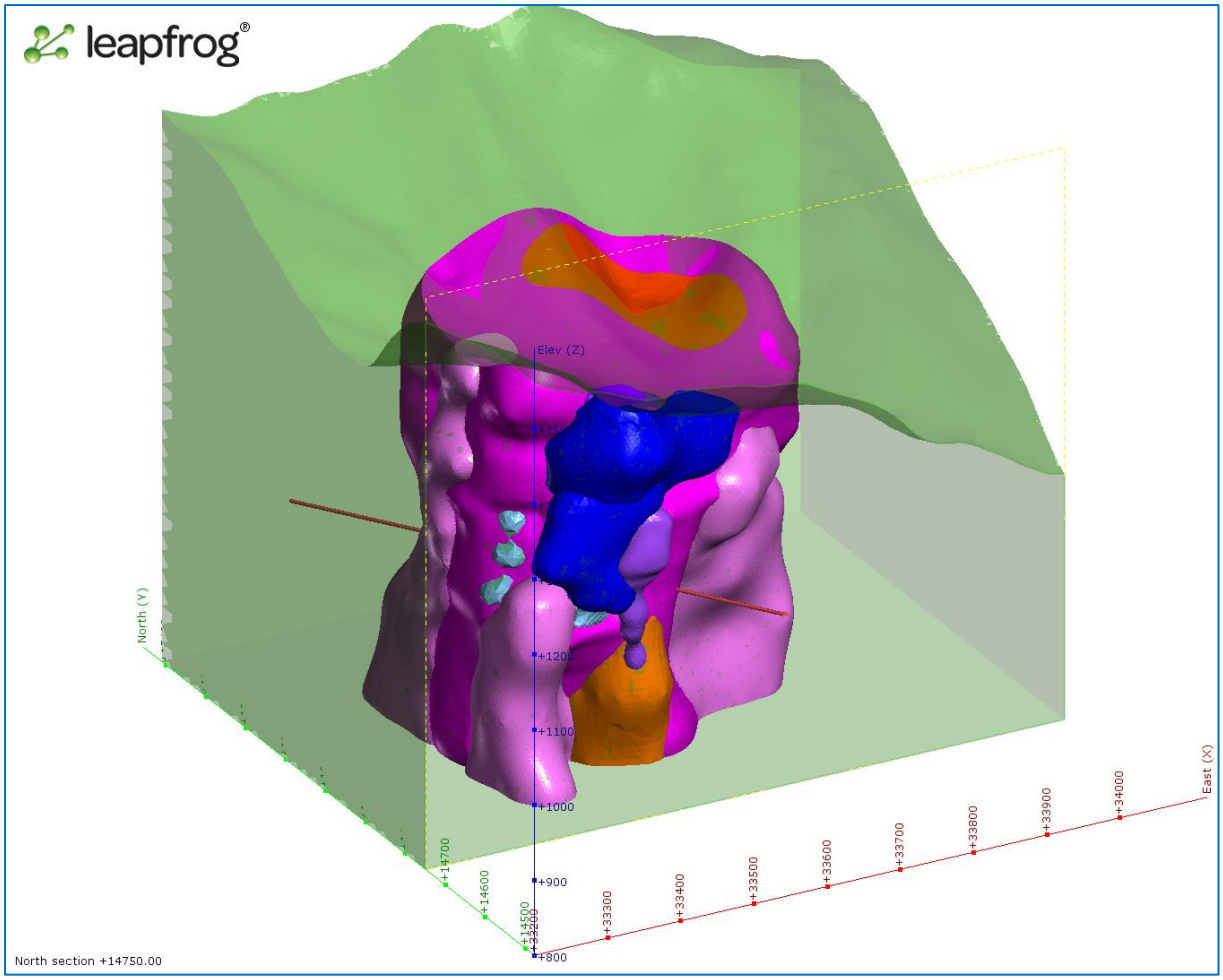

Figure 8. 3-D Geologic Model of Bumolo looking down oblique to the north east.

6.1 Basement Rocks (Meta-Andesite)

The oldest rock unit in Bumolo is the Meta-andesite (MA) which is subdivided into aphanitic basalt, diabase, porphyritic basalt, and sedimentary units. This form part of the Paleocene Pugo Formation and is considered as the country rock in the area (Figure 9). Diabase is commonly dark gray and fine-grained but grades to grayish white when silicified. Plagiophyric variety with almost 60-70% plagioclase feldspar phenocrysts is also noted, occasionally containing xenoliths of silicified rocks. Aphanitic basalts and porphyritic basalts are generally dark gray to greenish gray due to the chloritization of mafic minerals (Photo 2).

6.2 Clear Diorite (CD) and CD Breccia (CDBX)

The earliest diorite in the Bumolo intrusive complex is the fine to medium-grained Clear Diorite (CD). It is light gray to greenish gray when chloritized or pinkish gray in silicified portions. Xenoliths of MA and silicified rocks from older rock units and brecciation due to its intrusion into MA are locally observed. Petrographically, it shows porphyry texture with plagioclase and hornblende as the main phenocrysts in a microcrystalline quartzofeldspathic (i.e. aplitic) groundmass (Photo 4). CD is commonly affected by quartz - chlorite - magnetite ± secondary biotite (potassic) alteration and is believed to be the progenitor of copper mineralization. It formed a steep stock measuring about 400 x 400m in plan and cut at depth by the later intrusions (Figure 9).

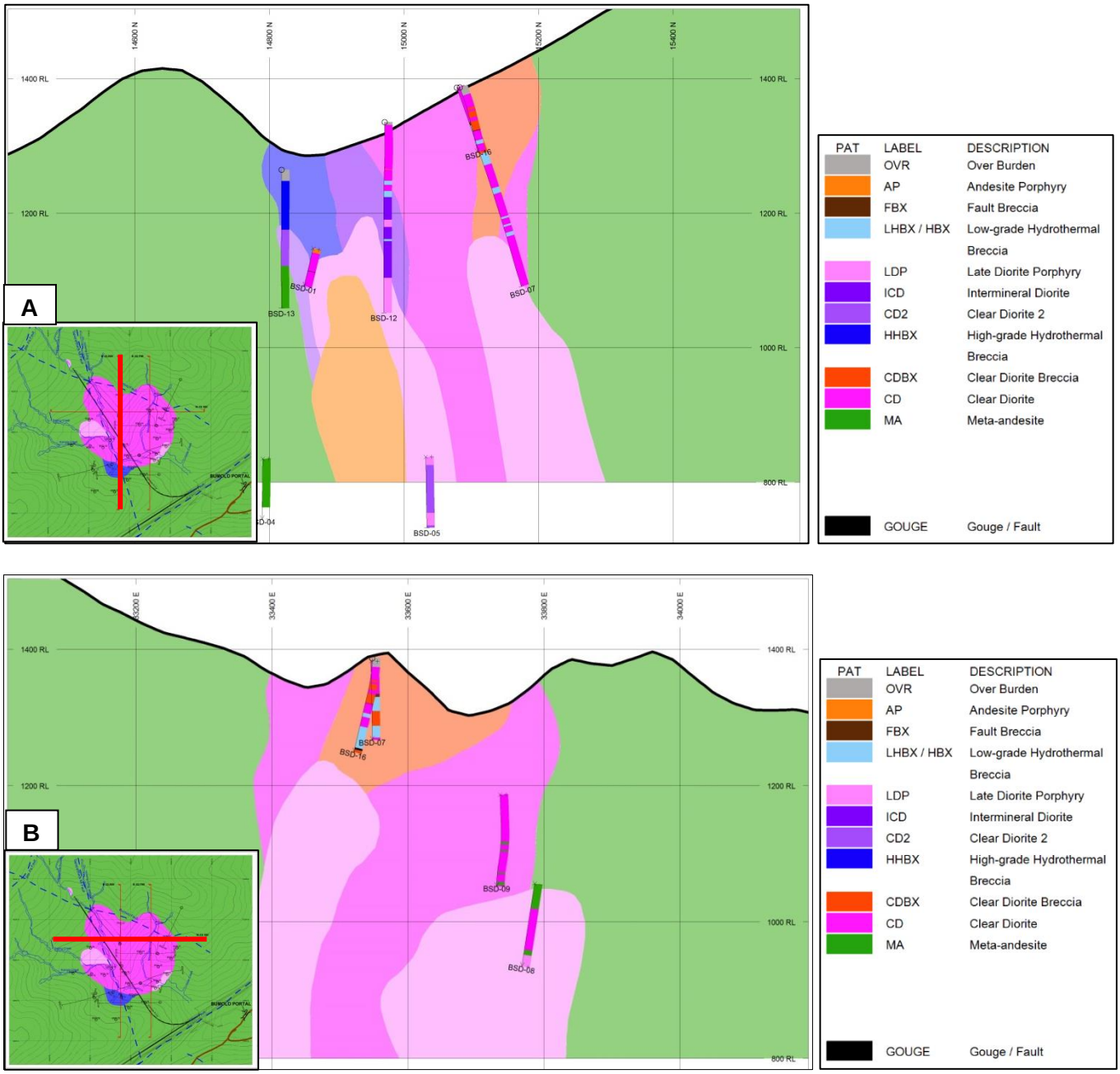

Figure 9. Bumolo deposit Section along A) 33550 looking west and B) 15100 looking north across the Bumolo intrusive complex**.**

6.3 High-grade Hydrothermal Breccia (HHBX)

High-grade hydrothermal breccias define an elongated SW-trending body on the southern contact of CD and MA (Figures 9 and 11). The clasts of this breccia include MA and mineralized CD cemented by quartz-magnetite-weak sulfides (Photo 5). It is inferred to be related to the main mineralization event associated with CD.

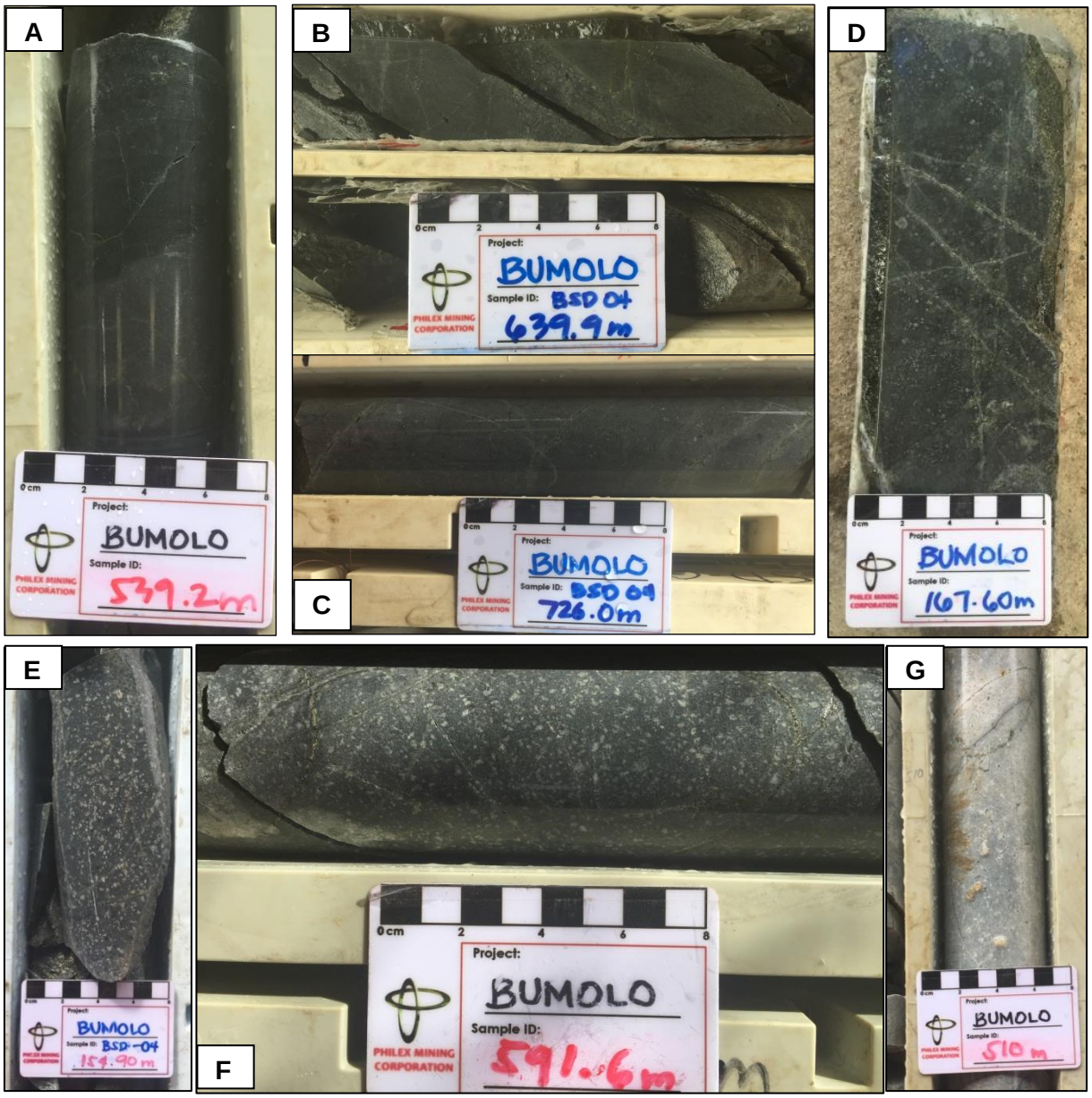

Photo 2. Photo of the facies of the Meta-Andesite (MA). A and C are silicified aphanitic basalts; B shows a propylitic-altered aphanitic basalt. D. Porphyritic basalt with chloritized pyroxene crystals shown at the center photo. E-F. Diabase with plagioclase phenocrysts G. Silicified diabase.

6.4 Inter-mineral Diorites (ICD and CD2)

Inter-mineral diorite porphyries ICD (Inter-mineral Clear Diorite) and CD2 (Clear Diorite 2) are porphyries emplaced after the progenitor, characterized by weaker mineralization relative to CD. ICD often displays gradational contacts with CD. It is cut by high volume of quartz veins (Photo 5) and shows distinct chlorite, sericite and magnetite alteration. CD2 has a porphyry texture with plagioclase and hornblende as the main phenocrysts in a finer groundmass. Isolated bodies of CD2 often have CD xenoliths, consistent with the relative age.

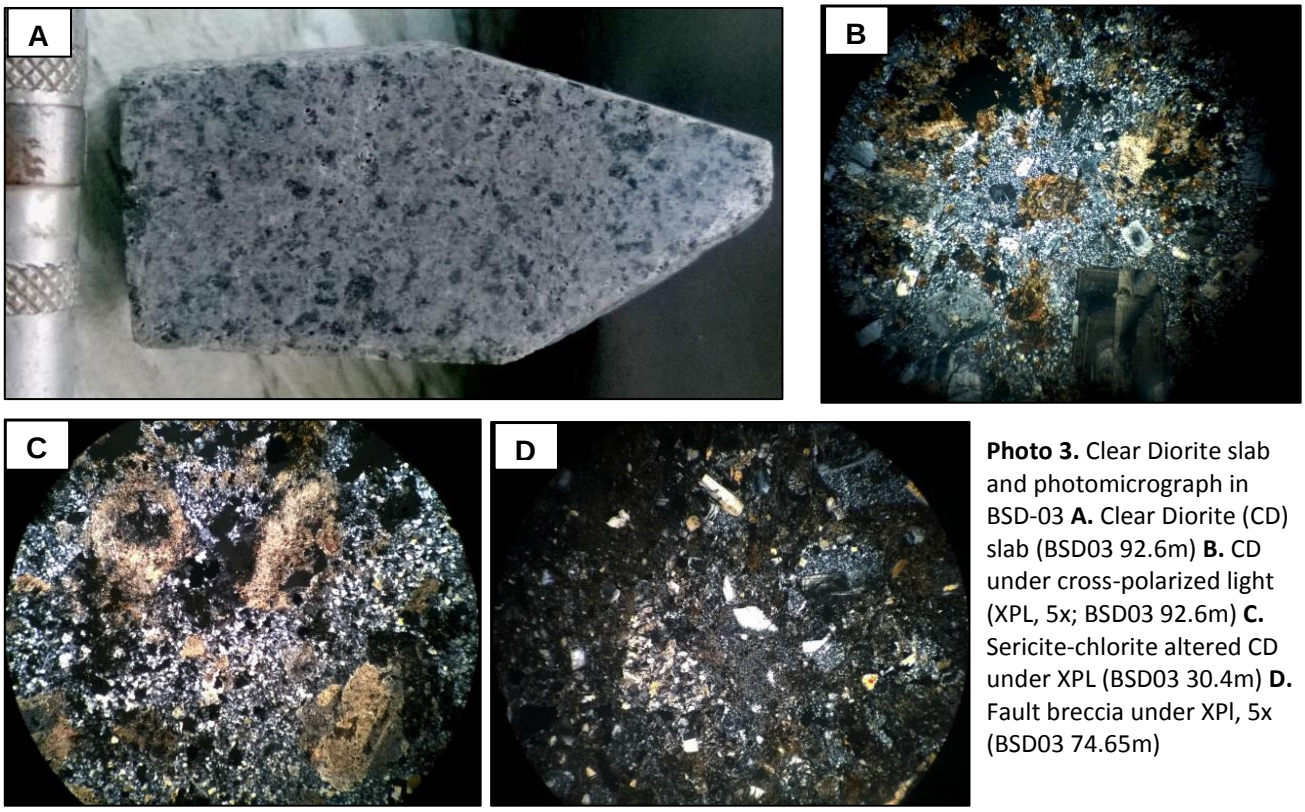

Photo 3. Clear Diorite slab and photomicrograph in BSD-03 **A.** Clear Diorite (CD) slab (BSD03 92.6m) **B.** CD under cross-polarized light (XPL, 5x; BSD03 92.6m) **C.** Sericite-chlorite altered CD under XPL (BSD03 30.4m) **D.** Fault breccia under XPl, 5x (BSD03 74.65m)

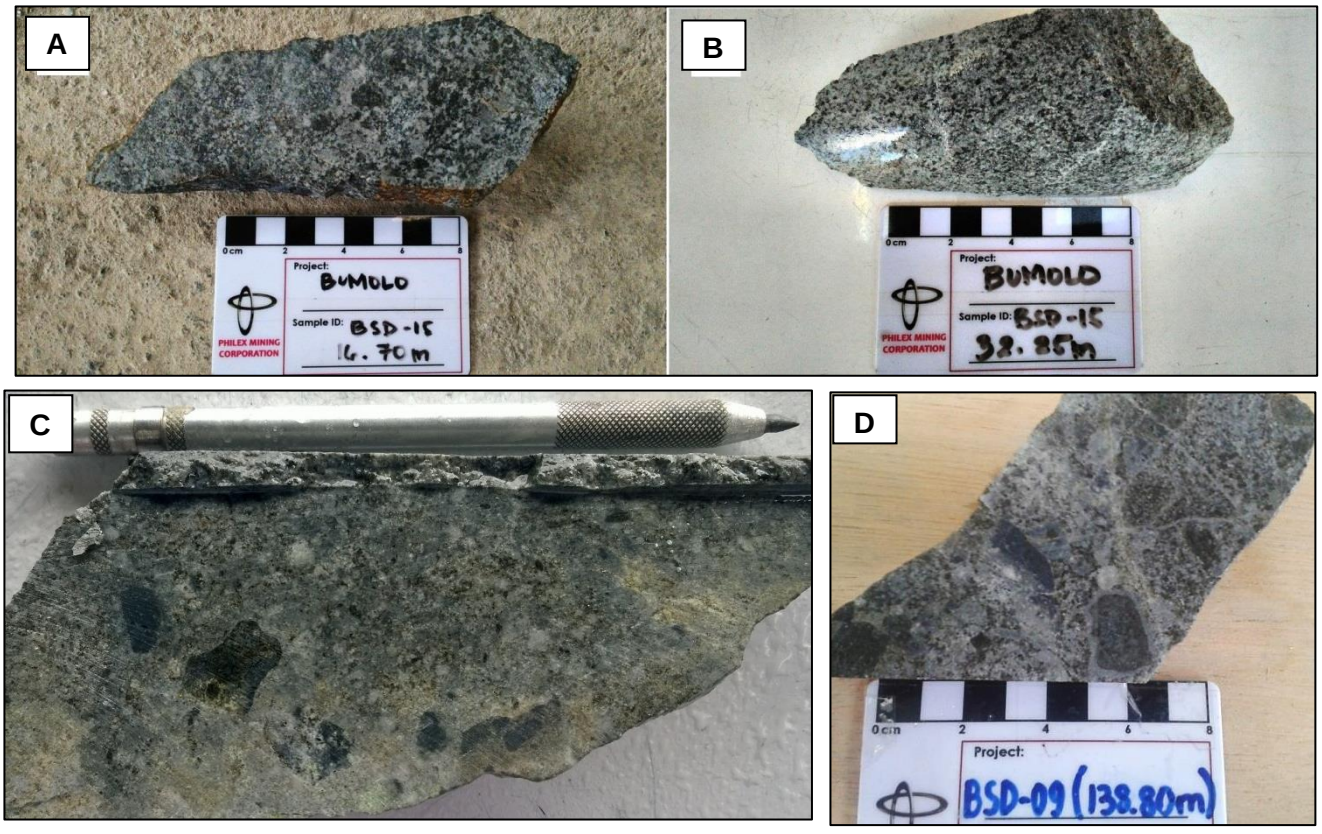

Photo 4. Varieties of Clear Diorite and Clear Diorite Breccia in BSD15. **A-B** Clear Diorite and **C-D.** CD Breccia, CD with abundant MA (dark) clasts

6.5 Late Diorite Porphyry (LDP) and LDP Breccia (LDPBX)

LDP is medium- to coarse-grained equigranular diorite that cuts through the earlier units (Figure 9 and Photo 5). Localized intrusion-related brecciation is also associated with LDP (LDP breccia). The body becomes larger at depth truncating the older diorites, CD and ICD.

6.6 Low-grade Hydrothermal Breccia (LHBX)

Low-grade hydrothermal breccias are more sporadic and generally occurring deeper compared to HHBX. The clasts are weakly mineralized MA and CD cemented by quartz-magnetite with localized sulfides.

6.7 Andesite Porphyry (AP)

AP is the youngest intrusion commonly intersected in the old BP drillholes. It is characterized by the strong porphyry texture in hand specimen and weak alteration. Under the microscope it exhibits a semi-seriate texture with plagioclase and hornblende as main phenocrysts in a relatively finer groundmass of same composition.

6.8 Brecciation

At least three types of breccias are identified at Bumolo. Intrusion-related breccias are locally formed in CD and LDP, named CDBX and LDPBX. They are characterized by the igneous cement same as the intruding rock and abundance of clasts of the older rocks.

The hydrothermal breccias are defined by the quartz, magnetite, and sulfide as cement on clasts comprising mainly of MA and CD. These are spatially and temporally unrelated as the high-grade hydrothermal breccias (HHBX) are associated with CD and the low-grade hydrothermal breccias (LHBX) are inferred to be related to the late mineral intrusions.

Breccias with rock flour matrix and commonly monomictic clasts are localized short intervals throughout the deposit. These are logged as fault breccias (FBX), inferred to be related to structures.

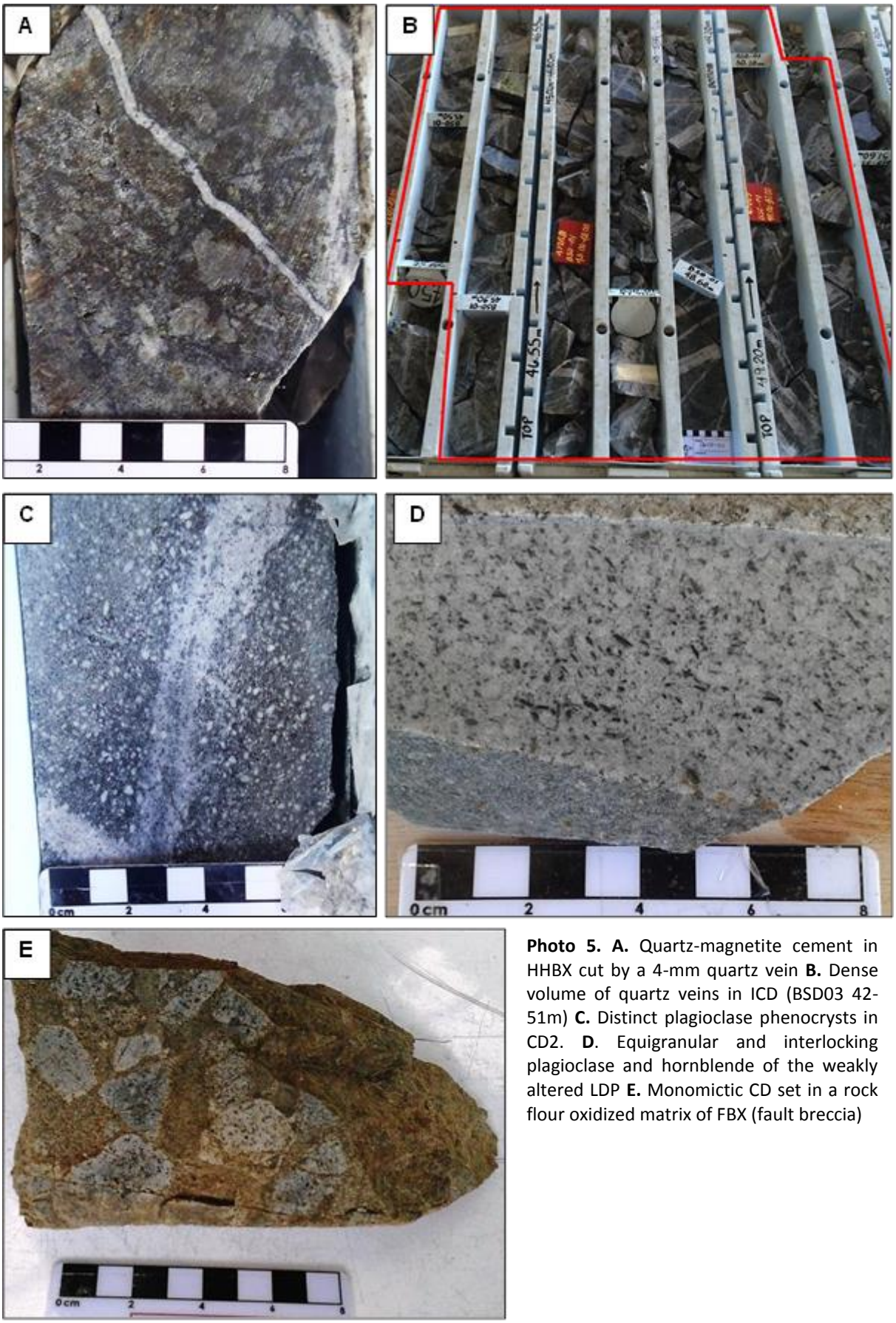

Photo 5. A. Quartz-magnetite cement in HHBX cut by a 4-mm quartz vein **B.** Dense volume of quartz veins in ICD (BSD03 42-51m) **C.** Distinct plagioclase phenocrysts in CD2. **D**. Equigranular and interlocking plagioclase and hornblende of the weakly altered LDP **E.** Monomictic CD set in a rock flour oxidized matrix of FBX (fault breccia)

8. MINERALIZATION IN THE MINERAL PROPERTY

7.1 Overview of the mineralization

Copper and gold mineralization alongside pervasive potassic alteration is associated with CD. The mineralized High-grade Hydrothermal Breccia (HHBX) is also believed to be temporally related to CD. Phyllic alteration usually overprinted both the country rock and the intrusives with varying degrees. Propylitic alteration is commonly observed in MA with occasional occurrence in LDP and AP. Localized silica flooding in MA is also noted.

The most dominant copper sulfide in Bumolo is chalcopyrite occurring as free grains, interlocked in magnetite and attached with coarse pyrite. Bornite is minimal and sporadic. Supergene copper enrichment is locally present as chalcocite rimming hypogene chalcopyrite and bornite.

Mineralization above 0.15% Cu and 0.20g/t Au is located at the upper portion and deepens towards the southwestern part of CD. The Cu-Au mineralization extends to 1125m RL with approximate thickness of 110m – 130m from the surface. Sharp drop of Cu and Au is observed when CD has been truncated by the late intrusive units. Mineralization however, is still open laterally on the western, southern, and northern portion of the deposit.

7.2 Type of mineralization as mapped

The Bumolo prospect shows typical porphyry style mineralization with characteristic magmatic-hydrothermal alteration and mineralization patterns. Alteration mapping was done on BSD holes to delineate the deposit's alteration zones. The mineral suite in Table 3 was used to create alteration assemblages while incorporating geological parameters such as lithology and structures in establishing the alteration zoning of the deposit. The drill cores were analyzed using TerraSpec™ 4 Spectral Analyser to identify the phyllosilicates and supplement the core logging and petrographic analysis.

Table 3. Summary of Alteration types and Mineral Assemblages for Bumolo

Alteration Type	Intensity	Mineral Suite		
		Key Minerals (Dominant)	Possible Ancillary Minerals	Primary Sulphides
Chloritic	Weak - Mod	Chlorite	± trace illite or Sericite ±clay	Pyrite ± trace specks Chalcopyrite
Propylitic	Weak - Mod	Chlorite + Epidote ± Carbonate		
Silicic	Mod - High	Quartz altered (silicified)	n/a	Pyrite ± Chalcopyrite (on some cases - abundant dissemination of cpy)
Intermediate Argillic	Mod - High	Mica (Muscovite/sericite) + Chlorite + Quartz	Magnetite + clay ± Epidote	Pyrite ± (trace of Chalcopyrite/ Bornite usually observed on the PT overprinted)
Phyllic	Mod - High	Mica (Muscovite/sericite) + Quartz	± trace of Chlorite	Pyrite ± (Chalcopyrite/ Bornite usually observed on the PT overprinted by PH)
Potassic	Weak	Mostly Secondary Bio	± Magnetite and trace of sericite	Pyrite ± trace specks Chalcopyrite
	High	Secondary Bio + Magnetite ± K feldspar	Actinotlite, Tourmaline, Gypsum / Anhydrite ± Chlorite, Sericite and Calcite	Pyrite + Chalcopyrite + Bornite ± Molybdenite

The potassic alteration zone with moderate to strong sericite overprint is interpreted to be associated with the main mineralizing phase in Bumolo. Overprint of late stage alteration was recognized but they do not contribute significantly to the mineralization. Supergene copper minerals have been observed within oxidized zones. Mineralization associated in the phyllic and propylitic alteration zones is minimal to null for both copper and gold. Silicification on localized portion near the intrusives and wall rock contact are poorly to moderately mineralized.

7.2.1 Potassic Alteration (Secondary Biotite + Magnetite ± K-Feldspar)

Potassic alteration at Bumolo is characterized by secondary biotite + magnetite ± k-feldspar. K-feldspar occurs as selvages on quartz veins locally observed in some holes. Magnetite occurs as stringers, fracture fills in quartz veins, and as abundant minute grains in the groundmass. Secondary biotite commonly replaces the primary mafic phenocrysts. Along with magnetite, minute grains of secondary biotite in the groundmass resulted to the dark gray appearance of the altered rock. The potassic alteration is most intense in CD while incipient secondary biotite alteration of hornblende phenocrysts was noted in the inter-mineralization CD2, and least developed in the late stage LDP and AP (see Fig. 10).

Hypogene sulfide minerals, chalcopyrite, bornite and weak pyrite, are mainly associated with this alteration. The upper portion of the potassic zone was affected by supergene weathering and oxidation. In this portion, minerals observed include cuprite, malachite, chalcocite and native Cu along with iron oxides göethite and hematite.

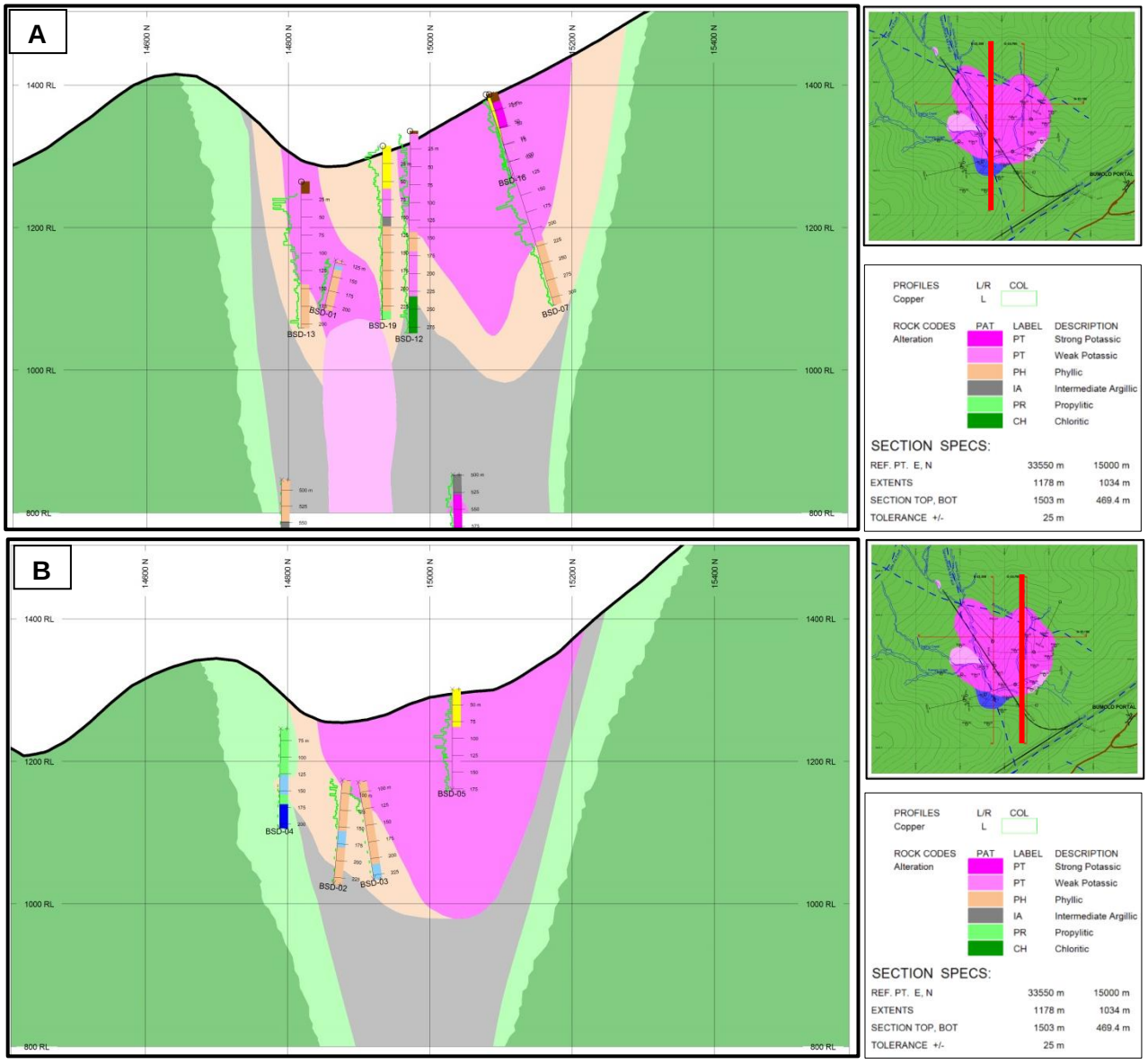

Figure 10. Section along A) 33550 looking west and B) 33700 looking west across the Bumolo intrusive complex

7.2.2 Sericitic/Phyllic Alteration (Sericite + Quartz)

The phyllic alteration at Bumolo occurs mostly adjacent to the contacts of CD and late stage porphyries (Figure 10). Macroscopic and petrographic observations revealed the occurrence of sericite + quartz minerals at depths, approximately 100m to 500m from the surface. This alteration differs with the typical phyllic alteration due to the relatively less pyrite content (generally <5%). Pyrite is the more dominant sulfide in the phyllic-altered zones, except where it overprinted mineralized, potassic-altered rocks. Sericite with substantial chlorite is found to also overprint the potassic altered cores.

7.2.3 Intermediate Argillic Alteration (Sericite/Illite + Chlorite +Clay)

Intermediate argillic alteration is evident on most of the LDP body and portions of MA. It is characterized by illite (or sericite in some cases) occurring as a weak dusting of plagioclase. Chlorite occurs as pervasive alteration in mafic minerals and in the groundmass along with traces of magnetite. Smectite occur as replacement of mafic minerals, plagioclase and

groundmass. This mineral assemblage is observed to overprint some portion of the potassic, phyllic and propylitic alteration zones (Figure 10).

7.2.4 Silicic Alteration (Quartz)

Intense silicification is mostly observed in the southern portion of the deposit near the contacts of the diorites and MA. The silicified portions of MA, appearing almost identical to the non-silicified, fine-grained MA, are distinguished on the basis of hardness. Petrographic and TerraSpec™ analyses confirmed this type of alteration.

7.2.5 Propylitic Alteration (Chlorite + Epidote + Carbonate)

The propylitic alteration bounds the potassic and phyllic alteration. It is characterized by mineral assemblage epidote + chlorite ± carbonate. This alteration is observed mostly on the country rock, MA, and in rare cases, portion of LDP. Chloritization of Fe and Mg rich mineral, and presence of epidote and calcite grains characterize this alteration. Pyrite as fracture fills and stringers with rare dissemination is the common sulfide with minimal chalcopyrite.

7.2.6 Chloritic Alteration

Meta-Andesite is regionally altered to chlorite. This alteration is often observed on the outer periphery of the propylitic zone. Drillhole intercept usually has limited zones of chloritic alteration. Chlorite partially altering secondary biotite is also noted.

7.3 Style of Mineralization

Copper and gold mineralization, pervasive potassic alteration and the development of the high-grade hydrothermal breccia were inferred to be temporally associated with the emplacement of the CD. Inter-mineralization diorite porphyries carried less mineralization and weaker potassic alteration. Weak to unmineralized late porphyries truncated the early diorites and resulted with phyllic overprint and localized low-grade hydrothermal breccias. Supergene mineralization was later developed on the central portion of the stock.

7.3.1 Main Copper Sulfide Mineralization

Copper and Au grades greater than 0.15% Cu and 0.20g/t Au respectively are confined at the upper portion of the stock associated with CD and High-grade Hydrothermal Breccia (HHBX), coinciding with the pervasive potassic alteration. Copper sulfides in Bumolo are occurring as disseminates, fracture fills, veinlets and quartz vein infill with magnetite ± secondary biotite ± pyrite and occasional specularite association (Photo 6). Chalcopyrite is the dominant Cu mineral with rare bornite (Photos 6 and 7). Gold is believed to be associated with Cu sulfide with 1:1 ratio to as high as 1:2. Pyrite is ubiquitous but more dominant in late phase intrusives and country rock. CD with stockworks and HHBX have elevated copper and gold grades.

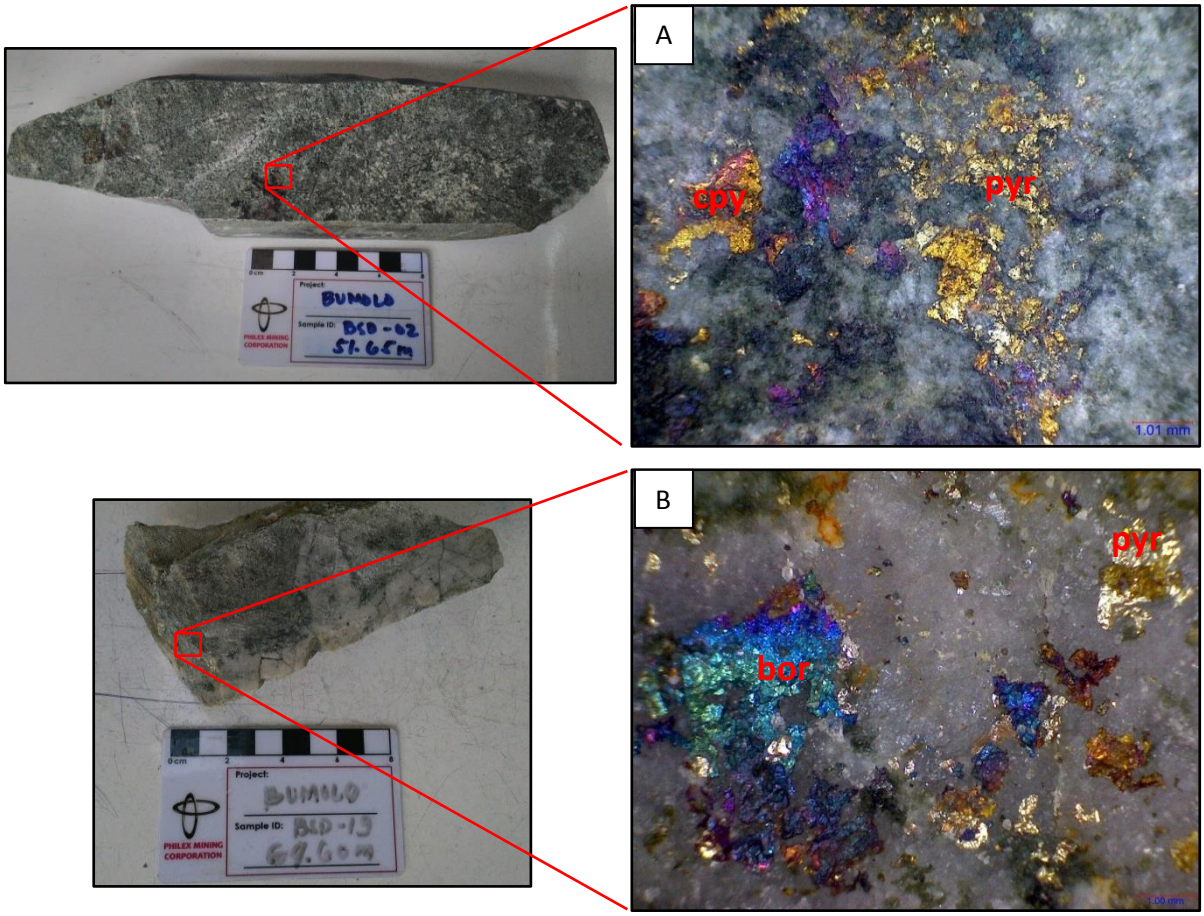

Photo 6. Cu sulfide mineralization (bornite and chalcopyrite) in fractures (A) and in veins (B)

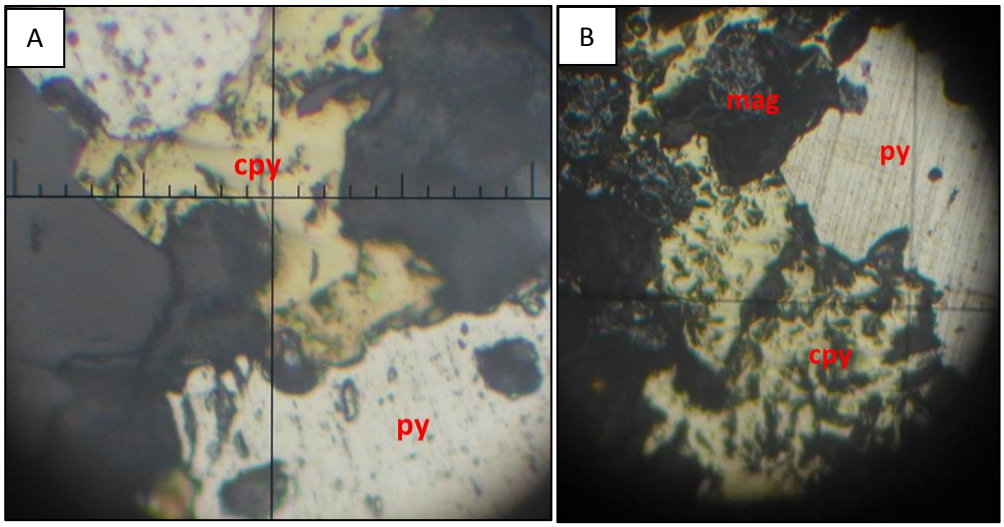

Photo 7. Photo under petrographic microscope using reflected light showing (A) chalcopyrite interlocked with pyrite and (B) chalcopyrite with magnetite and pyrite association.

7.3.2 Supergene Mineralization

The erosion of the upper portion Bumolo resulted to the development of localized supergene zone with a maximum thickness of 70m. Chalcocite characterized the supergene mineralization along with malachite, azurite, cuprite, covellite and native Cu (Photo 8). Chalcocite and covellite are observed rimming the chalcopyrite and bornite respectively under petrographic microscope (Photo 9). Cu mineralization in supergene is also commonly associated with Fe oxide minerals namely göethite and hematite.

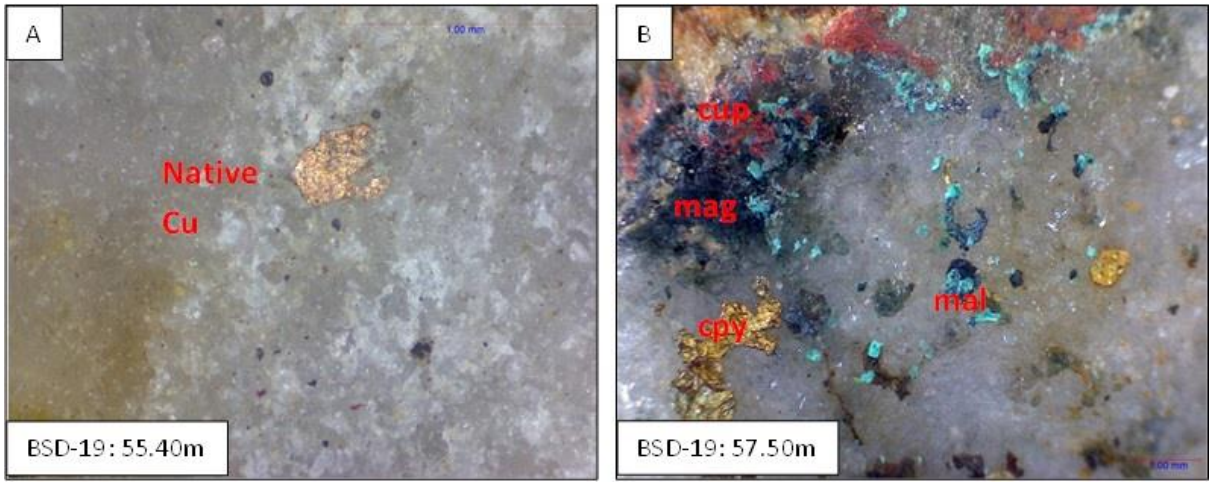

Photo 8. A. Native copper in veins and B. Cu Oxides and Cu carbonates replacing chalcopyrite.

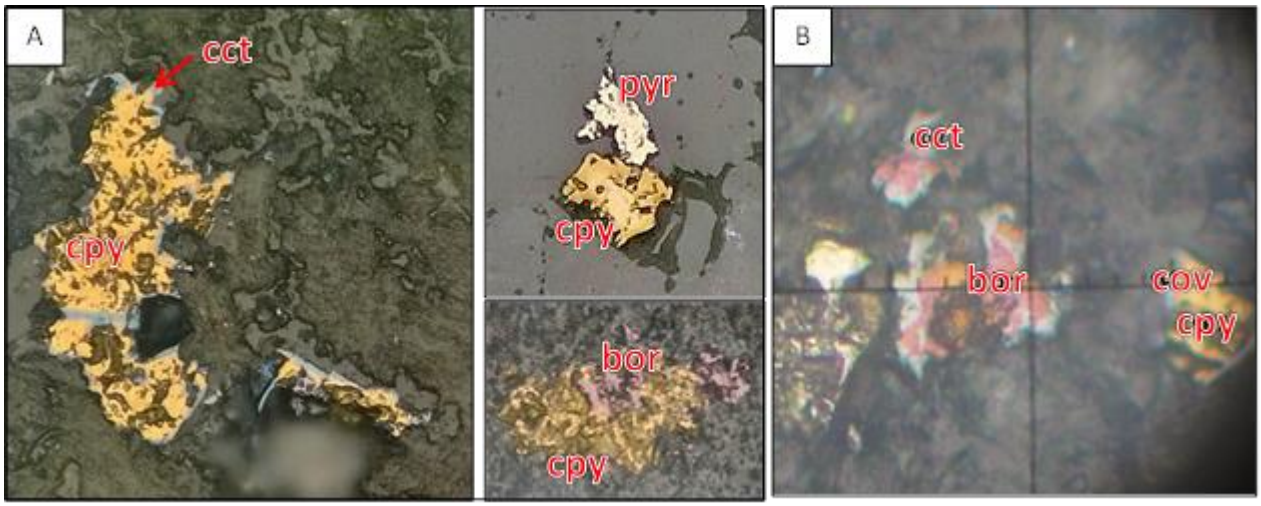

Photo 9. Photo under petrographic microscope using reflected light showing (A) chalcopyrite (cpy) with chalcocite (cct, also possibly digenite) rim, cpy attached to pyr, and cpy to bornite (bor); (B) chalcopyrite (cpy) and bornite (bor) rimmed by covellite (cov) and chalcocite (cct) respectively.

7.3.3 Wall Rock Alteration and Paragenesis

The country rock is MA with members from both Pugo Formation and Zigzag Formation. It is regionally chloritic altered and proximal to the Bumolo intrusives. Due to the influence of increasing temperature and hydrothermal fluids, a thin alteration zone of propylitic and some silicic alteration were observed and interpreted. Silicification was noted and is localized near

contacts. Contacts with the intrusive body are either sharp with bake and chill margins or is associated with intrusives and hydrothermal breccia.

7.3.4 Geological Structures

Bumolo porphyry Cu-Au deposit is hosted in and around a multiphase diorite complex found to be bounded by the Tapaya-Black Mountain fault to the west and by the Bumolo fault on the northern portion (Figure 11) No structures have been mapped or interpreted in the main Cu sulfide mineralization that contributed to the improvement of the grade. Fault gouges were noted in the cores showing no significant change in Cu and Au grades.

7.3.5 Localization of the Deposit

Significant mineralization in Bumolo is associated with CD and HHBX, which are truncated by late and less mineralized porphyries at depth (Figure 9). The portion with >0.15% Cu and 0.20g/t Au is at the upper part of the stock forming a tabular pattern associated with CD and HHBX. The deposit deepens towards southwest associated in High-grade Hydrothermal Breccia. The cupulas of late porphyries serves as the limit of the main mineralization at its bottom and Meta-Andesite to the sides.

7.3.6 Length, Width, Depth of Mineralization

Horizontal and tabular shape of the main Cu mineralization that extend deeper at southwestern portion was formed due to the emplacement of Clear Diorite that were truncated later on at depth by younger porphyries. Drilling data confirms a thickness of 110m to 130m of mineralized zone from the surface with an approximate depth down to 1125masl.

The current geologic model has revealed a 400 x 400 x 600m (length x width x depth) intrusive complex at Bumolo. The mineralization is observed at near surface and is overlain by overburden, i.e. colluvium. Size of mineralization with cut-off grade of 0.15% Cu was measured to have similar length and width as the lithologic model while its depth and thickness at its largest is about 130m from present surface.

7.3.7 Development of “Ore Shoots”

Significant Cu and Au grades are associated with the heavily veined Clear Diorite and High-grade Hydrothermal Breccia. These two zones are believed to be related to the emplacement of the Clear Diorite at Bumolo. It is also pervasively altered to potassic with selective overprinting of phyllic alteration.

Localized and minimal supergene enrichment on the central part of the deposit was a later development after extreme erosion and exhumation the upper portion of the Bumolo porphyry stock.

7.3.8 Continuity of Mineralization

A Drilling data confirms the horizontal tabular shape of the main copper and gold mineralization at the upper portion of the stock. However, the extension of mineralization around the stock is still to be well defined. Vertically, mineralization was truncated by the younger intrusives at depth. Though, on the southwest side the mineralization possibly

extends deeper. Drilling is still ongoing and has not defined the limits of mineralization. The Bumolo deposit is still open on all sides.

9. EXPLORATION

8.1 Geological Work

Detailed geological mapping covering approximately 64 has was conducted to update the existing surface geological map, define surface drill targets, and further refine the geological model of Bumolo. Mapping activities using compass and tape creek traverse on 1:500m scale commenced on the 16th of December 2014 and was completed early 2015. Mapped lithologies on surface include the Clear Diorite (CD), Late-phase Diorite Porphyry (LDP) and Meta-andesite (MA, subdivided into basalt and diabase).

8.1.1 Rock Types

The oldest rock unit is the MA subdivided into basalt and diabase. MA forms part of the Pugo Formation and is considered as the country rock in the area. Generally, it is aphanitic (basalt) and porphyritic (diabase) in texture, primarily composed of subhedral to anhedral plagioclase crystals. Textural destruction due to silicification and moderate bleaching is common. Alteration is propylitic to phyllic with pyrite being the main sulfide mineral.

CD is characterized by the interlocking medium-grained granular altered plagioclase and hornblende. Pervasive potassic alteration of quartz + magnetite - biotite ± sericite ± actinolite is overprinted by weak chloritic alteration. In parts, quartz stockwork and sheeted quartz veins (<4cm thick) were noted. Magnetite veinlets or stringers prominently cut the CD. The magnetite-sulfide veins generally trend NE/SE and NNE/NW. Sulfide mineralization includes pyrite, chalcopyrite and rare bornite. It is bounded on the west by the SSE draining third-order Bumolo creek and on the south by its ESE draining continuation. The S to SSE draining second-order creek limits the eastern section (Figure 11).

LDP is the youngest intrusive body mapped on the surface. It occurs as dikes cutting the older rock units. In general, the LDP is highly jointed, fresh to chloritic altered, and lacking Cu-sulfides. LDP dikes measure up to 20 m in diameter. These were mapped along the first-order ESE draining “Saging” creek near the junction of “Kaingin” creek and along the second-order SSE draining Bumolo creek.

At lithologic contacts, intrusive breccias occur with typical chaotic texture on chilled margins and assimilation of the older wall rocks into the younger intrusions. When in contact with MA, intrusive breccias are usually light gray in color; strongly weathered, and contain basalt xenoliths.

8.1.2 Structures

Structures in Bumolo occur as northwest and northeast trending faults. The NNW-SSE Tapaya-Black Mountain fault traverses the CD stock and the NW-SE Bumolo fault on the north (Figure 11). The northeast-trending Sta. Fe fault lies further northwest and the Albian fault occurs towards the south.

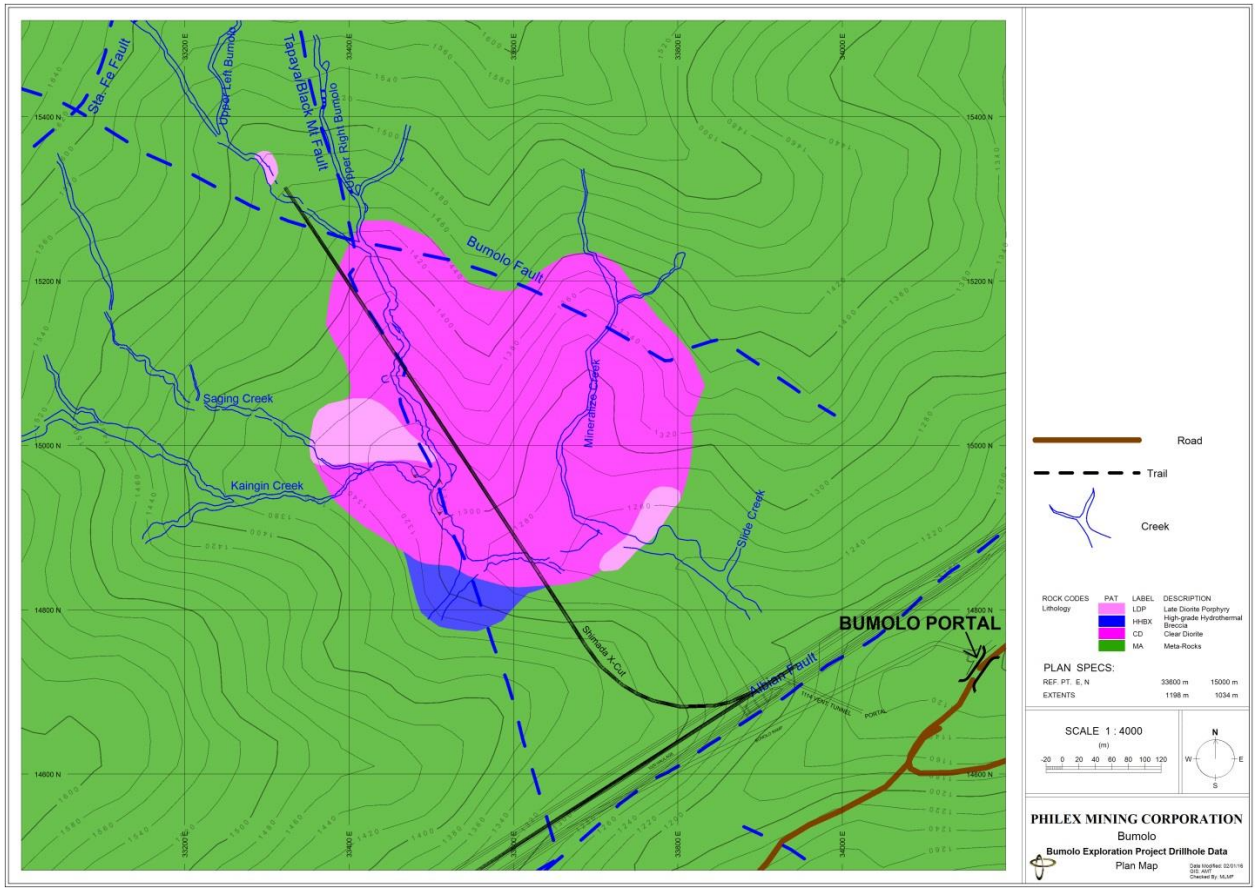

Figure 11. Bumolo Geologic Map based on results of field mapping and drilling

8.1.3 Surface Sampling

Channel sampling from January to March 2015 in the western portion of the potassic-altered CD exposed along the "Bumolo" creek yielded an average of 0.07% Cu and 0.24 g/t Au. This represents the 110-m stretch of 22 channel samples following a 3 to 5 m sampling interval. Furthermore, 6 samples equivalent to 26-m interval yielded an average grade of Cu and Au values of 0.16% and 0.51g/t, respectively.

Propylitic and phyllic alteration developed over MA and locally, over the youngest intrusive LDP dikes. In some portions, LDP is relatively fresh to chloritic. Potassic alteration with quartz + magnetite - biotite ± sericite ± actinolite (potassic) with weak chlorite overprint is commonly observed in CD.

Microscopic analysis of mold polished section from the potassic altered CD outcrop shows that Cu-sulfide mineralization includes chalcopyrite and bornite interlocked in magnetite, attached into pyrite, and as free minute grains in the rock mass.

8.2 Geophysical Surveys

8.2.1 Induced Polarization (IP)-Resistivity Survey

IP-Resistivity survey of twenty-eight (28) stations, which are located along three (3) 500-m E-W lines with eleven (11) points per line and spaced 50m apart (Figure 12), was conducted to

determine the resistivity-chargeability anomalies around the proposed drillholes in the area. The layout aims to cover the upper 100m of the ground and did not take into account any mineralization trend. Location of stations was done by the field staff before the survey through compass-and-tape traverse.

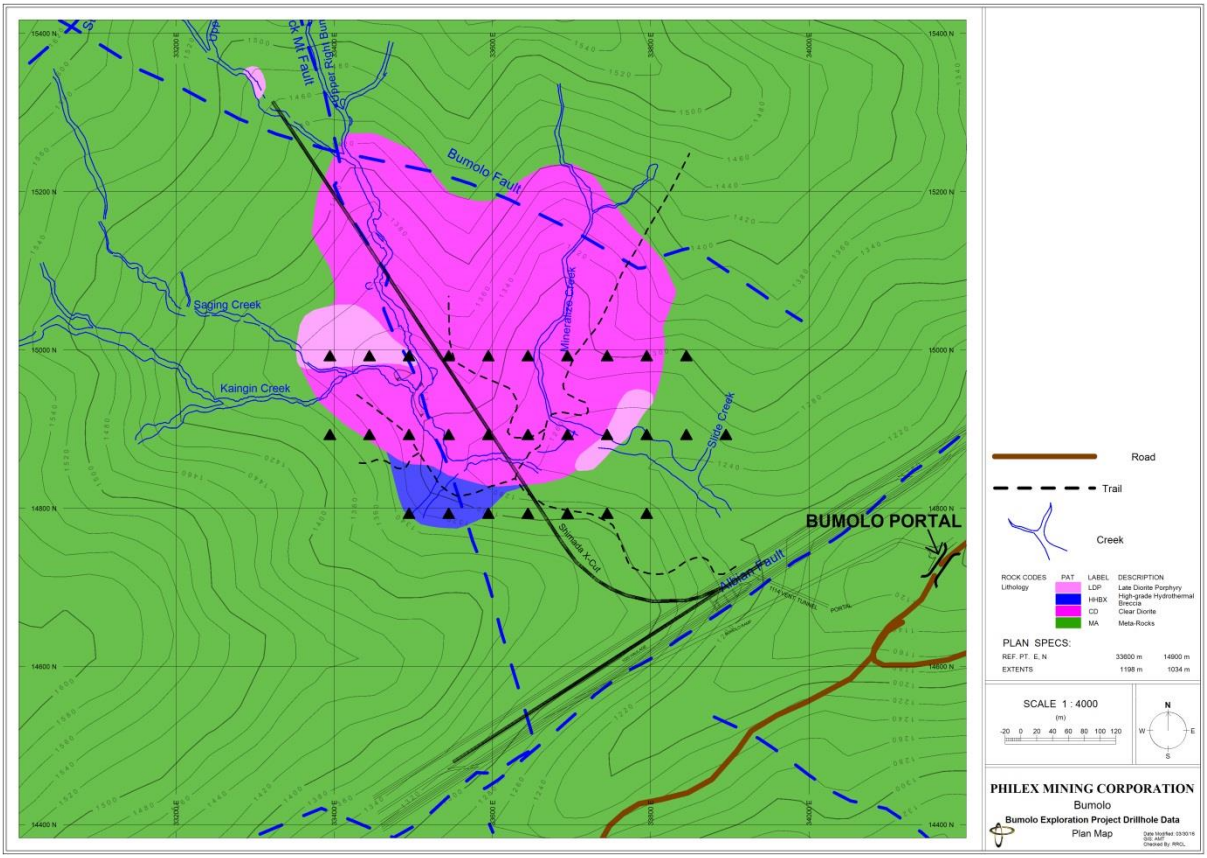

Figure 12. Lithological map of Bumolo showing the IP-chargeability survey lines

The IP-Resistivity survey was done in roll-along system, dipole-dipole, 6-channel array at 50 m intervals. Equipment included Iris™ Elrec Pro receiver and VIP 5000 transmitter operated by a 5kVA, 220V, single-phase motor generator. During the survey, data accepted for processing were ensured to have maximum Q (or error of the reading) values of 5%.

Syscal Prosys II software was used to download the survey data from the receiver. Further, AGI EarthImager 2D software was used in 2D data processing with noise-reduction procedures based on the 1) default settings, and 2) data misfit histogram of measured vs. computed values of resistivity and chargeability.

Three-dimensional (3D) modeling was done in Geosoft Oasis Target using ordinary kriging (OK) of previously-generated 2D inverted IP and resistivity data.

Chargeability anomaly zones were correlated with previous and currently-proposed drillholes to determine coinciding anomalies.

In general, noise limits the quality of output profile by eliminating the unwanted points. It was observed in seven (7) points of Line 2 and can be attributed to lack of clayey soil and

presence of loose pebble- to boulder-sized rocks along the creek and slope where some stations near the proposed drill pad are located. Generally, moderate to high noise can be attributed to shallow or absence of soil profile and fine (or clayey) materials on the ground surface.

Figure 13 shows the compiled inverted cross-sections of resistivity (top) – IP (or chargeability, bottom) in 2D along the different survey lines. The "area(s) of concern" characterized by resistivity low (blue) and chargeability high (red) can be observed between L1-300 and L1-350 (dashed circle in Figure 13).

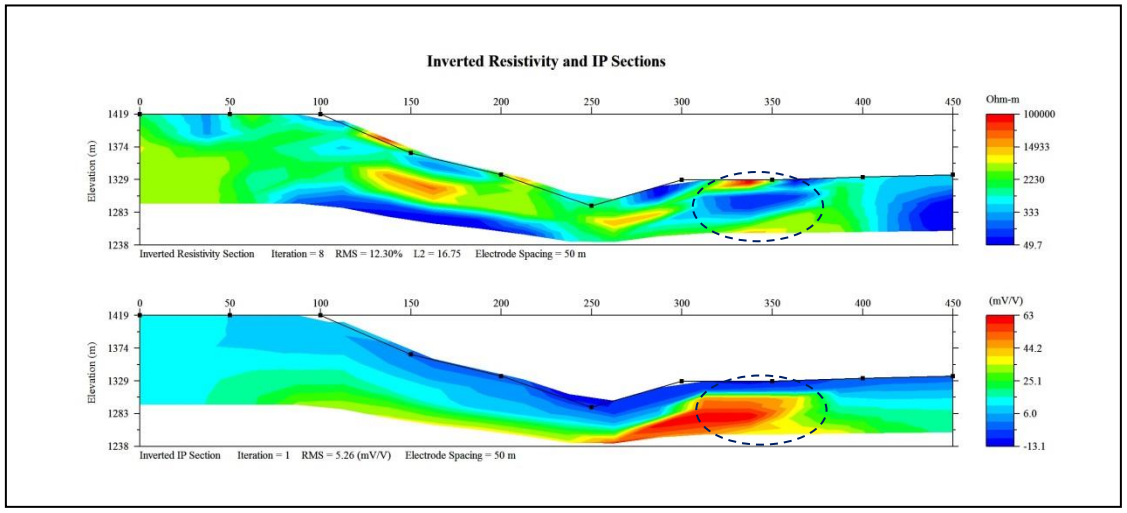

Figure 13. West-east cross sections of inverted IP-resistivity anomalies along survey Line 1

Upon generation of the 3D model and inclusion of proposed drillholes (elevation = 1249m; bearing = 255°; BSD-1 of -70° dip, BSD-2 of -50° dip) in plan, a chargeability high (red) to the NNE of the collar (Figure 14A) does not coincide very well with the resistivity low (blue) to the NW (Figure 14B).

The "area of concern" characterized by resistivity low (blue) and chargeability high (red), associated to the sulfides in the phyllic zone of a possible porphyry system, was not spatially distinct in the plan section of the 3D model at the drillhole collar elevation. This can be explained by either: 1) lack of a distinct phyllic zone in the area, or 2) otherwise, supposedly wider and more continuous resistivity-low area that is more spatially correlatable, which is basically affected by removal of significant amount of data along Line 2. Correlation to magnetics survey data is needed to prove either inference.

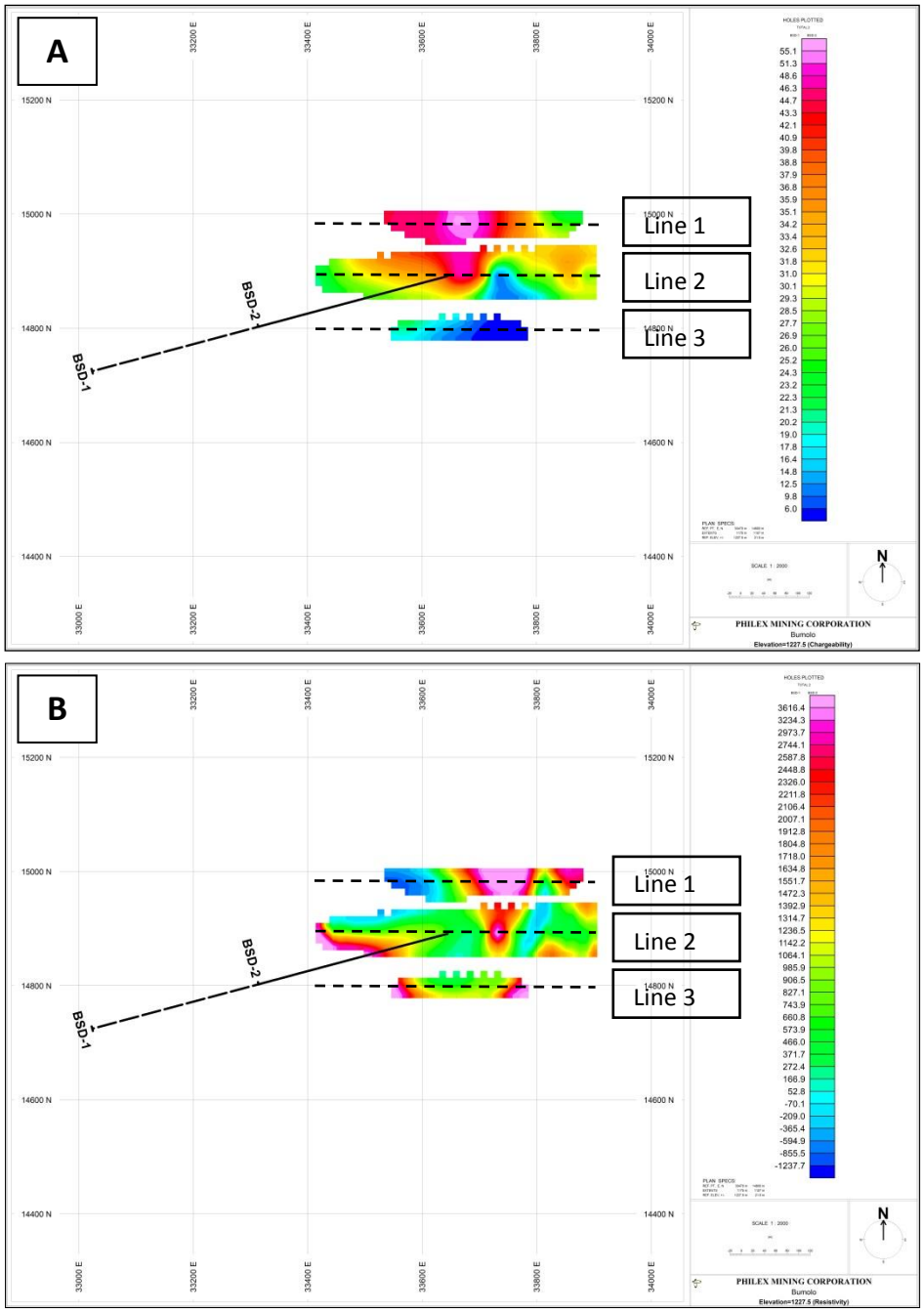

Figure 14. A) Chargeability and B) Resistivity anomaly plan map of Bumolo Prospect with the survey lines and drillholes BSD-1 and BSD-2

8.2.2 Magnetics Survey

Survey grid for the magnetics survey is the same as the IP-resistivity survey grid but with three (3) additional lines to the south and one (1) line to the north, with a total of sixty (60) stations (Figure 15). The survey aims to determine the magnetic susceptibility signature around the proposed drill pad in the area enough to cover the upper 100m of the ground. No mineralization trend was taken into consideration in the survey layout. Line brushing, survey proper and re-survey were conducted from February 26 until March 17, 2015 by in-house field personnel. Location of stations was completed before the survey through compass-and-tape traverse.

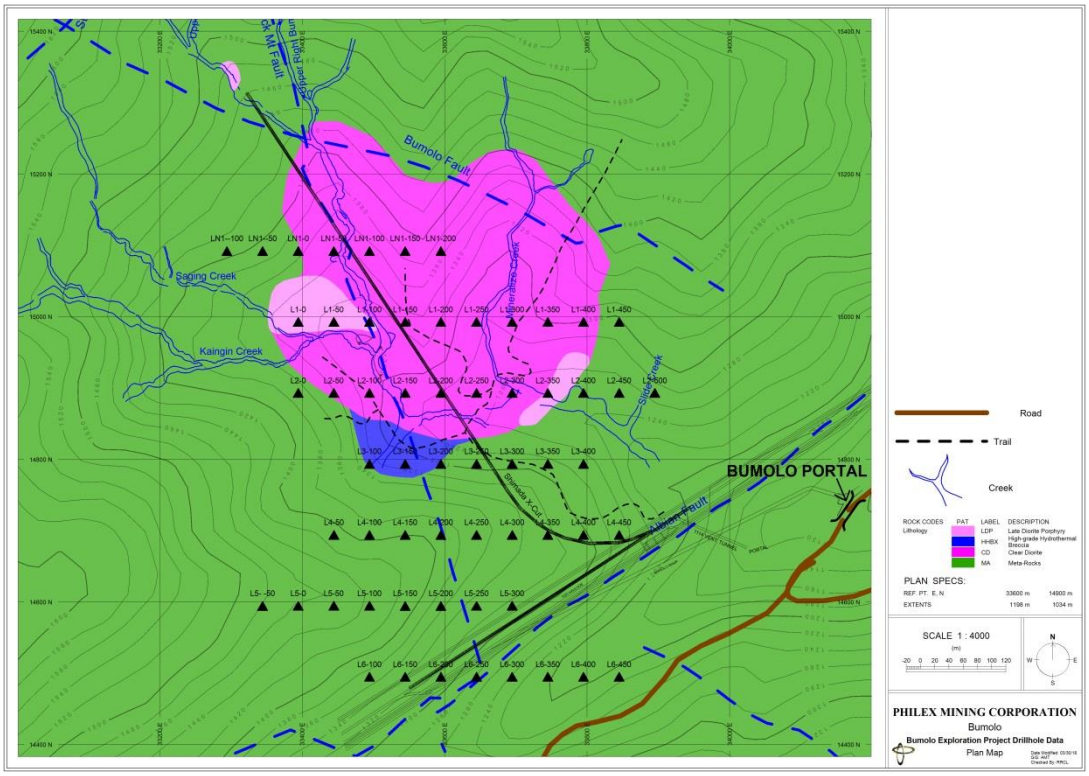

Figure 15. Lithological map of Bumolo Prospect showing the magnetics survey lines

The magnetic survey uses a Scintrex Envi Pro magnetometer system of base and rover. A stop-and-go method was used, wherein at least ten (10) total magnetic field intensity readings were recorded in each station by the rover while the base station, located at a site about 1km from the survey area, took magnetic intensity readings of the area simultaneous with the rover survey.

After each survey day, all base and rover data were downloaded through the Data Logger software. Microsoft Excel was then used in noise reduction, diurnal correction, levelling and anomaly computation. Noisy rover and base data were detected as outliers in the smooth time-series (for base) and distance-series (for rover) plot and were subject for removal.

Diurnal or base correction was done by subtracting the magnetic intensity reading of the rover from simultaneous base station intensity measurement to obtain the magnetic anomaly. The subtraction was done after adding an arbitrary value of 1000 to the rover value in order to avoid getting negative difference value.

As a QA-QC measure, trend analysis was done on anomaly plots of points along the N-S direction. Sudden change in consecutive anomaly values can be attributed to noise and requires re-survey. Seven stations (namely, L1 200, L1 250, L2 150, L2 200, L4 100, L5 150 and L5 200) were re-surveyed and showed that noise wasn't involved. After which, the final anomaly data was prepared.

The magnetic anomaly values are then fed to Surfer for gridding and contouring. The grid data saved from Surfer is fed to Magpick for Reduction-to-Pole at 30 degrees. Further, Geosoft Oasis Montaj was used to ordinary krige (OK) the output magnetic data and to generate a better-looking anomaly map.

Based on the raw magnetic anomaly (plan) map in Figure 16, a distinct magnetic high (red) of 150-200m radius in Line 2 appears to be intersected by the proposed drillholes. To the south, two magnetic highs (~50m in radius) in Lines 5 and 6 are interpreted to be continuous. Reduction-to-pole procedure was not employed at this point due to irrelevance at the survey location, which is near the equator.

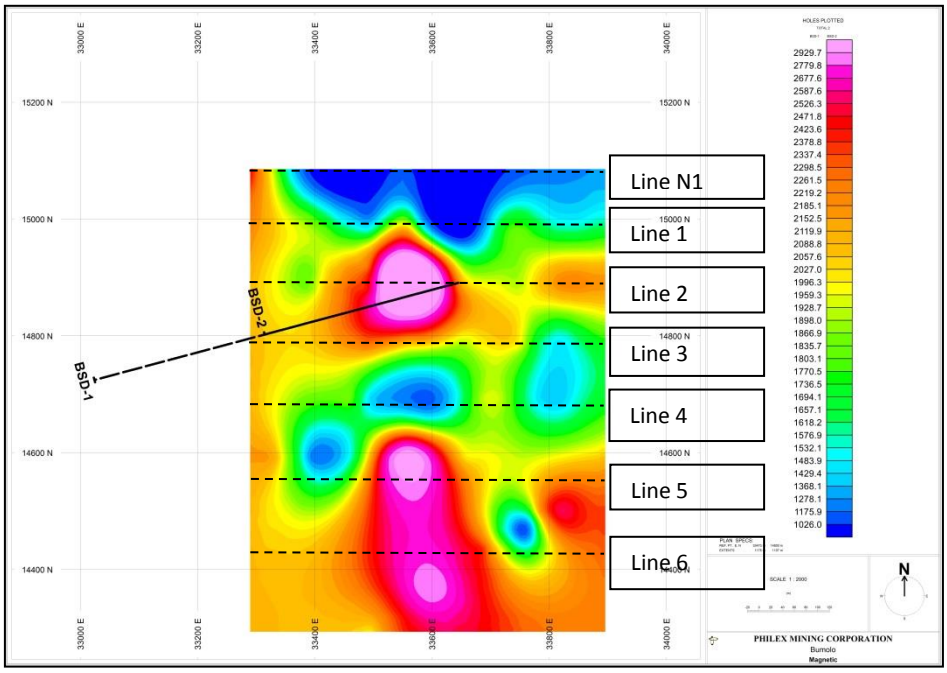

Figure 16. Magnetics (raw) anomaly plan map of Bumolo Prospect with the survey lines and drillholes BSD-1 and BSD-2

The "area of concern" characterized by distinct magnetic high in Line 2 can be attributed to magnetite mineralization in the potassic zone of a possible porphyry system, as strongly supported by the presence of mapped diorite (intrusive) lithology. Further, the area is located near an assumed phyllic zone that was identified by IP-chargeability anomaly. With this, the area has been strongly proposed for drilling.

The two smaller magnetic highs in Lines 5 and 6 were found on basalt rocks and seem to arise from too few data points, which can be called point anomalies. No significant implication to mineral exploration is seen based on current survey results. Confirmatory mapping and/or further magnetics survey can be programmed to verify this claim.

8.3 2015 to Present Drilling and Sampling Program

8.3.1 2015 to Present Drilling Program

The consent to conduct surface exploration drilling in Bumolo was granted in December 2014. Scout drilling program at Bumolo commenced that commenced in March 2015 was elevated to definition drilling program by the 4th quarter of the year. Drilling was conducted by the in-house exploration drilling section of Philex and by one drill contractor - DrillCorp Philippines, Inc. (DCP). The company's #1 CS-10 rig was commissioned to drill the first three surface boreholes. The #2 CS-10 rig started drilling the 4th borehole on the 13th of June.

The first CS-14 drill rig (Rig #75) of DrillCorp Philippines, Inc. (DCP) was commissioned to drill the 5th hole on July 22, 2015. This was followed by the second CS-14 machine (Rig #75) on the 23rd of September that drilled the 8th hole.

By the fourth quarter of 2015, the scout exploration drilling progressed to definition drilling after blocking significant Cu-Au mineralization. Two additional man-portable (RV machine) rigs from DCP were mobilized. The first man-portable Rig #58 drilled the 11th hole on the 29th October while the second Rig #59 drilled the 14th hole on the 19th of November.

A total of 20 drillholes were completed as of February 1, 2016 with an aggregate meterage of 7981.05m (Fig. 17). Data generated were then incorporated in the drillhole database from the previous underground drilling campaigns (Table 4) which translated to 11, 382 meters of drill cores.

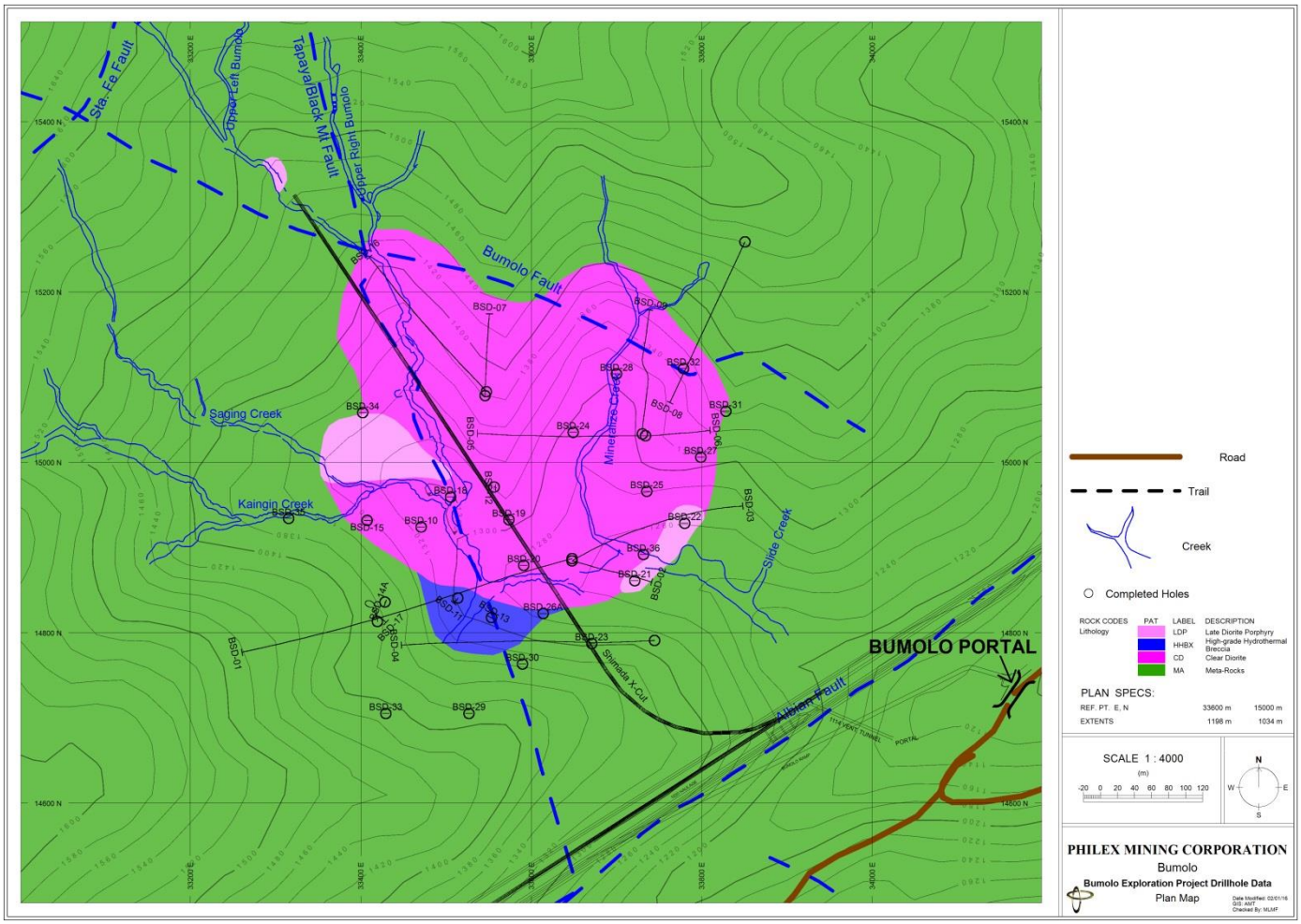

Figure 17. Bumolo deposit drillhole location map

Table 4. Bumolo Project Combined Drillhole Database

BP (Underground) DrillHoles

Hole ID	Northing	Easting	Elevation (m)	Azimuth (°)	Inclination (°)	Depth (m)	Projection	Date Started	Date Completed	Rig ID
BP-1	14886.99	33602.74	1036.56	254.51	74.48	198.45	SurfGrid	17-Nov-01	27-Feb-02	In-house
BP-2	14886.91	33601.08	1031.27	270.00	10.5	222.60	SurfGrid	17-Oct-02	12-Mar-03	In-house
BP10-3	14885.42	33602.29	1035.17	290.00	68	260.65	SurfGrid	19-Jun-10	16-Jul-10	Philex - LM 90-1
BP10-4	14886.42	33603.03	1035.84	0.00	70	308.10	SurfGrid	18-Jul-10	13-Aug-10	Philex - LM 90-1
BP10-5	14887.36	33605.30	1031.16	60.00	60	278.80	SurfGrid	19-Aug-10	31-Aug-10	Philex - LM 90-1
BP10-6	14883.69	33601.57	1034.38	240.00	48	524.75	SufGrid	5-Sep-10	5-Nov-10	Philex - LM 90-1
BP10-7	14886.02	33601.23	1033.84	310.00	50	321.50	SurfGrid	14-Nov-10	7-Dec-10	Philex - LM 90-1
BP10-8	14887.08	33601.64	1028.82	335.00	-50	383.80	SurfGrid	18-Dec-10	5-Feb-11	Philex - LM 90-1
BP11-9	14887.45	33606.09	1028.62	70.00	-50	550.10	SurfGrid	7-Mar-11	28-Apr-11	Philex - LM 90-1
BP11-10	14883.06	33602.90	1028.79	205.00	-50	352.20	SurfGrid	6-May-11	29-May-11	Philex - LM 90-1
				Total Meterage		**3400.95**				

Surface Drillholes

Hole ID	Northing	Easting	Elevation (m)	Azimuth (°)	Inclination (°)	Depth (m)	Projection	Date Started	Date Completed	Rig ID
BSD-01	14887.18	33647.78	1249.30	255.00	-51.05	680.75	SurfGrid	16-Mar-15	26-Apr-15	Philex - CS 10-1
BSD-02	14884.49	33647.70	1249.16	105.00	-70	287.45	SurfGrid	4-May-15	17-May-15	Philex - CS 10-1
BSD-03	14885.82	33647.55	1249.30	60.00	-70	586.35	SurfGrid	22-May-15	3-Jul-15	Philex - CS 10-1
BSD-04	14784.47	33750.78	1279.29	267.00	-70	801.60	Surfgrid	13-Jun-15	17-Aug-15	Philex - CS 10-2
BSD-05	15031.11	33735.60	1326.42	270.00	-70	626.10	Surfgrid	22-Jul-15	28-Aug-15	Drillcorp Rig #75
BSD-06	15031.30	33734.01	1326.41	90.00	-70	241.20	Surfgrid	1-Sep-15	12-Sep-15	Drillcorp Rig #75
BSD-07	15078.45	33545.69	1386.85	0.00	-70	311.15	Surfgrid	14-Sep-15	1-Oct-15	Philex - CS 10-1
BSD-08	15258.88	33850.69	1477.54	205.00	-70	608.90	Surfgrid	23-Sep-15	18-Nov-15	Drillcorp Rig #74
BSD-09	15033.56	33730.31	1326.24	0.00	-70	492.90	Surfgrid	5-Oct-15	6-Nov-15	Drillcorp Rig #75
BSD-10	14924.23	33470.68	1290.30	0.00	-90	273.00	Surfgrid	24-Oct-15	17-Nov-15	Philex - CS 10-2
BSD-11	14840.87	33513.71	1270.39	0.00	-90	299.20	Surfgrid	29-Oct-15	16-Nov-15	Drillcorp Rig #58
BSD-12	14971.21	33556.36	1335.49	0.00	-90	283.55	Surfgrid	10-Nov-15	11-Dec-15	Philex - CS 10-1
BSD-13	14818.00	33553.21	1264.67	0.00	-90	206.00	Surfgrid	18-Nov-15	28-Nov-15	Drillcorp Rig #58
BSD-14A	14836.18	33428.24	1335.75	0.00	-90	245.20	Surfgrid	7-Dec-15	8-Jan-16	Drillcorp Rig #59
BSD-15	14932.01	33407.32	1314.45	0.00	-90	344.90	Surfgrid	28-Nov-15	10-Dec-15	Philex - CS 10-2
BSD-16*	15083.04	33547.24	1387.05	320.00	-70	671.60	Surfgrid	6-Dec-15	31-Jan-16	Drillcorp Rig # 75
BSD-17	14813.34	33419.36	1354.66	135.00	-70	225.70	Surfgrid	12-Dec-15	8-Jan-16	Drillcorp Rig #58
BSD-18	14959.48	33505.24	1291.71	0.00	-90	274.95	Surfgrid	29-Dec-15	18-Jan-16	Philex - CS 10-2
BSD-19	14932.83	33573.67	1314.74	0.00	-90	243.75	Surfgrid	7-Jan-16	21-Jan-16	Philex - CS 10-1
BSD-20	14879.25	33591.06	1266.52	0.00	-90	276.80	Surfgrid	7-Jan-16	16-Jan-16	Drillcorp Rig # 74
**Drillhole depth considered as of this reporting cut-o*					**Total Meterage**	**7981.05**				

The project site drilling operation follows a sequential activities which include pad preparation and drill core handling. Philex assigned rig and field geologists monitored and supervised these activities to ensure that core handling protocol is properly implemented. Details of the chain of custody is shown in Figure 18.

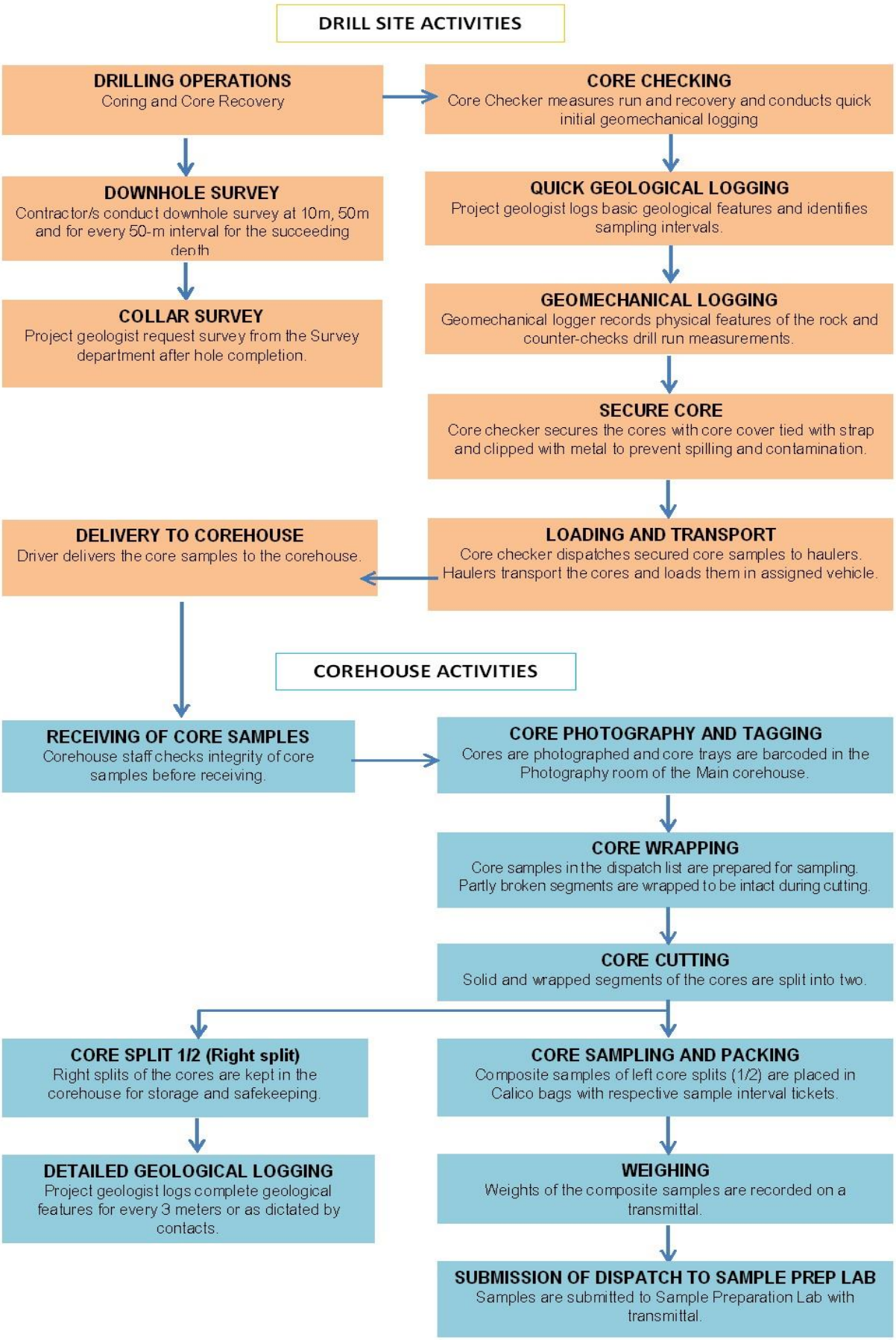

Figure 18. Modified Chain of Custody of DC samples for Padcal from drill site to core house

8.4 Drilling Methodology

The drilling program in Bumolo was carried out by Philex's in-house drilling arm and later on supplemented by Drill Corp. Both drillers used CS rigs with Drill Corp adding two man portable rigs in the 4th quarter of 2015. All rigs were capable of drilling more than 400 m with CS rigs capable of reaching more than 700 m depth. They utilized triple tube diamond coring using PQ3, HQ3 and NQ3 core diameter. For both drillers, drill runs range from 3m in competent ground to less than 1.5m in broken ground. Core recoveries from both companies in the bedrock averaged above 90%.

8.5 Downhole Survey

Down hole surveys are conducted at 10-m, 50-m depths and every 50-m interval thereafter until the end of hole or instructed otherwise. In-house drilling uses Deviflex borehole survey tool with instrument assembly limited to HQ and NQ rod size. Survey data are then digitally recorded and stored into the equipment's PDA and downloaded directly to a personal computer/laptop through adaptor cable.

DCP utilizes Camteq multi-shot (Proshot) survey camera fitted to PQ, HQ, and NQ size rods. Survey readings are handed written on a survey ticket/report which is signed by the driller and cross verified by the crew. A digital soft copy is provided to Philex as requested.

8.6 Collar Survey

Drillhole collars are initially located on ground by the field geologist using handheld GPS or compass and tape traverse from a known survey point. Verification of the collar location is conducted by a licensed geodetic engineer of Philex using South© Total Station. Collar survey is tied to the local surface grid datum. The survey data are provided through email.

8.7 Core Data Management

8.7.1 Core Checking

Once the core samples recovered from a drill run were laid out, the core checker measures the run and core recovery. These data are recorded in the logbook and in the daily drilling shift report. The corresponding depths of each run are labeled in the core tags placed on the core tray. The core checker also takes a photo of the core tray and conducts an initial geomechanical logging of the core samples, determining RQD (Rock Quality Determination) and IRS (Intact Rock Strength).

8.7.2 Geomechanical Logging

The physical features (such as RQD categories, joint patterns, weathering, IRS, etc.) of the core samples are recorded by a geomechanical logger in a log sheet[1] utilizing the wizpad computer. The filled-up log sheet is reviewed by the project geologist before uploading to acQuire© database. The logger also counter-checks the drill run measurements by the core checker.

[1] Geomechanical_Log_Sheet_for_Padcal Version 2.13 012-02-17

8.7.3 Geological Logging

The geological logging is conducted by the project geologist, mainly determining the geological features such as rock type, mineralization, alteration and structures of the core samples. An initial quick mineralogical log is completed by the field geologist at the drill site every day, marking the intervals for sampling. A comprehensive detailed log is completed at the core house after the cores have been split in half. A mineralogical logsheet[2] filled up using a wizpad computer.

8.7.4 Secure Core

After logging, the core checker secures the cores in the core tray by covering it with upholstered plywood, tied with strap and clipped with metal to prevent the samples from spilling or being contaminated. A Drill Core Transmittal is filled up and given to the haulers upon dispatching of core samples.

8.7.5 Core Transport

Designated haulers transport the secured core samples from the drill site with the respective transmittal. The core trays are loaded properly to the assigned vehicle and delivered to the main core house.

8.7.6 Receiving of Samples

Core samples are received by the core house staff and laid out on a respective area outside. Integrity of the samples is checked by counter-checking the transmittal with the core tags, labels, and sequence of the actual delivered core samples. Any form of tampering on the core cover and core tray as a whole is also checked.

8.7.7 Core Photography

After receipt at the core house, the core samples are then brought inside for photography. The core tray is laid out flat on the metal rollers with a photo header above it. A camera is set-up on the ceiling, parallel to the core tray, with 2 strobe lights at its sides. The designated core house staff takes at least 2 photos of each core tray. The cores are photographed wet, as it better shows the features of the cores. Meterages of cores photographed are listed in the worksheet Core Photo List Form and core photos are then uploaded in the acQuire© database.

Afterwards, core boxes are barcoded for proper archiving. Barcodes show the following information: (Top) Project name; (Bottom) Hole ID_From (m)_To (m)_Box no., as shown in Figure 19.

[2] Semi_Detailed_or_Detailed_Geological_Mineralogical_Log_Sheet Version 2.55 03-08-14

Figure 19. Core photography. Sample of the core photo (top image) and sample barcode (bottom) used in tagging of the core boxes

8.7.8 Core Wrapping

After photography, the cores are prepared for sampling. Fractured solid segments of the cores are pieced together and wrapped securely with transparent packaging tape. This ensures that the fractured parts remain intact during the cutting process. Highly fractured and clay-rich intervals are not wrapped.

A dispatch list prepared by the QA-QC geologist that has the drillhole intervals to be sampled is given to the core house staff for reference (see Sample Dispatches to Intertek and Padcal). The start and end meterages of the sampling intervals are labeled on the core box.

The following are considered in choosing the sampling intervals and is decided upon by the project geologist and QAQC geologist:

- Routine 3m composite sampling involves Clear Diorite (CD) intercepts and other lithologies with estimated Cu content ≥ 0.1%. Otherwise, sampling is done for every 15m interval.
- When shifting from every 3m to 15m sampling interval, two additional consecutive 3m composite samples must be chosen before changing the sampling interval to 15m.
- Special samples requested by the site geologist/logger should be included upon approval from the Project Manager. They must be minimum 1.0 to maximum 3.5m in length.
- End of hole must be sampled for 3m composite.

8.7.9 Core Cutting

The wrapped core samples are marked in the center, lengthwise along the core axis. This will serve as guide for the core cutter during splitting. Only solid and wrapped core segments are cut and broken to clayey intervals are left as is.

8.7.10 Core Sampling and Weighing

After cutting, dark red wooden blocks indicating sample numbers and intervals are placed on the start of the sampling interval. The left core-split, 3-m composite sample is placed in a calico bag. A sample ticket is placed inside the bag and the sample number is also written in the bag itself. The samples are weighed (Wet Weights_CH) and weights are recorded in the core house worksheet.

8.7.11 Core Storage

The remaining right core splits of the core are kept for storage and detailed logging in the core house. Core trays are barcoded for archiving and safekeeping.

8.7.12 Submission to Philex Sample Preparation Laboratory

Composite samples (left half split) are submitted to the sample preparation laboratory with its corresponding transmittal form.

10. SAMPLE PREPARATION, QUALITY ASSURANCE AND QUALITY CONTROL, QAQC

9.1 Security, Chain of Custody and Preparation of Samples

Recent exploration being undertaken in Bumolo for resource definition focused mainly on diamond drilling program, which generated drill cores as main products of the exploration. A chain of custody, as well as protocols, that govern sample handling procedures from the drill site, where the drill cores are recovered, to the corehouse, where drill cores are sampled, and ultimately, to the sample preparation laboratory, where cores are prepared for assaying has been put into practice to ensure integrity of the data collected. Samples are sent to a commercial laboratory and assay returns are uploaded in the database.

9.2 Sample Preparation Activities

9.2.1 Dispatch Method

Dispatches from core house are accompanied by a transmittal that provides a list of samples to be prepared. The integrity of the samples is checked before receiving the dispatch. The samples are then weighed upon receipt and recorded in the worksheet as Wet Weights_SP.

9.2.2 Oven Drying

The samples are transferred from the sample bags to steel trays, still accompanied by the sample tickets. The samples are oven-dried for at least 8 hours at 115^{o}C. After drying, the

samples are weighed again to determine moisture content (Dry Weight). Weights obtained throughout the sample preparation are noted on the Pulp Sample Preparation Form worksheet.

9.2.3 Primary Crushing

After drying, the samples are fed into the jaw crusher, reducing samples into 1/4 to 3/4-inch fragments.

9.2.4 Specific Gravity Measurement

An aggregate of 500 grams sample consisting of core chips are handpicked and collected with 15-m interval for Specific Gravity determination using the liquid immersion method. The graduated cylinder is filled with 500mL of water. The initial volume is measured using the upper meniscus. The collected 500g of rock chips are put in the gradated cylinder. The combined final volume of water and rock chips is recorded. It is ensured that there are no more bubbles when taking the final volume.

9.2.5 Secondary Crushing

The product of the primary crusher are fed to the Boyd crusher, an integrated crusher-splitter that reduces samples to about 2 to 4 mm fragments and splits the composite into desired proportions. The rotary splitter is set to separate 1 kilo from the sample composite. The rest of the samples that are coarse rejects are stored.

9.2.6 Pulverization

The 1-kg sample split from the secondary crushing is pulverized in LM2 ring mill and is ground to -200 mesh pulp for 6 to 8 minutes. Grind size of every sample is tested using spatula method and every 10th sample using wet sieving (with at least 90% -200 mesh passing). The ring mill is cleaned up with running water every after use.

9.2.7 Rifle Splitting, Weighing and Barcoding of Pulps

The 1-kg pulverized sample is rifled split into four portions (labeled A-D), with each split weighing about 250 grams. Pulp splits are weighed and packed in pre-numbered/barcoded kraft envelopes. The kraft envelopes are then placed in sealed plastic bags.

9.2.8 Insertion of QA/QC Samples

As part of the QA/QC protocol of Philex, controls and standards are included anonymously in the dispatches sent to the assay laboratory, maintaining continuous sample numbering. The following are the QA/QC inserts (Table 5) currently incorporated and their respective frequencies.

Table 5. Bumolo QA/QC Insert Frequency

QA/QC Sample	Frequency
Pulp Duplicate	1:10
Coarse Duplicate	1:20
ICS Sample	1:15
Blank Sample	1:25

9.2.9 Pulp Duplicates

These refer to routine samples in a batch that are selected randomly and analyzed twice (pulp aliquot B). They are inserted at a frequency of 1:10 for the purpose of testing for in-batch and between-batch types errors.

9.2.10 Coarse Duplicates

Coarse duplicates pertain to the samples prepared from coarse rejects from the sample preparation that are re-analyzed on a selective but regular basis (pulp aliquot W). They will check for representativity and will determine if the sample preparation has been undertaken properly from the coarse fraction to provide reproducible results. They are regularly inserted at a frequency of 1:20.

9.2.11 Internal Control Standards

These are standard control samples to check for accuracy of analysis of the laboratory. These are prepared by the company to match the mineralogical matrix, ore type and grade range of the target deposit being explored and are analyzed by a large number of reputable laboratories and whose final consolidated results are certified.

Currently, PCL-32009 is incorporated in the dispatches at a frequency of 1:15. Having certified values of 0.13 g/t Au and 0.057% Cu, it is prepared from pulverized Cu-Au tailings (TSF # 3) materials.

9.2.12 Blank Standards

These refer to internally prepared samples having background levels of the element(s) of interest. They are inserted at a frequency of 1:25 for the purpose of testing for contamination imparted during analysis by the laboratory. Currently being used samples are Blank 2 lahar samples.

9.2.13 Dispatch to Assay Laboratory

Two dispatches are prepared for each batch of samples. One is sent to Intertek-McPhar laboratory in Muntinlupa (with accompanying Waybill and Sample Submission Form to Intertek Lab) and the other to the assay laboratory in Padcal for parallel assay (Sample Submission Form to Padcal Lab. Pulp A is utilized as routine samples for Intertek, while pulp C is for Padcal laboratory.

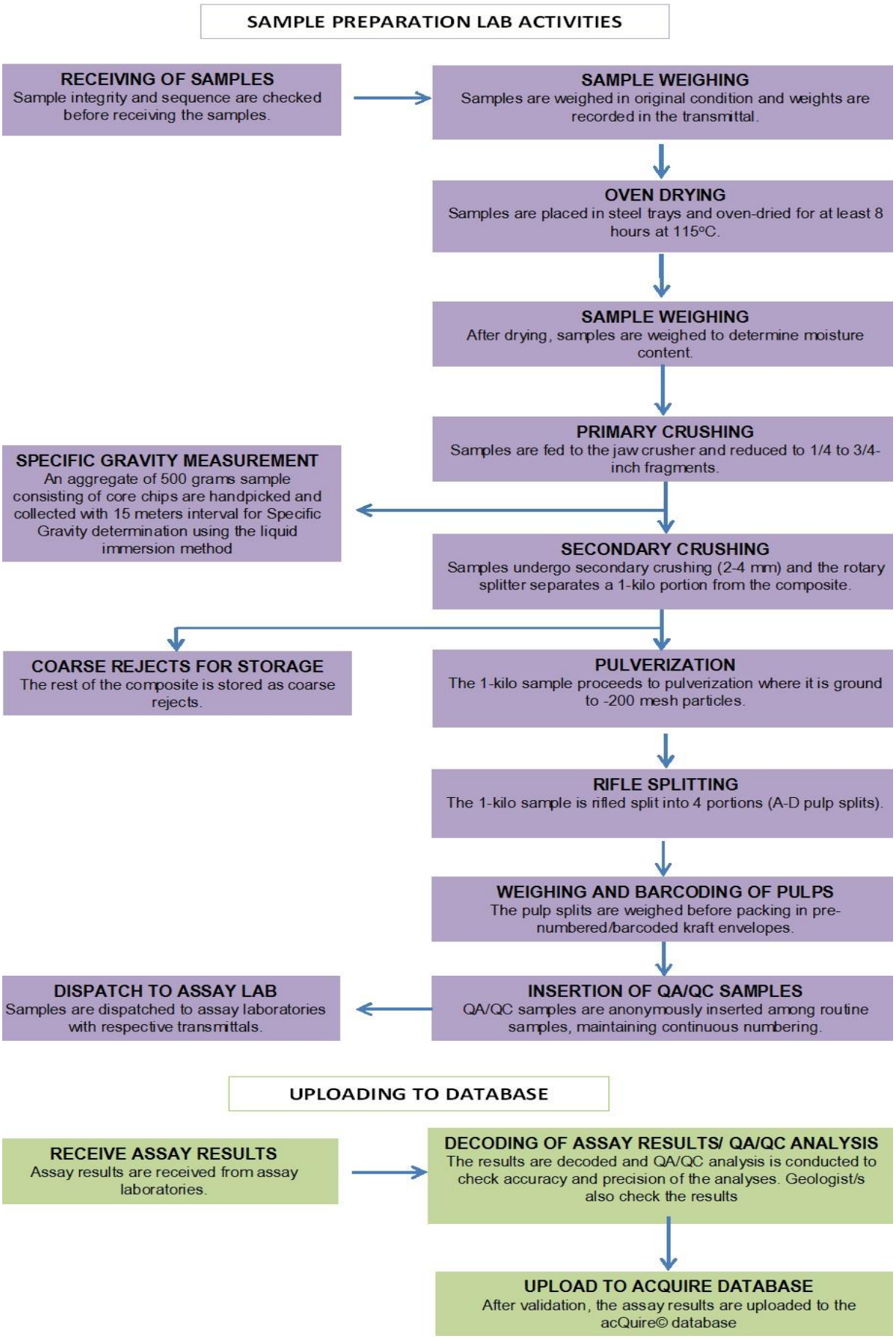

Figure 20. Flowchart for Sample Preparation Activities

9.3 Analytical Methods Used

Routine samples are primarily analysed for Cu, Ag, and Au. The procedures of determinations used by the commercial laboratory, Intertek McPhar, are prescribed by Philex as PHX-01, method code for Au analysis, and PHX-02, for Cu and Ag.

PHX-01 is an ore grade method of analysis for Au in DDH core samples, "measured" rock samples and samples where grade values are to be used for resource and reserve estimation. The finely ground sample (-200 mesh) is fused with a suitable flux under reducing conditions which separates the precious metals as a lead alloy from the gangue. Subsequently, the lead is removed by absorption into a cupel at about 930°C, the resultant Au-Ag bead is dissolved in HNO3 and HCI, and finally the gold concentration is determined by AAS. Apart from the usual Certificate of Analysis, the weights of Pb buttons are included in the report for additional QA/QC purposes.

PHX-02 is an ore grade method of analysis for Cu and Ag by AAS in DDH core samples, "measured" rock samples and samples where grade values are to be used for resource and reserve estimation. The analytical scope of the method includes a range of elements that could be determined from the same leach but will be specified in the sample submission forms.

The sample is digested with HCIO4, HNO3 and HCI under regulated heat to incipient dryness, followed by further heating with concentrated HCI to dissolve salts. The solution is then diluted to 100 ml in a volumetric flask. The solution is allowed to settle then the element concentration is measured in the AAS. This method follows common 3-acid digestion methods in mineral assay laboratories for ore grade determination of elements.

9.4 Quality Assurance and Quality Control (QA/QC)

Drill core samples handled in the core house and processed in the sample preparation laboratory produce pulp samples are dispatched to laboratories for assaying. Samples are sent routinely to Intertek Mcphar (Intertek), a third-party commercial laboratory based in Muntinlupa, with the official final results used in the resource database. Parallel assaying was also put into practice since resumption of drilling last March 2015, employing in-house Padcal Assay Laboratory (Padcal), for faster return of preliminary results and as additional QAQC monitoring (interlab checks).

A total of 20 dispatches for the earlier BP holes and 71 dispatches for the recent BSD holes are included in this report. This consists of a total of 620 QA/QC samples among 2917 routine samples which were dispatched to Intertek for the period. The samples were analyzed primarily for Au, Cu, and Ag. All dispatches are within the analytical quality of 10-20% QA/QC sample percentage.

QA/QC samples are anonymously incorporated among routine samples as part of the protocols and procedures instituted by Philex. For the BP holes, pulp duplicates have a frequency of 1:10, while coarse duplicates, ICS samples, and blank standards all have 1:25. Last June 2013, recommendations and internal discussions with Dr. RC Obial, a Philex consultant, modified the frequencies of inserts to improve precision and accuracy monitoring, as well as to avoid sample swaps, which were a bit frequent before 2013 but were already corrected.

The evaluation of assay results are presented as plots of MPRD[3] (Mean Percent Relative Difference) and RD[4] (Relative Difference) against time reported and metal grades. Analysis of QA/QC samples

[3] **MPRD** = (Assay value of parent sample – Assay value of duplicate sample)/ Mean assay value x 100%
[4] **RD** = (Assay value – Certified assay value)/ Certified assay value x 100%

will indicate precision and accuracy, as well as contamination, of determinations of the laboratory. Weights of lead buttons are also analyzed.

9.4.1 Duplicate Assays

Duplicate assays obtained from the pulp duplicates of routine samples are used to monitor precision of the laboratory determinations. A total of 257 pulp duplicates were assayed for the period. Most samples are within the acceptable 10% MPRD band for Cu. One low-order outlier was identified, but may be attributed to minor analysis errors of the laboratory. Overall, Intertek exhibited good precision for copper assays. No significant bias was observed.

Most Au assays are also within the acceptable 20% MPRD band for Au. All outliers are within below grade range of interest (<0.1 g/t Au). Overall, Intertek exhibited good precision for gold assays. No significant bias was observed (Figs. 21-22).

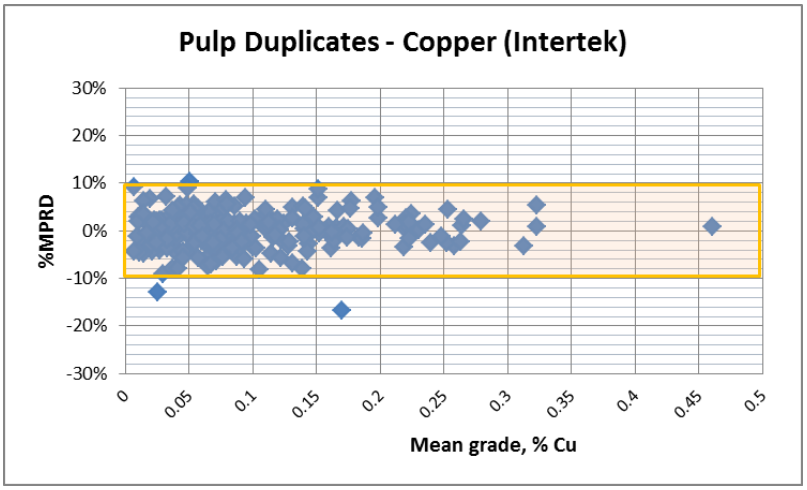

Figure 21. Cumulative QA/QC performance for pulp duplicates for Cu Assays

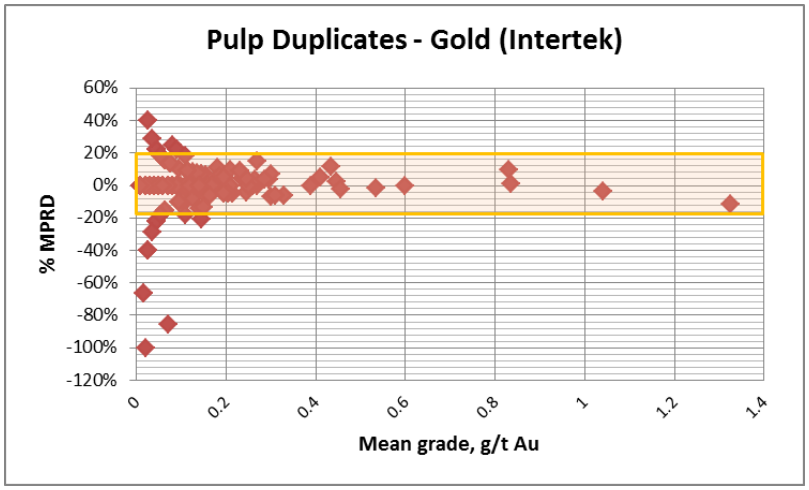

Figure 22. Cumulative QA/QC performance for pulp duplicates for Au Assays

9.4.2 Duplicate Rejects

Duplicate rejects obtained from the coarse duplicates of routine samples are also used to monitor precision, as well as repeatability, of the laboratory determinations. A total of 118 coarse duplicates were assayed for the period. Most samples are within the acceptable 10% MPRD band for copper. Two significant outliers were identified to be sample swap cases from the laboratory based on QAQC evaluation and interlab checking. One is from BP-10-3 (142.51% MPRD) and the other from BSD-11 (60.74% MPRD). Overall, Intertek exhibited good repeatability for copper assays (Fig. 23).

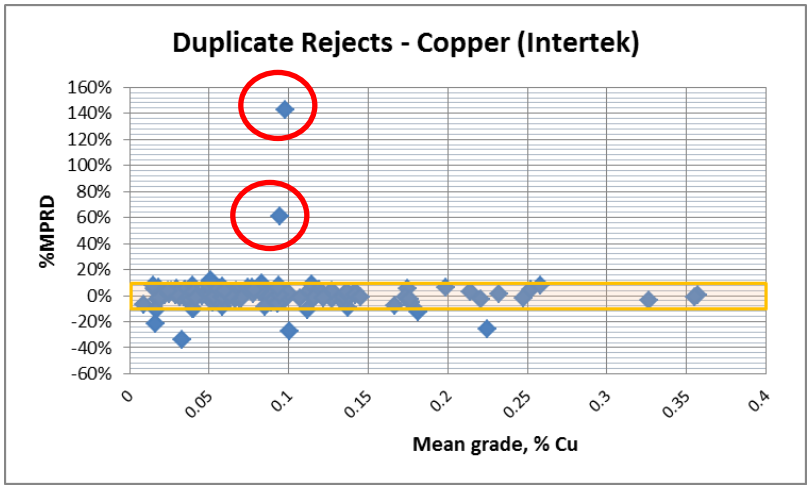

Figure 23. Cumulative QA/QC performance for coarse duplicates for Cu assays

A number of outliers were also identified in the Au assays but most are below grade range of interest. The significant outliers identified in Au assays are also the same outliers in the Cu assays, confirming the sample swap errors of the laboratory. These errors will be discussed with the laboratory. Overall, Intertek exhibited good repeatability for gold assays. This also indicates that the pulps sent to the laboratories are good representative for their sample composites, reflecting efficient sample preparation (Fig. 24).

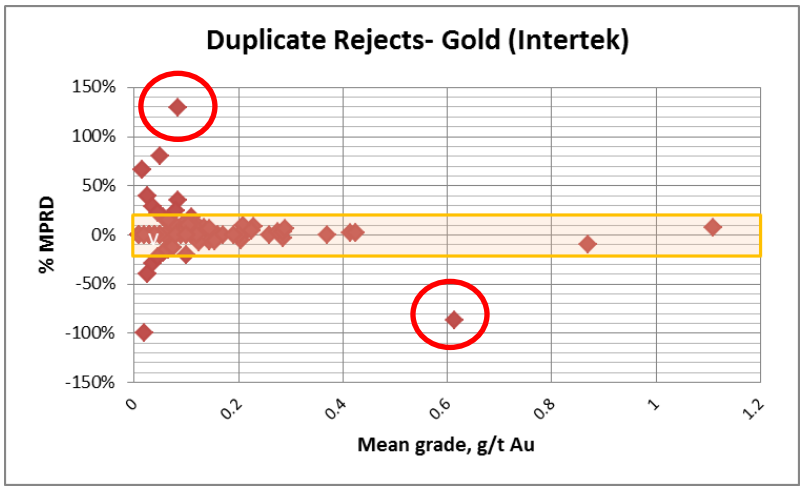

Figure 24. Cumulative QA/QC performance for coarse duplicates for Au assays

9.4.3 Blank Standards

A total of 96 blank samples were assayed for the period. Blank standards are incorporated among dispatches to monitor possible contamination in the analysis. Most samples are of the expected low grade Cu and Au grades, however 2 significant outliers were identified. A check on the QA/QC evaluation and interlab results reveal the outliers to be sample preparation errors, possibly a sample swap case. Overall, no significant contamination was identified in Intertek assays (Fig. 25).

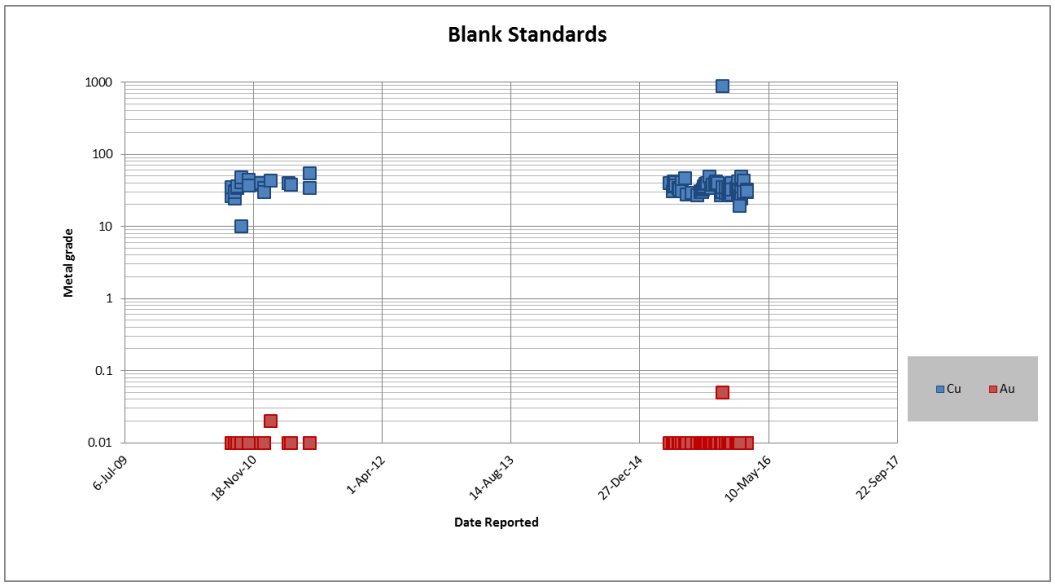

Figure 25. Cu and Au assays reported for blank standards

9.4.4 Internal Control Standards

A total of 149 ICS samples were assayed for the period. Internal Control Standards (ICS) are incorporated in dispatches to monitor accuracy of determinations. Results for most Cu and Au assays are within the acceptable RD bands. Consistent negative bias can be observed in the Cu plot but is acceptable since the predetermined Cu value is low and difficult to reproduce precisely. Based on evaluation and interlab checking, two low-order outliers (Fig. 26) were identified in the Cu assays, one due to sample preparation error (possibly sample swap) and the other, an analysis error from the laboratory, which is for further discussion.

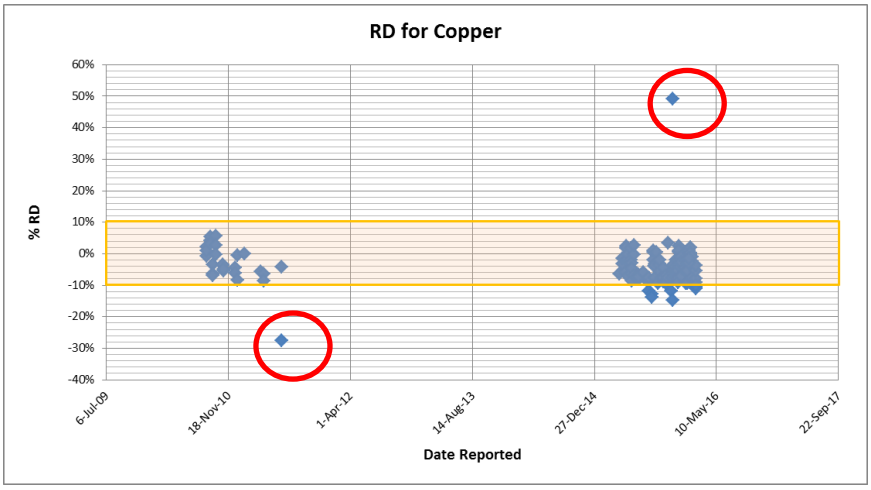

Figure 26. Cumulative QA/QC performance for ICS samples for Cu assays

On the other hand, more significant outliers were identified. Three outliers (Fig. 27) from older Au assays from the BP holes are from analysis errors from the laboratory, while there are two outliers from recent Au assays identified as a sample preparation error and an analysis error. Overall, Intertek exhibited good accuracy in its determinations.

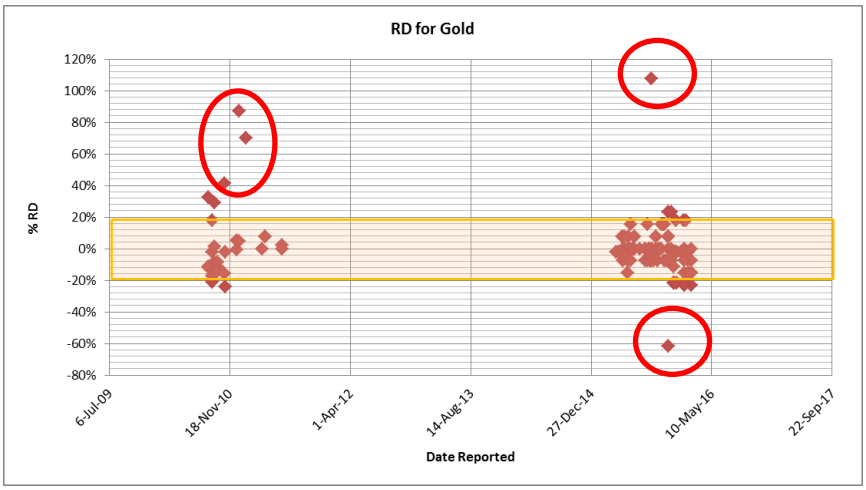

Figure 27. Cumulative QA/QC performance for ICS samples for Au assays

9.4.5 Parallel Assays (Inter-laboratory Check by In-house Assay Lab)

Parallel assaying practiced since the start of drilling last March 2015 allowed comparison of assays between Intertek and Padcal laboratory, serving as additional QA/QC check called Inter-laboratory checking. MPRD (Mean Percentage Relative Difference) between Intertek and Padcal results were obtained and used to determine the degree of precision (how close) of the results.

Cu assay results of the laboratories appear to be precise within ±20% MPRD, as exhibited by the clustering of points in Figure 28. The plot tends to be erratic below 0.05 % Cu, which is expected since lower grades tend to be more difficult to reproduce precisely. Slight positive bias was also identified with grades above 0.20% Cu, indicating Intertek having slightly greater assays in the said grade range.

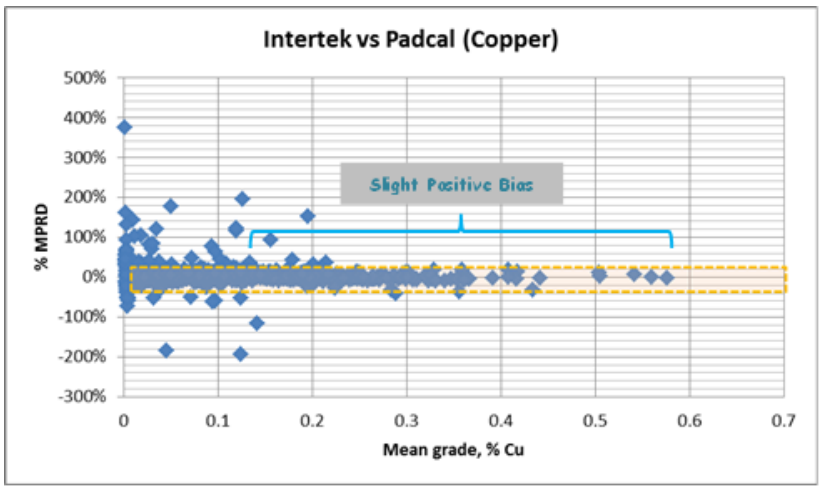

Figure 28. MPRD of Intertek and Padcal for Cu

On the other hand, Au assay results of the laboratories appear to be precise within +30% to -10% MPRD, as exhibited by the clustering of points on Figure 29. The plot also tends to be erratic below 0.05 g/t Au, However, significant positive bias was observed with grades above ~0.2 g/t Au, indicating Intertek having greater assay values for grades within range of interest.

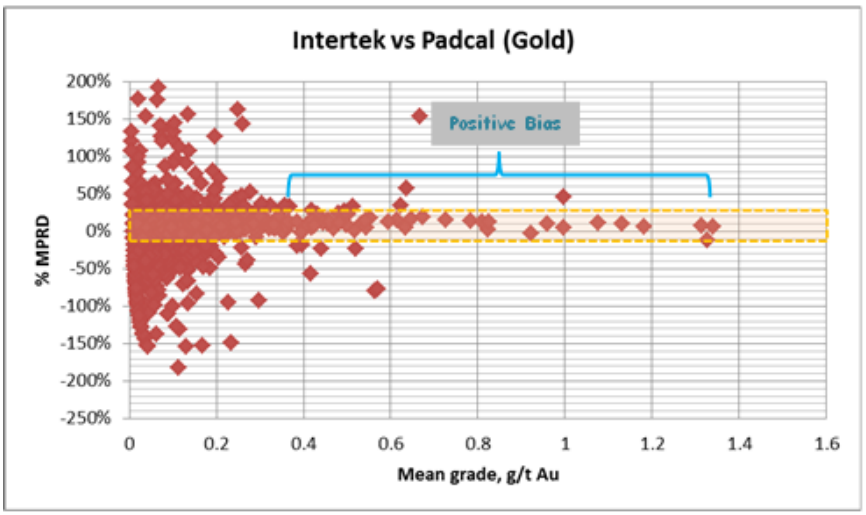

Figure 29. MPRD of Intertek and Padcal for Au

Cu is more precisely determined by the laboratories, in comparison to Au. This is due to the random errors encountered in Padcal assays, as well as the systematic bias of Padcal Au assays being lower than Intertek. Precision between Intertek and Padcal assay, as shown by the figures, is acceptable, increasing confidence in the determinations of Intertek, which provides the official data for resource estimation.

9.4.6 Lead Button Weights

The lead button weights covered in the dispatches to Intertek range from 22.76 to 58.04 grams, with a dense cluster at 30 to 52 grams (Fig. 30). The weight range of the samples is within the 30 to 50 g capacity of the cupels used by the laboratory. Samples with weights not within the cupel range may indicate that the lead may not have optimally captured the gold in the sample melt during fire assay. This might result to a possible underestimation of gold grades. A check on the Au assays of outliers and adjacent samples show no significant errors identified. One case of typo error on the Pb button data from BP assays of Intertek was identified but has been corrected by the laboratory. Overall, the plots show good clustering of points. Thus, fluxing and fire assaying was done by the laboratory satisfactorily.

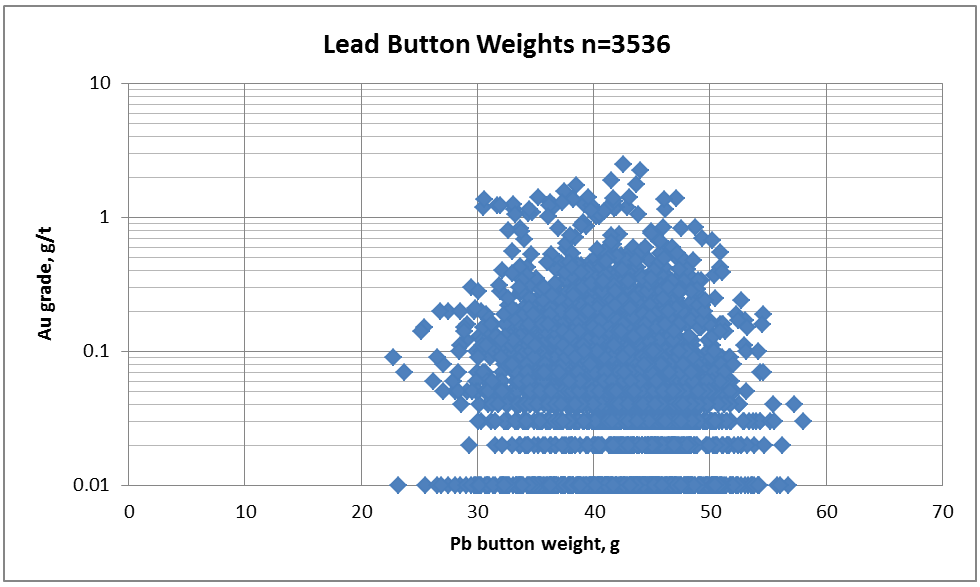

Figure 30. Lead button weights of Intertek for the period

10 MINERAL RESOURCES ESTIMATE

10.1 Summary

Philex has conducted an internal Mineral Resource Estimation (MRE) for the Bumolo porphyry Cu-Au deposit utilizing Cu-Au assay data collected as of February 01, 2016 from its ongoing resource definition drilling program. The PMRC table guideline is presented in Appendix A.

The total maiden MRE at 0.274% copper equivalent (CuEq) cut-off grade is 21.7 MT at 0.20% Cu and 0.30 g/t Au, which can be translated to in-situ contained metals of 95.7 million pounds of Cu and 0.21 million ounces of Au (Table 6). Copper equivalent calculation for Bumolo is: %CuEq = %Cu + (0.693*g/t Au) calculated based on Padcal Mine's parameters using an estimated metal prices of US$2.35/lb for copper and US$1,145/oz for gold with metal recoveries of 82% for copper and 80% for gold as of October 2015.

Table 6. Bumolo Copper-Gold Deposit Inferred Mineral Resource

Bumolo MRE at 0.274% CuEq						
Classification	**MT**	**% Cu**	**g/t Au**	**Cu Mlb**	**Au Moz**	**% CuEq**
Inferred	21.7	0.20	0.30	95.7	0.21	0.41

10.1.1 Domains

Geology domains for Bumolo were defined by creating wireframes of the interpreted geological section profiles generated from the drillhole detailed logs. For the time being, only lithological domains were considered for use in the MRE; as such, the deposit was initially subdivided into nine domains: Andesite Porphyry (AP), Clear Diorite (CD), Clear Diorite 2 (CD2), Clear Diorite Breccia (CDBX), High-grade Hydrothermal Breccia (HHBX), Inter-mineral Clear Diorite (ICD), Late Diorite Porphyry (LDP), Low-grade Hydrothermal Breccia (LHBX) and Meta-Andesite (MA).

Basic geostatistical runs using the initial nine (9) lithologies were done to test the model. However, due to limited data in some lithologies, statistical results are not well supported

and reassessment of the model was done to possibly regroup similar lithologies. The final domains used for Bumolo MRE was based on a combined geological and statistical parameters were intrusive phases and data population for each domain were put into consideration. Lithologic units with few data points were grouped with adjacent rock units of similar statistical distribution. The resulting domains were reduced to five (5) namely; Host, CD, BX, Inter Min and Post Min. Similar set of domains were also utilized for both copper and gold estimates.

10.1.2 Data Used

Total of 30 validated drillholes equivalent to 11,382 meters of core samples were used in this study. Assay values for gold and copper were assigned to each sampling interval. Specific gravity was computed for every 15 meters using the dry-water immersion test. QA/QC checks were conducted regularly and sampling errors were found to be within acceptable standards.

10.1.3 Summarized Statistics

In Bumolo, gold noticeably has higher coefficient of variation than copper, which is addressed primarily through segregation into the working estimation domains. Additional data manipulation such as compositing further reduces this value for the deposit. These methods worked particularly well across all domains suggesting that multiple distributions are substantially present in the deposit.

Visual analysis of location map of drill data points was done to arrive at a decision that declustering is not necessary due to the dispersed nature of drilling data used. Looking at the histograms within each domain, skewed distributions were observed that normalization of the data would be done to aid in variography. The histograms also suggested the lack of significant outliers, thus eliminating the need for a top cut.

10.1.4 Variography

Experimental variograms were made for both metals in all domains. Four directions were created along the XY plane for every 45 degrees and in one direction perpendicular to this plane. The sill was modeled using the down-the-hole variograms and up to two additional spherical structures were chosen for the variograms. Anisotropies were observed in almost all variograms. The resulting model variograms validated the difference in both statistical and spatial distribution within each domain.

10.1.5 Kriging

Kriging was done in a 20x20x10 block model. Each domain was treated independently and kriged in a separate grid file. Two kriging passes were done in each domain. The first pass has relatively stricter kriging parameters to ensure the quality of estimation by considering blocks that have sufficient data close enough to the block as defined by the full range of the variogram. The second pass was done to ascertain that all blocks within the limits have been estimated, regardless of their location. A top cut was assigned to blocks estimated using the second pass to avoid giving high grades to poorly-estimated extrapolated blocks.

10.1.6 Resource Classification

Drill hole spacing for assayed holes varies from around 80 by 80 meters and locally closer in central portions to around 125 by 125 meters in peripheral zones and is classified as Inferred Resources. The Bumolo Project exploration program is professionally managed and the database is acceptable for use in mineral resource estimation. Preliminary but robust geological and resource domains of the Bumolo deposit are defined and found suitable for the maiden MRE. There is continuity for both the copper and gold grades within the established domains with low nugget effects and large ranges. The QA-QC programs and core logging procedures follow the best industry practice and generally exceed commonly accepted standards. The copper and gold grades are estimated using Ordinary Kriging interpolation method as the mineralization is relatively homogenous. The Competent Person believes that the methodology used in the MRE is appropriate and that the result will have accuracy suitable for the intended mining method.

Further petrographic and mineragraphic studies, however, are still in progress to support the in-depth geological understanding on the nature of mineralization and the domains used in the estimation. More detailed exploration through closely-spaced drilling aims to develop a more robust geological model and possibly upgrade the mineral resource to Indicated category.

10.2 Objective

This report aims to outline the process employed to arrive at the resource estimate for the Bumolo Project. Tonnage and grade are the block characteristics that were computed at this resource estimation run. Ordinary kriging was performed for every domain to compute for block grades. On the other hand, tonnage was computed per block based on the assigned specific gravity and block volume. Classification was pegged at the Inferred category due to the generally low confidence in the current geological knowledge and mineralization continuity in the area.

10.3 Domains

The deposit has been subdivided into various lithological types that were eventually combined to obtain a statistically homogenized domain for the resource estimation. Domain classification details are discussed below.

10.3.1 3D Modeling

Creation of 3D models was done to limit the estimation into volumes or domains that are geostatistically similar. For this estimation run, the approach was to build a series of geological models representing the different intrusive phases and group those that are geologically and statistically associated to finally arrive at statistically robust domains.

The geologic solids were created using cross sections (100-meter spacing) and level plans (50-meter spacing) across the deposit. Project geologists manually interpreted and delineated the boundaries of the domains before doing computer-assisted digitization in Geosoft Oasis Montaj and AutoCAD v2015. The solid modeling was finally generated in Leapfrog Geo v3.1. Validation of generated solids was done in GEMS v6.7 through physical checking of triangulation errors and visual assessment of contacts. Final “cleaned” solids were then used in the resource estimation.

10.3.2 Concept of Homogeneous Domains

Domains (also called solids or wireframes) are three-dimensional spatial entities that subdivide a deposit into various solids/zones based on the geologic feature(s) (e.g. lithology, alteration, ore type, structure, etc.) that control(s) or characterize(s) mineralization. Ideally, only one type of material exists within each domain ('physical continuity') and therefore, only one distribution is considered ('statistical continuity'). Most estimation methods are intended to be used on homogeneous domains assuming unimodality and certain predictability within that distribution. Multiple distributions require consideration of methodologies as correlation and data segregation, which creates additional complexity and grounds for error. In practice, a perfectly homogeneous domain cannot exist in reality; however, the more similar the material is inside a domain, the better the estimation methods used in this resource estimation will work.

10.3.3 Bumolo Geologic Domains

Geology domains for Bumolo were defined by creating wireframes based on flagged rock types within the drill data (Fig. 31). At this time of reporting, only lithological domains were deemed acceptable for use; as such, the deposit was subdivided into nine domains (Figure 30): andesite porphyry (AP), Clear Diorite (CD), Clear Diorite 2 (CD2), Clear Diorite Breccia (CDBX), High-grade Hydrothermal Breccia (HHBX), Inter-mineral Clear Diorite (ICD), Late Diorite Porphyry (LDP), Low-grade Hydrothermal Breccia (LHBX) and Meta-Andesite (MA). Future resource estimates will explore the validity of alteration, ore type and structure as possible estimation domains.

10.3.3.1 Andesite Porphyry (AP)

This rock unit was observed only on underground BP holes and is modeled in the lower central portions of the Bumolo deposit. Interpreted as one of the young intrusives, AP is generally unmineralized and has soft boundaries with adjacent LDP lithology in terms of statistics.

10.3.3.2 Clear Diorite (CD)

Being the main mineralized intrusive, CD dominates the middle to northern part of the deposit, with its single root found to the northwest. Due to dense drilling data, it was decided to be treated as a single domain. Statistically, it has soft boundaries only with the CDBX that it encloses.

10.3.3.3 Clear Diorite 2 (CD2)

CD2 is a barren intrusive that is part of the late mineralization phase to the south of the deposit. With the very few drilling data, soft boundaries are present between this and adjacent LHBX and MA units statistics-wise.

10.3.3.4 Clear Diorite Breccia (CDBX)

This breccia body is found in the northern portion of the much larger CD unit. It has quite few drilling data whose grades are greatly influenced by the CD unit surrounding it.

10.3.3.5 High-grade Hydrothermal Breccia (HHBX)

Located to the south of ICD and CD units, HHBX has been intersected by significant drilling density that merits treatment as a single domain. Although the distinctly elevated grades can be explained by association with adjacent lithologies, hard boundaries are notable statistically and lithologically.

10.3.3.6 Inter-mineral Clear Diorite (ICD)

ICD is a medium-sized body at the center of the deposit that is contiguous with CD to the north and HHBX to the south. It is part of the late mineralization suite and has noticeable hard boundaries with adjacent lithologies.

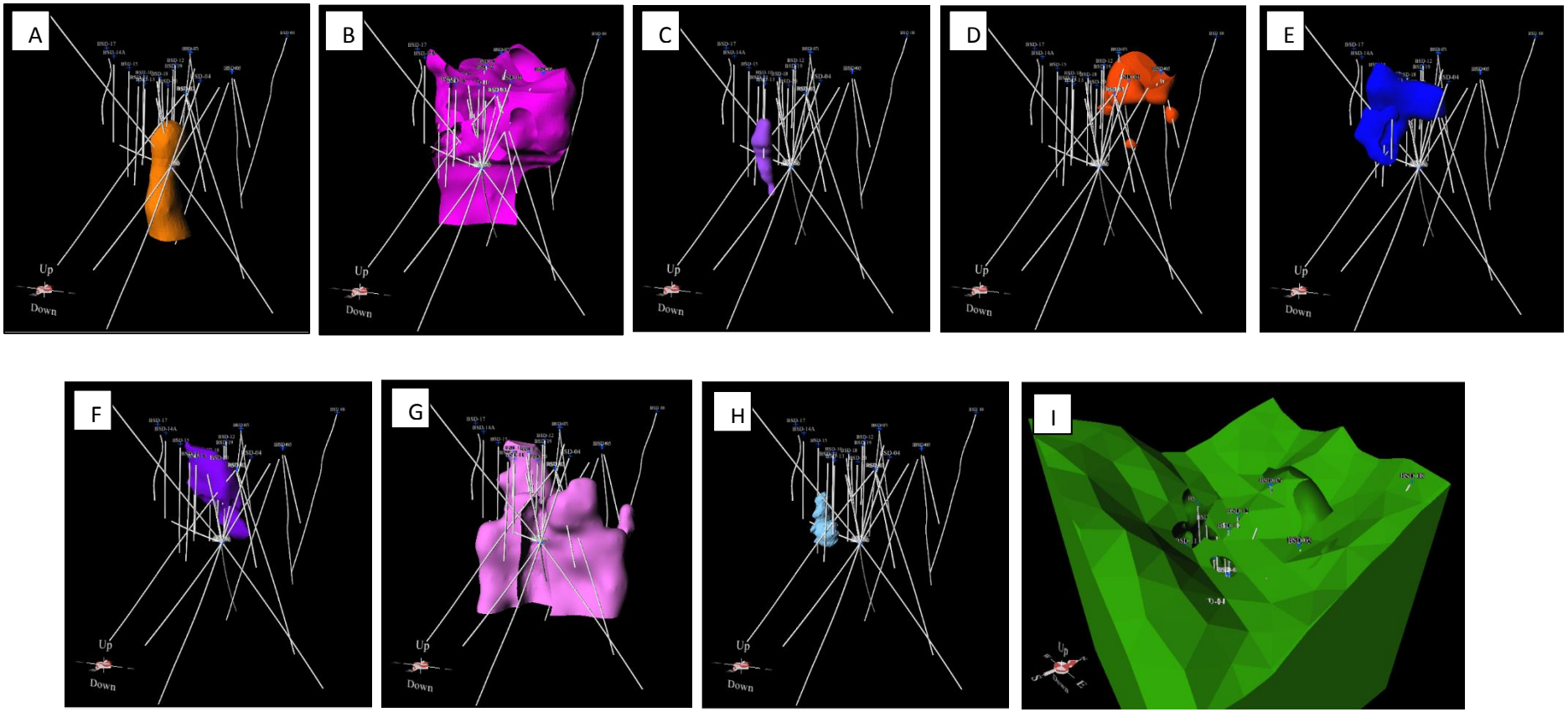

Figure 31. Generated lithologic solids for Bumolo: A) AP, B) CD, C) CD2, D) CDBX, E) HHBX, F) ICD, G) LDP, H) LHBX and I) MA.

10.3.3.7 Late Diorite Porphyry (LDP)

Also a late mineralization intrusive, LDP almost surrounds the deeper portions of CD and is basically weakly mineralized. It has hard boundaries with adjacent CD based on statistical and lithologic observation.

10.3.3.8 Low-grade Hydrothermal Breccia (LHBX)

This occurs as two relatively small pockets to the west of the area and is located adjacent to LDP and CD. It has very few drilling data and quite similar statistical and lithological association with LDP, which merits lumping into one domain.

10.3.3.9 Meta-andesite (MA)

Meta-andesite constitutes the pre-mineralization basement rock of the deposit. It is generally un-mineralized except along contacts with other highly mineralized domains. Drilling density falls off rapidly as it moved further away from the deposit and, as such, this domain is treated as strictly background.

10.3.3.10 Bumolo Estimation Domains

Final estimation domains for Bumolo were identified based on intrusive phases (Table 7). Lithologic units with few data points were grouped with neighbouring rock units of similar lithologic character and statistical distribution. MA and HHBX domains were treated as a single domain, only with corresponding change in naming. Similar set of domains was utilized for both copper and gold.

Table 7. Final estimation domains for Bumolo

Estimation domains	Lithologic domains	Basis
Host	MA	
CD	CD, CDBX	Too few data points in CDBX; similar statistical distribution and close spatial location of CDBX and CD.
BX	HHBX	
Inter Min	CD2, ICD	Too few data points in CD2; similar statistical distribution and close spatial location of CD2 and ICD.
Post Min	AP, LDP, LHBX	Similar statistical distribution and close spatial location of AP and LDP; too few data points in LHBX.

10.4 Mineral Resource Database

The drillhole data cut-off used in the MRE is February 01, 2016. It is consists of 30 validated drillholes equivalent to 11,382 meters of drill cores including meters drilled from ten (10) underground drillholes (BP holes) in the previous drilling campaign. Assayed core samples represent the 3,053 data points with values for both gold and copper grades.

The database used was exported from AcQuire™ software in csv (comma-separated variable) format (Table 8). These files contain the drill hole data used for mineral resource estimation and domain creation, as follows:

Table 8. Drillhole Database Used

File Name	Data Imported
BP_BSD_collar_20160201	Hole ID, Easting, Northing, RL, End of hole, Dip, Azimuth
BP_BSD_survey_20160201	Hole ID, Dip, Azimuth, Depth
BP_BSD_assay-litho-alt_20160201	Hole ID, From, To, pct Cu, g/t Au, Rock type, Alteration
BP_BSD_SG_20160201	Hole ID, From, To, SG

The CP has decided to include in this resource run the analytical results from the early underground (BP) drilling campaign despite the absence of down-the-hole survey. Further stringent and systematic QA-QC protocol implemented by Philex in the analysis of drill core samples warrants acceptable database inclusion for resource estimation.

10.5 Exploratory Data Analysis

10.5.1 Initial Data Statistics and Analysis

Gold and copper grades are the focus of analyses in this section of the report. Using the wireframes created earlier, data points were segregated into their respective domains. A data point within a wireframe was flagged as part of that domain along with all other points inside. The simple statistics of the raw data is presented in Tables 9-10.

Table 9. Raw drillhole stats for gold by lithologic domain

Bumolo Raw Ddh Stats by Lithologic Domains						
g/t Au						
	Host	CD	BX	Inter Min	Post Min	Total
Number of samples	620	675	302	277	845	2719
Minimum value	0.01	0.01	0.01	0.01	0.01	0.01
Maximum value	1.24	1.24	1.38	0.59	0.47	1.40
Mean	**0.07**	**0.16**	**0.22**	**0.09**	**0.07**	**0.10**
Standard Deviation	0.13	0.16	0.22	0.06	0.06	0.13
Variance	0.02	0.02	0.05	0.00	0.00	0.02
Coefficient of variation	1.85	0.96	1.00	0.72	0.81	1.31

Table 10. Raw drillhole stats for copper by lithologic domain

Bumolo Raw Ddh Stats by Lithologic Domains						
% Cu						
	Host	CD	BX	Inter Min	Post Min	Total
Number of samples	620	675	302	277	845	2719
Minimum value	0.00	0.01	0.04	0.01	0.00	0.00
Maximum value	0.35	0.53	0.57	0.28	0.28	0.57
Mean	**0.06**	**0.12**	**0.18**	**0.08**	**0.07**	**0.09**
Standard Deviation	0.06	0.07	0.11	0.04	0.05	0.07
Variance	0.00	0.01	0.01	0.00	0.00	0.01
Coefficient of variation	0.93	0.59	0.59	0.55	0.70	0.83

10.5.2 Sample Spacing

Sample spacing varies depending on the domain. In both enriched zones, samples are 30m apart, on average. In the oxide zones, samples are, on average, 55m to 60m apart. In the early mineralized domains, samples are, on average, 35m apart. In the primary and mixed host, samples are, on average, 85m apart. There is preferential drilling in the areas of greater interest which is expected of exploratory drill data.

10.5.3 Compositing

Since the estimation method does not use a weighting system based on the length of samples, it is possible that bias is created when extreme grades represent a relatively small amount of material compared to the other samples. In an attempt to negate the effects of this bias introduced by samples of varying length, data points are composited to a uniform length. Compositing also reduces human errors in assaying samples. Raw data has been composited to 3-meter lengths and all composites below one (1) meter were discarded. Presented in Table 11-12 are the statistics of domained and global composites for copper and gold.

Table 11. Composite drillhole stats for gold by lithologic domain

Bumolo 3m Composite Stats by Lithologic Domains						
g/t Au						
	Host	CD	BX	Inter Min	Post Min	Total
Number of samples	571	639	281	248	816	2555
Minimum value	0.01	0.01	0.01	0.01	0.01	0.01
Maximum value	1.24	1.24	1.37	0.59	0.47	1.40
Mean	**0.07**	**0.16**	**0.23**	**0.09**	**0.07**	**0.10**
Standard Deviation	0.12	0.14	0.23	0.06	0.06	0.13
Variance	0.01	0.02	0.05	0.00	0.00	0.02
Coefficient of variation	1.72	0.92	1.00	0.72	0.79	1.29

Table 12. Composite drillhole stats for copper by lithologic domain

Bumolo 3m Composite Stats by Lithologic Domains						
% Cu						
	Host	CD	BX	Inter Min	Post Min	Total
Number of samples	571	639	281	248	816	2555
Minimum value	0.00	0.01	0.04	0.01	0.00	0.00
Maximum value	0.35	0.53	0.56	0.28	0.28	0.56
Mean	**0.06**	**0.12**	**0.18**	**0.08**	**0.07**	**0.09**
Standard Deviation	0.05	0.07	0.11	0.04	0.05	0.07
Variance	0.00	0.00	0.01	0.00	0.00	0.01
Coefficient of variation	0.91	0.58	0.60	0.54	0.69	0.82

After compositing, there was generally ~6% decrease in the total number of samples as a result of significant number of raw drillhole points with <3 meter sampling length (~6%; 164 out of 2719). There is totally no change in the deposit-wide mean for both metals. The coefficients of variations after compositing are expectedly lower due to volume-variance effect. The results mentioned above are to be expected of proper compositing because man-made errors are reduced when data is composited.

Tables 11-12 of composited drillhole data shows that the means of the different domains vary to around double the mean of unsegregated data suggesting that multiple distributions are present in the entire deposit. Also noteworthy is the reduction in the coefficient of variation after compositing for almost all domains, which is also a sign of multiple distributions segregated through the domains used.

10.5.4 Declustering

Unlike kriging which takes into account the increased number of data points in the areas of interest, variography prefers an evenly-spaced drilling grid to better model changes in grades over an entire domain given certain distances. Shown in Figure 32 are base maps of the data available per domain.

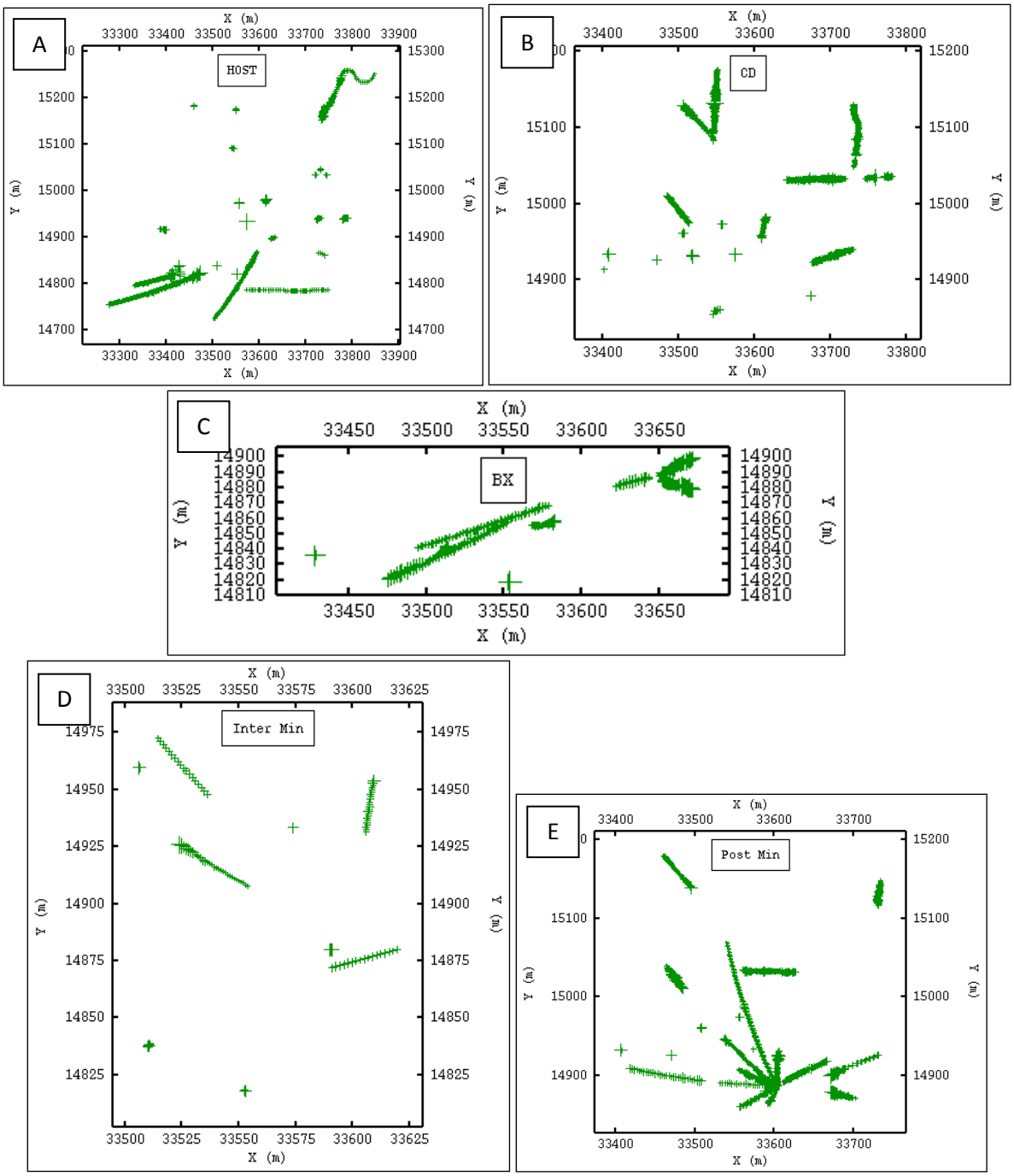

Figure 32. Plan maps showing drill data distribution per domain: A) Host, B) CD, C) BX, D) Inter Min and E) Post Min.

The base maps suggest that there is generally no clustering of data observed per domain as it is still in the early stages of resource definition drilling. With this, variogram modeling was seen to be more objective due to its significant dependence on drilling data density and will tend to be more efficient in well-sampled portions. In the opinion of the estimator, declustering is not warranted at this point. Also, as each domain is assumed to be homogeneous, declustering is not as critical since the resulting distribution should remain the same.

10.5.5 Treatment of Grade Outliers

Special care should be taken when deciding whether high-grade values are part of the distribution or outliers in each domain data set. Histograms were looked at to identify potential outliers and to plan how to deal with these specific points. Spatial analysis of the high-grade data points was also done to ensure that the presumed outlier is significantly different from data points adjacent to it. The analysis of these outliers will greatly affect how they are handled during the estimation process.

No correction for outliers was done in this part of data analysis. As seen in the histograms in Figures 33 and 34, high-grade samples are part of the distribution as the right-end tail extends to sizable distances for some domains.

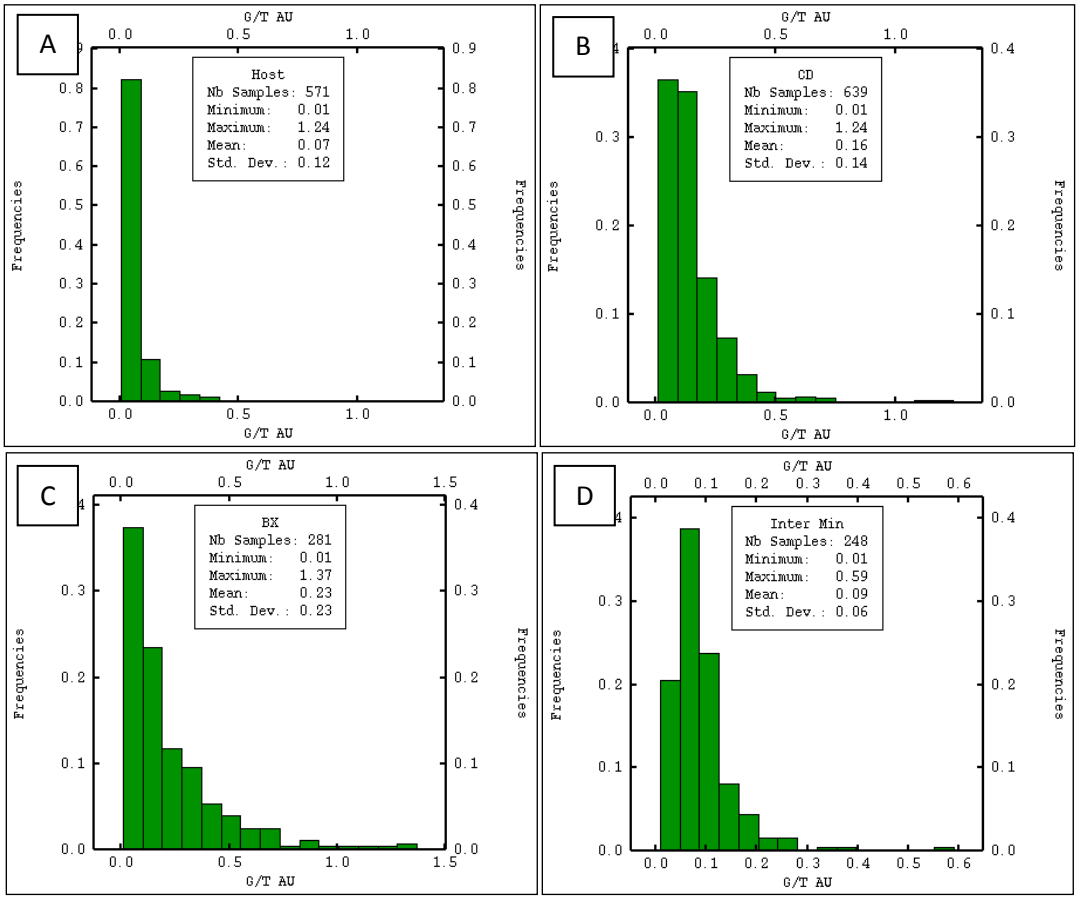

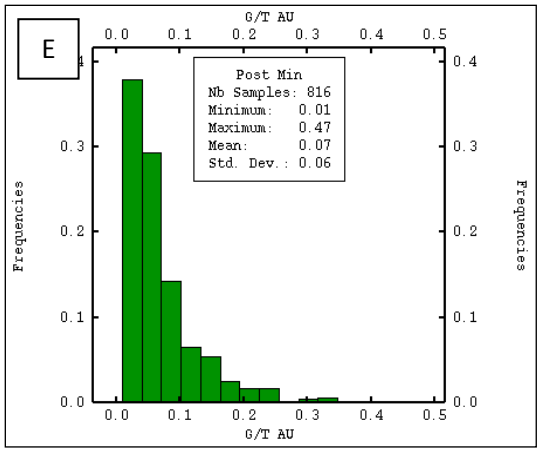

Figure 33. Histograms for gold grades per domain: A) Host, B) CD, C) BX, D) Inter Min and E) Post Min.

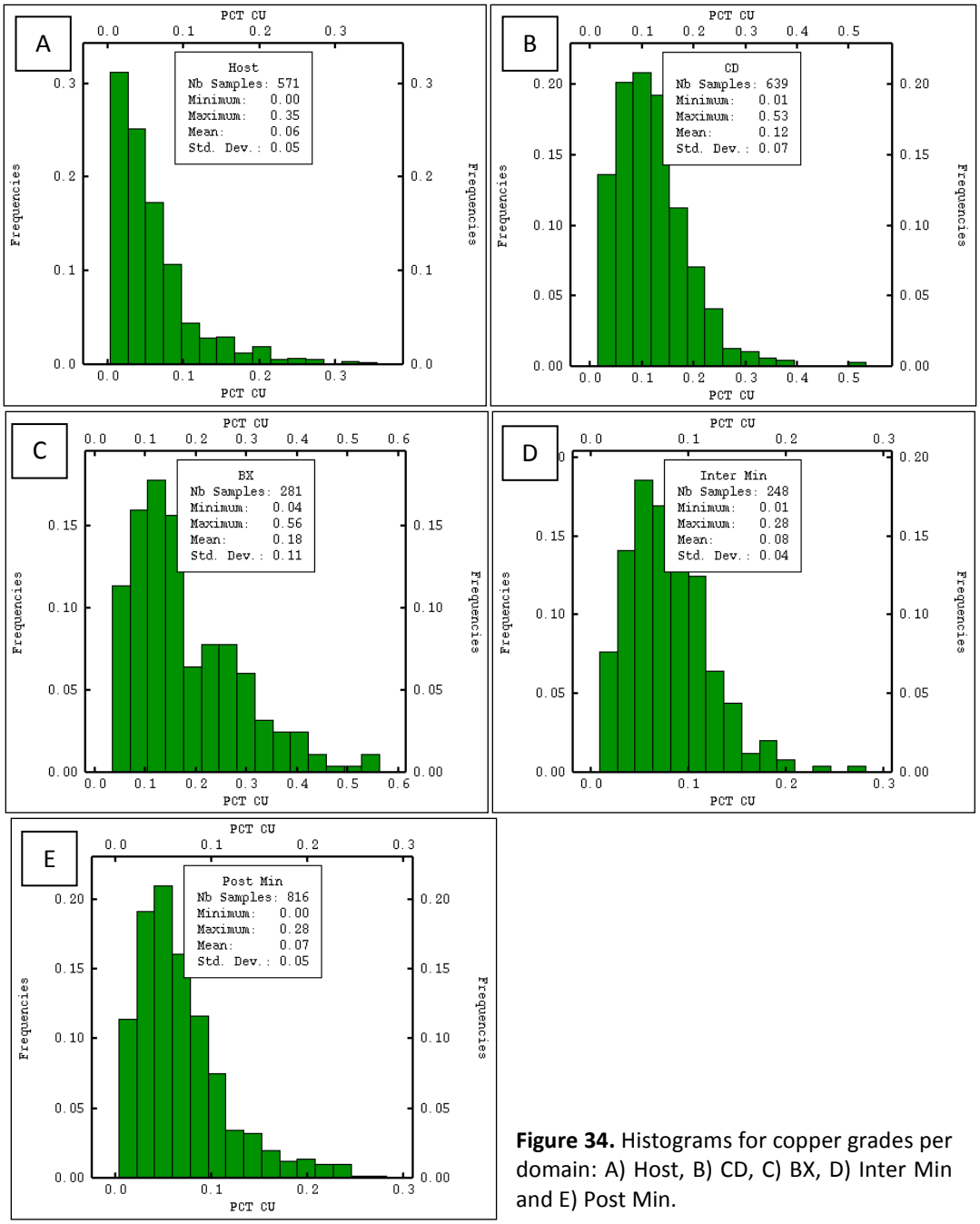

Figure 34. Histograms for copper grades per domain: A) Host, B) CD, C) BX, D) Inter Min and E) Post Min.

10.5.6 Data Normalization

Similar to most mathematical formula, variography and kriging work best with normalized data. The log-normal nature of geologic data and the linear computation of the two mentioned processes tend to incur potential bias towards isolated high-grade points in the resulting estimation. In variography, the simple solution to this bias is the normalization of data. For actual kriging, multiple passes will have to be done to ensure isolated high-grade points do not influence farther than the geologic interpretation.

Gaussian anamorphosis is done as a way of managing skewed grade distributions of data points in each domain. Given that the grade distributions are skewed to the left and the variograms follow linear computation, much importance is not given to changes near zero; thus, changes in grades far to the right of zero are over-valued. If this holds, normalizing the data allows the original variogram to work more efficiently in determining the correlation of two points given their distance. This transforms the data to the normal curve but does not change the order of data with respect to increasing grades.

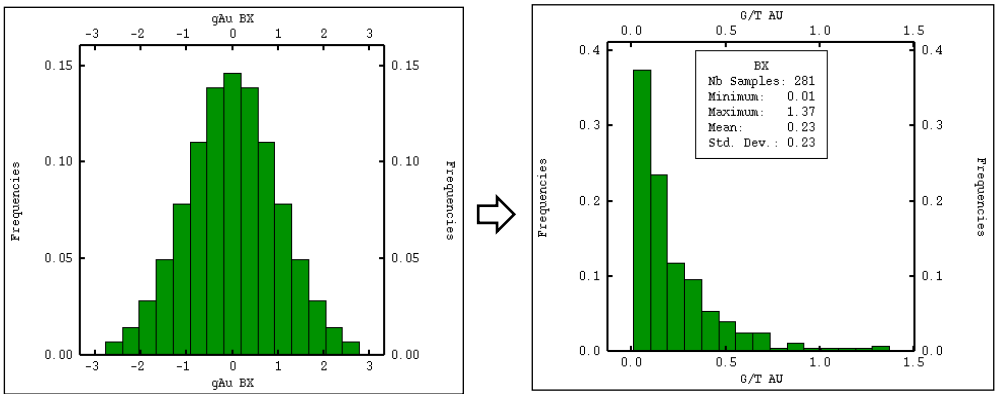

Figure 35. Data transformation through Gaussian normalization

As seen in the histogram for gold grades inside the BX domain (Figure 35), half of the data points fall into the first three (3) bars, which are arguably just as important as the other half of the data set in variogram computation. With the variogram working only with absolute grade differences, lesser weight is placed on these points as the difference between the lowest grade to the mean is only ~0.2 compared to the difference between the mean to the highest grade of more than 1.0. Normal transformation attempts to remedy this condition by spreading out the lower half of the distribution, which allows the variogram to give more weight to numbers closer to zero.

10.6 Variography

Variography was performed independently on the Gaussian-transformed data in each domain for both metals. All instances of the word variogram(s) mentioned here, unless otherwise stated, also refer to the semi-variogram(s).

10.6.1 Variogram Creation

Data was flagged into the respective domains depending on which wireframe encases them. Variogram maps (Figure 36A) were then constructed on the XY plane to assist in determining the dominant direction of continuity.

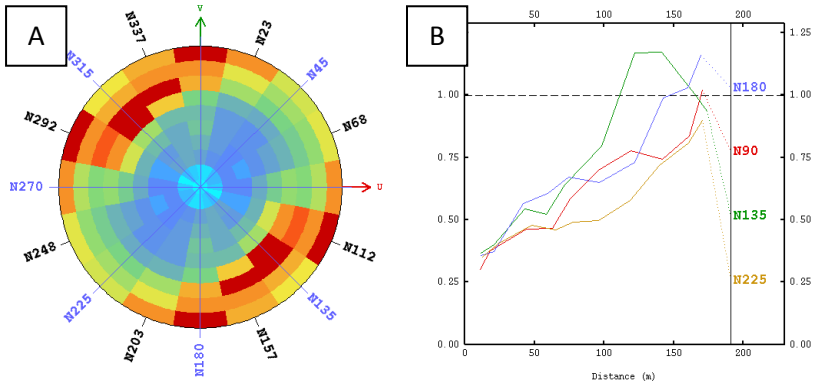

Figure 36. Example of A) variogram map and (B) variogram

Four (4) experimental variograms (Figure 35B) were created on the XY plane, with the first direction made parallel to the major direction while three others made for every 45°. These experimental variograms have 10 lags in each direction with 30-meter lag distance. Lag tolerance of 15 meters was allowed when considering two points for variogram calculations while a 22.5° angular tolerance was set when checking if two points are along the same direction. Slicing height of 100 meters was used for points with a different Z value.

A fifth experimental variogram was created perpendicular to the XY plane, which is referred to as the down-the-hole variogram as it is calculated along the drill lines. This variogram has 300 lags with 1-meter distance per lag. A 0.5-meter lag tolerance was allowed when considering two points for variogram computations. Angular tolerance of 90° was used when checking if two points lie along the correct direction.

Model variograms were then created based on the experimental variograms. These contain one nugget structure and two spherical structures. Anisotropies are expected in these models; thus, three directions were created based on the five experimental variograms. These model variograms were then back-transformed to represent the untransformed (or raw) composited data in the respective domains.

The table below (Table 13) presents the complete parameters arrived at during the variogram modeling for both gold and copper metals. Figures 37-54 show all modelled experimental and back-transformed variograms per domain for both metals.

Table 13. Summary of gold and copper variograms

Bumolo Variogram Parameters										
Domain	Host		CD		BX		Inter Min		Post Min	
Element	Au	Cu	Au	Cu	Au	Cu	Au	Cu	Au	Cu
Major Direction (°)	45	0/90	135	0	Isotropic	Isotropic	45	Isotropic	0	0/90
Semi Direction (°)	135	0/90	45	90	Isotropic	Isotropic	135	Isotropic	90	0/90
Minor Direction (°)	D-90	D-90	D-90	D-90	Isotropic	Isotropic	D-90	Isotropic	D-90	D-90
Nugget	0.0025	0.00039	0.004	0.001	0.007	0.0019	0.0009	0.0004	0.0004	0.0003
Sill 1	0.0047	0.00125	0.0058	0.0011	0.0205	0.0041	0.0031	0.0014	0.0015	0.00065
Range Major 1	55	120	20	30	80	60	40	50	50	30
Range Semi 1	40	120	50	30	80	60	30	50	60	20
Range Minor 1	50	120	30	30	80	60	45	50	25	15
Sill 2	0.0062	0.00123	0.0104	0.0027	0.023	0.0052	---	---	0.0012	0.0013
Range Major 2	160	160	200	150	100	80	---	---	160	120
Range Intermediate 2	90	160	155	120	100	80	---	---	105	120
Range Minor 2	120	130	95	80	100	80	---	---	115	120

10.6.2 Gold Variograms

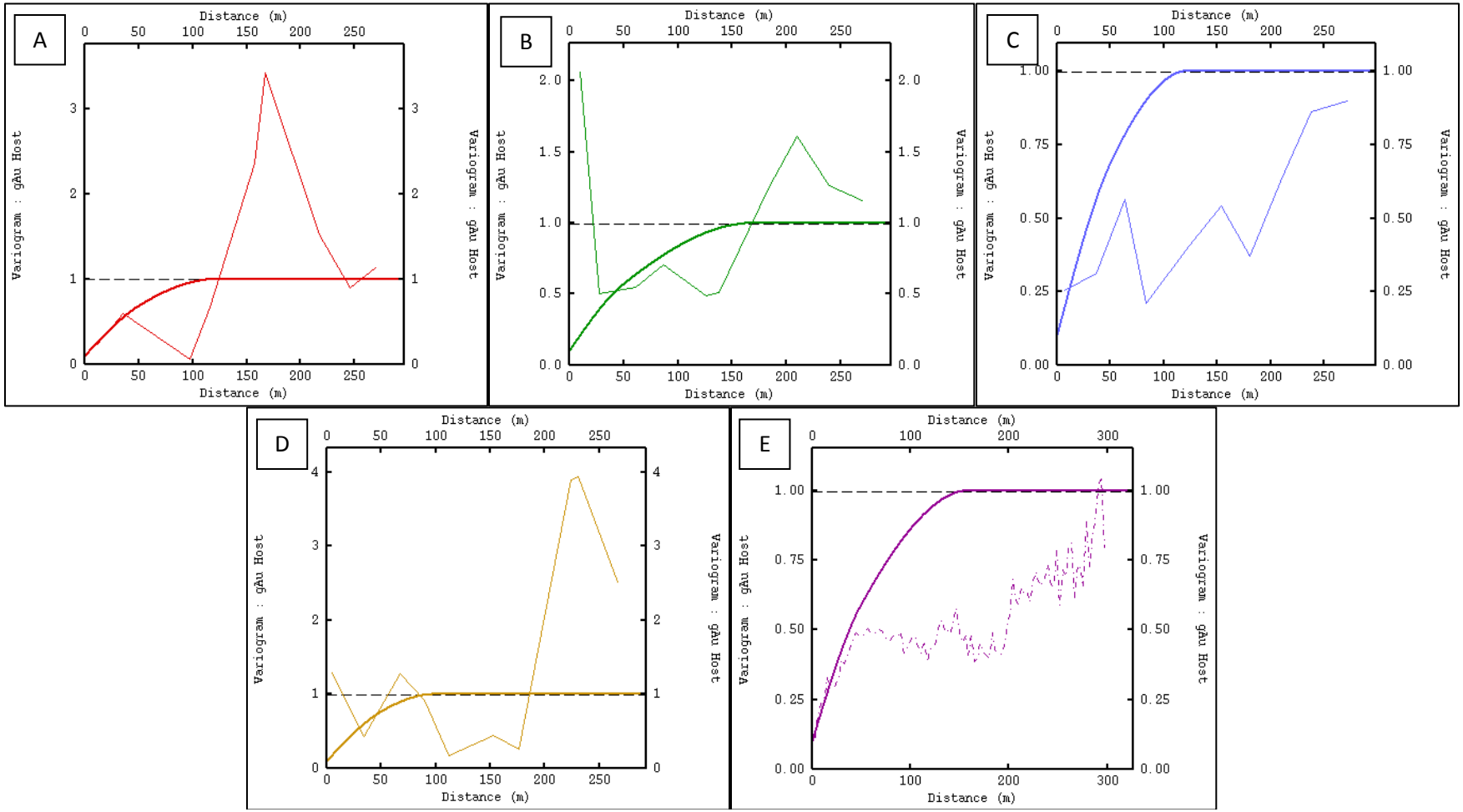

Figure 37. Host experimental variograms with modeled variograms for gold along various directions: A) 0°, B) 45°, C) 90°, D) 135° and E) D-90°

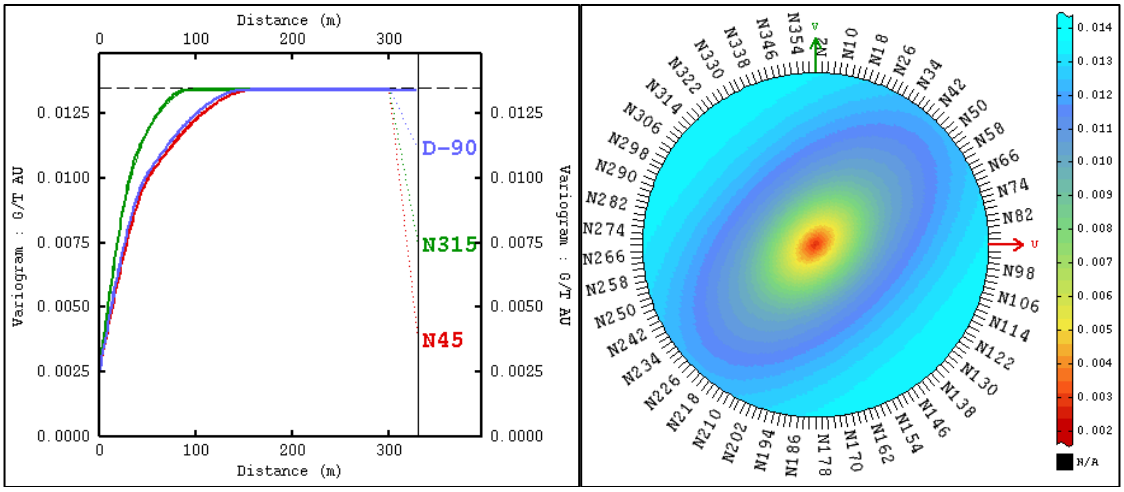

Figure 38. Host back-transformed variograms for gold

For the experimental variograms, the first data point in the N45 and N135 directions was not strictly modeled due to its impractical effect on the entire model and the low number of pairs that it represents. The back-transformed variograms showed relatively short ranges, which imply less smoothing in the kriging process. The N45 and D-90 directions have almost the same ranges on both first and second spherical structures.

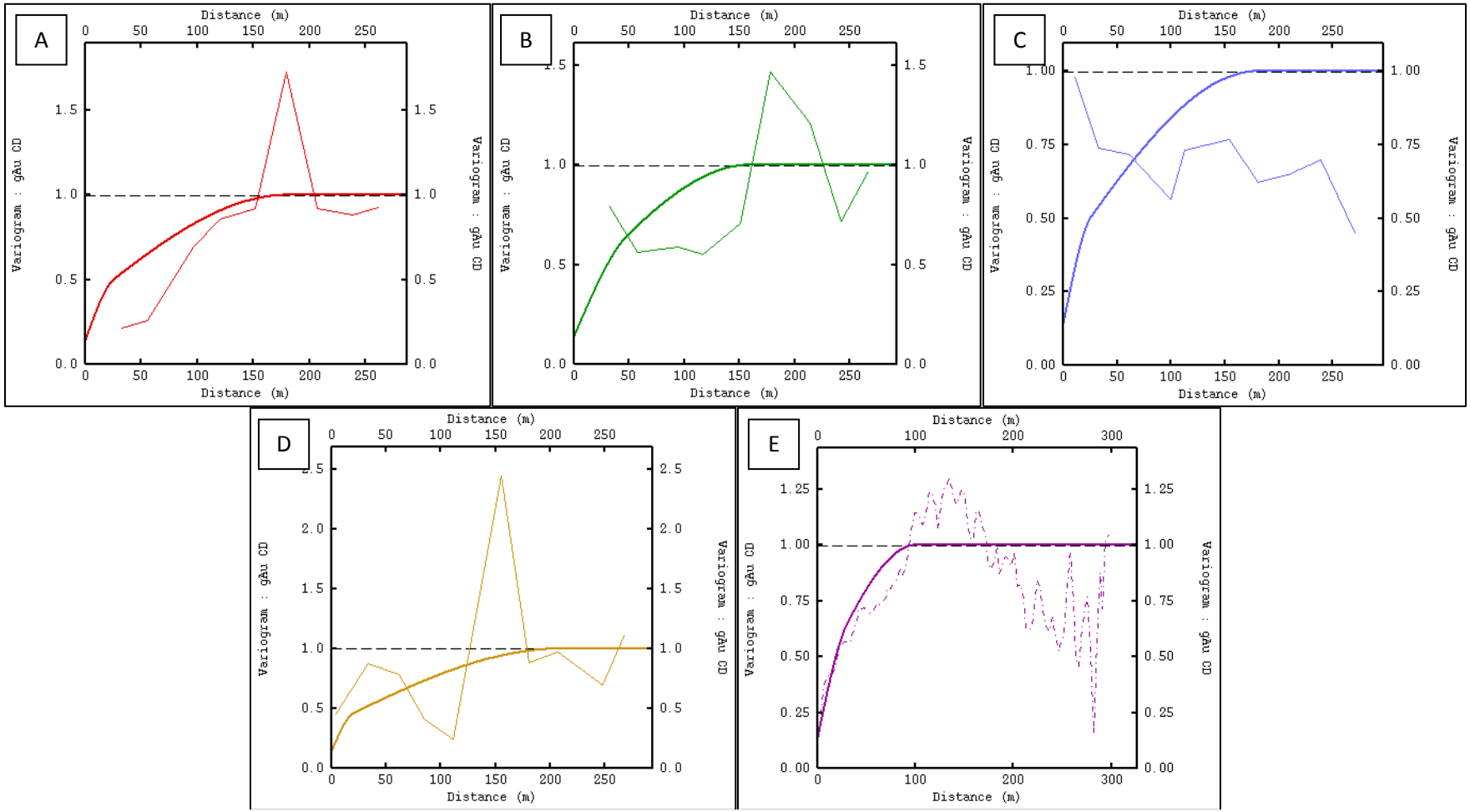

Figure 39. CD experimental variograms with modeled variograms for gold along various directions: A) 0°, B) 45°, C) 90°, D) 135° and E) D-90°

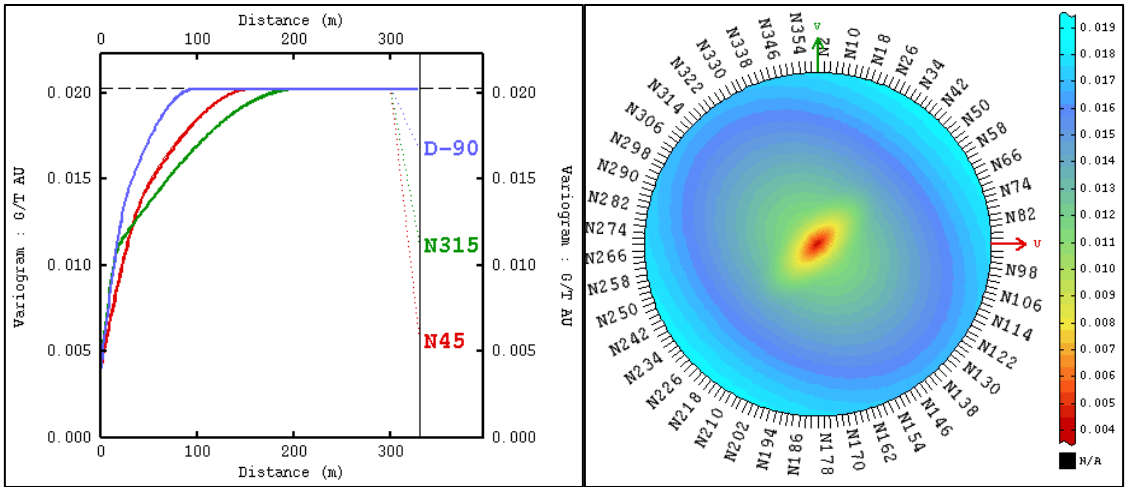

Figure 40. CD back-transformed variograms for gold

For the experimental variograms, the first data point in the N45 and N90 directions was not strictly modeled due to its impractical effect on the entire model and the low number of pairs that it represents. The N315 direction has the longest range on the second spherical structure compared to other directions. The D-90 direction has notable short range, which makes the data directly above or below the block to have little effect on the estimate.

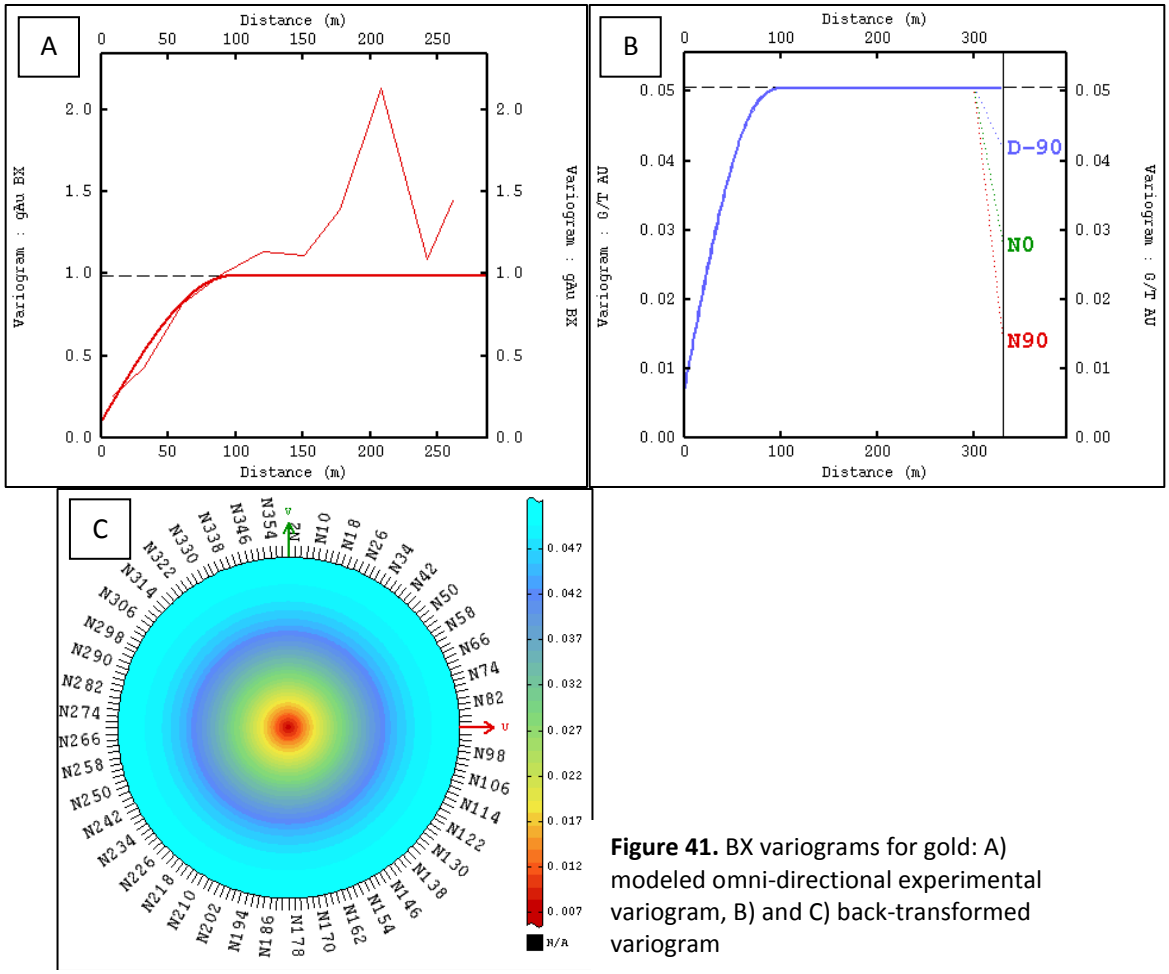

Figure 41. BX variograms for gold: A) modeled omni-directional experimental variogram, B) and C) back-transformed variogram

Experimental variograms were modeled under omnidirectional condition as data points are too few to warrant directional variogram modeling. With this, the back-transformed variogram has relatively short range, which implies less smoothing in the kriging process across all directions.

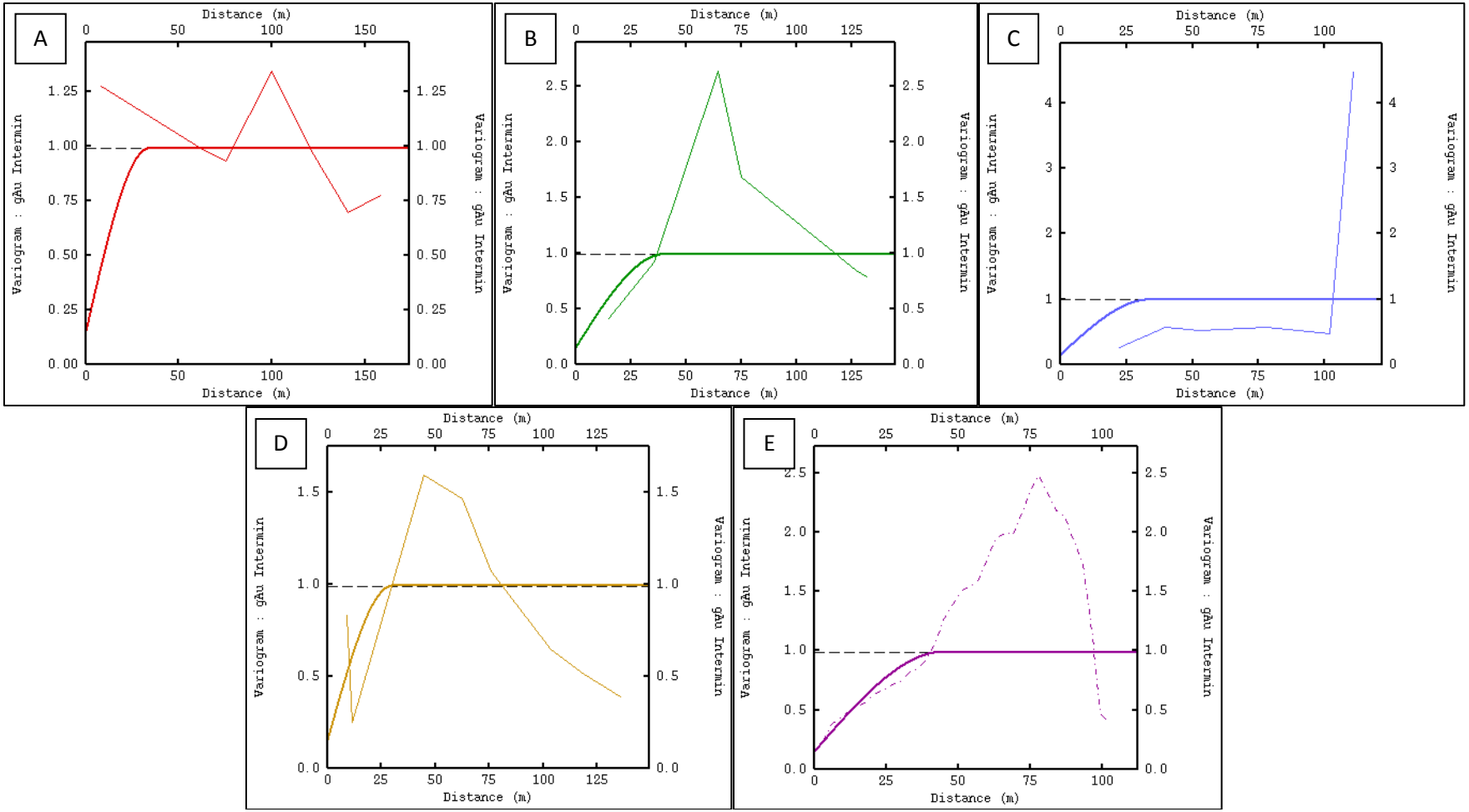

Figure 42. Inter Min experimental variograms with modeled variograms for gold along various directions: A) 0°, B) 45°, C) 90°, D) 135° and E) D-90°

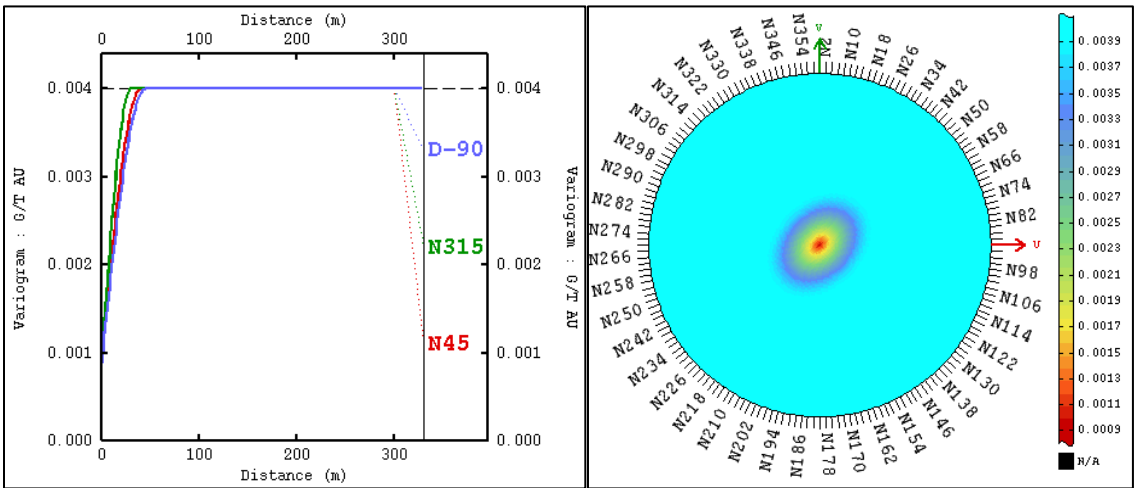

Figure 43. Inter Min back-transformed variograms for gold.

For the experimental variograms, the first data point in the N0 and N135 directions was not strictly modeled due to its impractical effect on the entire model and the low number of pairs that it represents. The back-transformed variograms showed notably short ranges on both first and second spherical structures, which imply less smoothing in the kriging process.

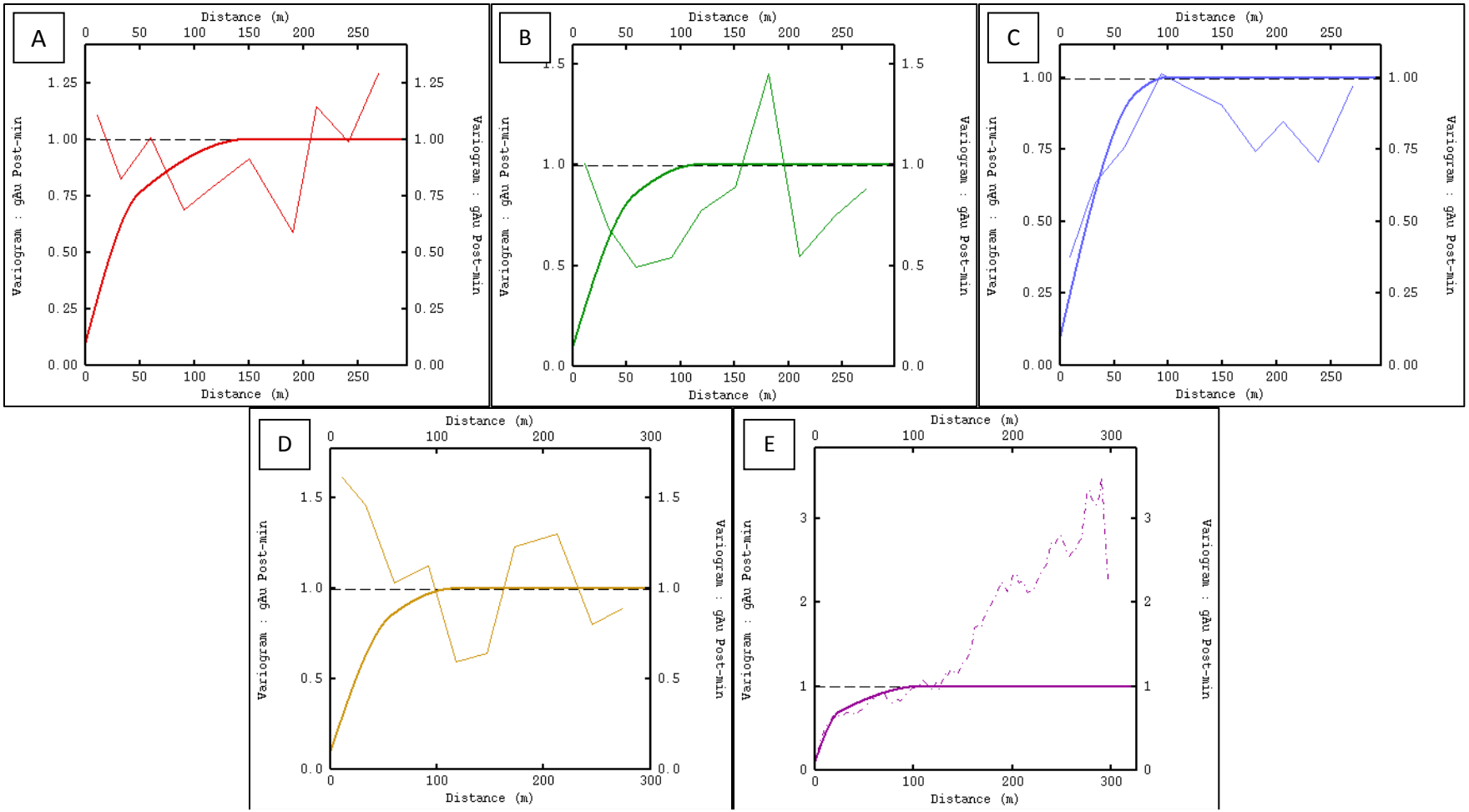

Figure 44. Post Min experimental variograms with modeled variograms for gold along various directions: A) 0°, B) 45°, C) 90°, D) 135° and E) D-90°

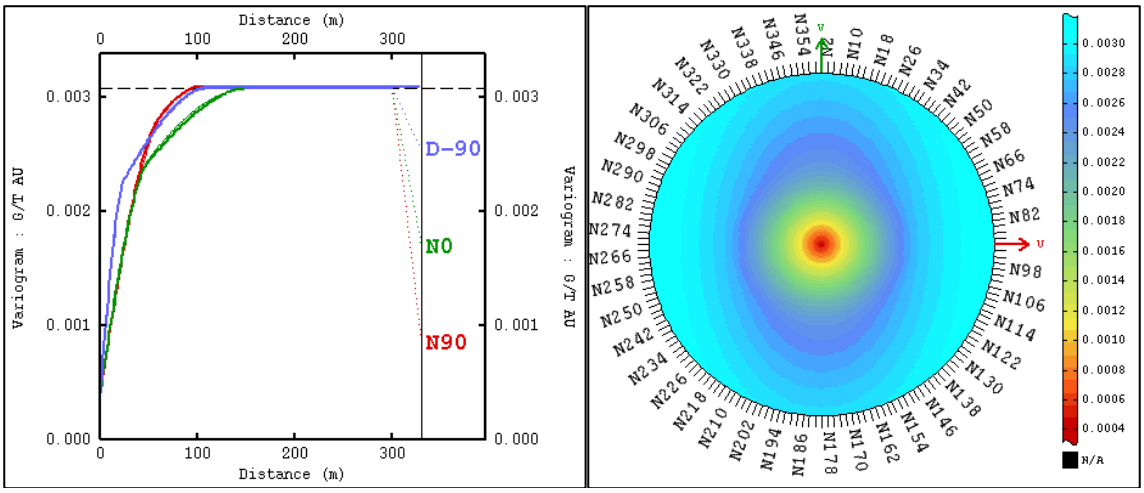

Figure 45. Post Min back-transformed variograms for gold

For the experimental variograms, the first data point only for N90 and D-90 directions was strictly modeled due to its significant effect on the entire model and significant number of pairs that it represents. The back-transformed variograms showed relatively short ranges, which imply less smoothing in the kriging process. The N0 direction has the longest range on the second spherical structure.

10.6.3 Copper Variograms

The copper variograms for various lithologic domains were also generated similar to gold. The figures and analyses are also shown and discussed.

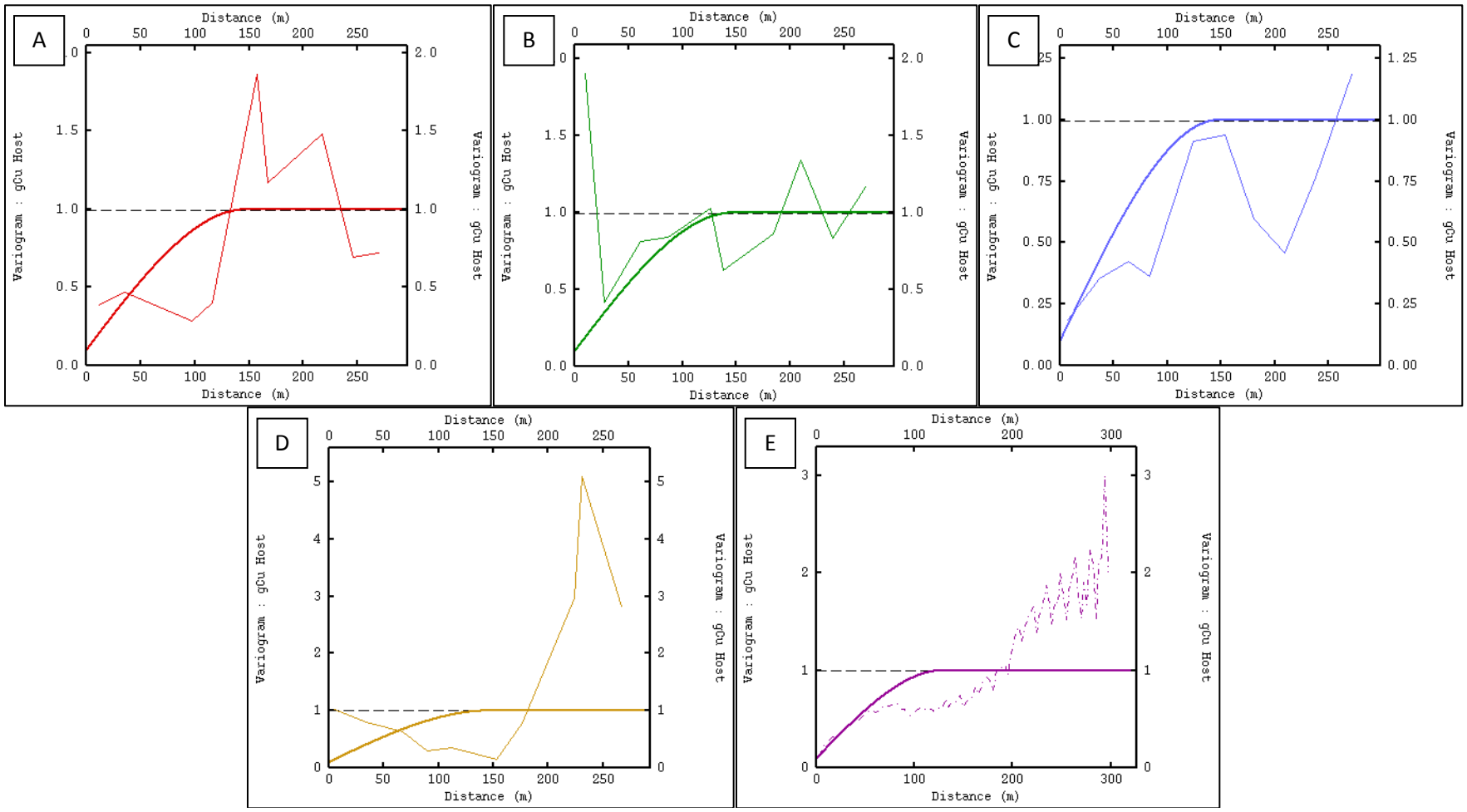

Figure 46. Host experimental variograms with modeled variograms for copper along various directions: A) 0°, B) 45°, C) 90°, D) 135° and E) D-90°

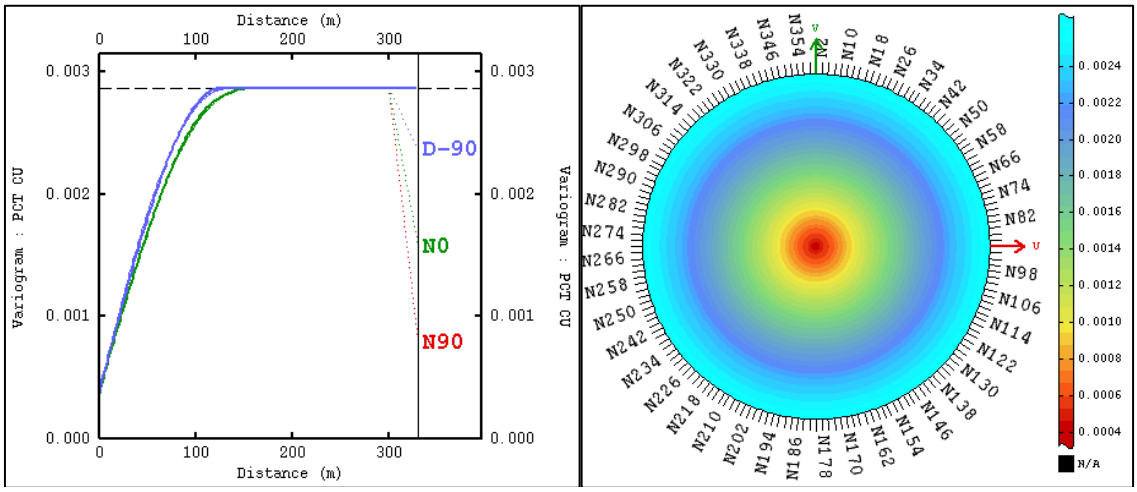

Figure 47. Host back-transformed variograms for copper

For the experimental variograms, the first data point for the N45 and N135 directions was not strictly modeled due to its impractical effect on the entire model and the low number of pairs that it represents. The back-transformed variograms exhibited isotropic behavior as shown by very close model ranges. Relatively short ranges and low nugget effect (compared to the sill) imply less smoothing in the kriging process. The N0 direction has the longest range on the second spherical structure while D-90 direction has notable short range, which makes the data directly above or below the block to have little effect on the estimate.

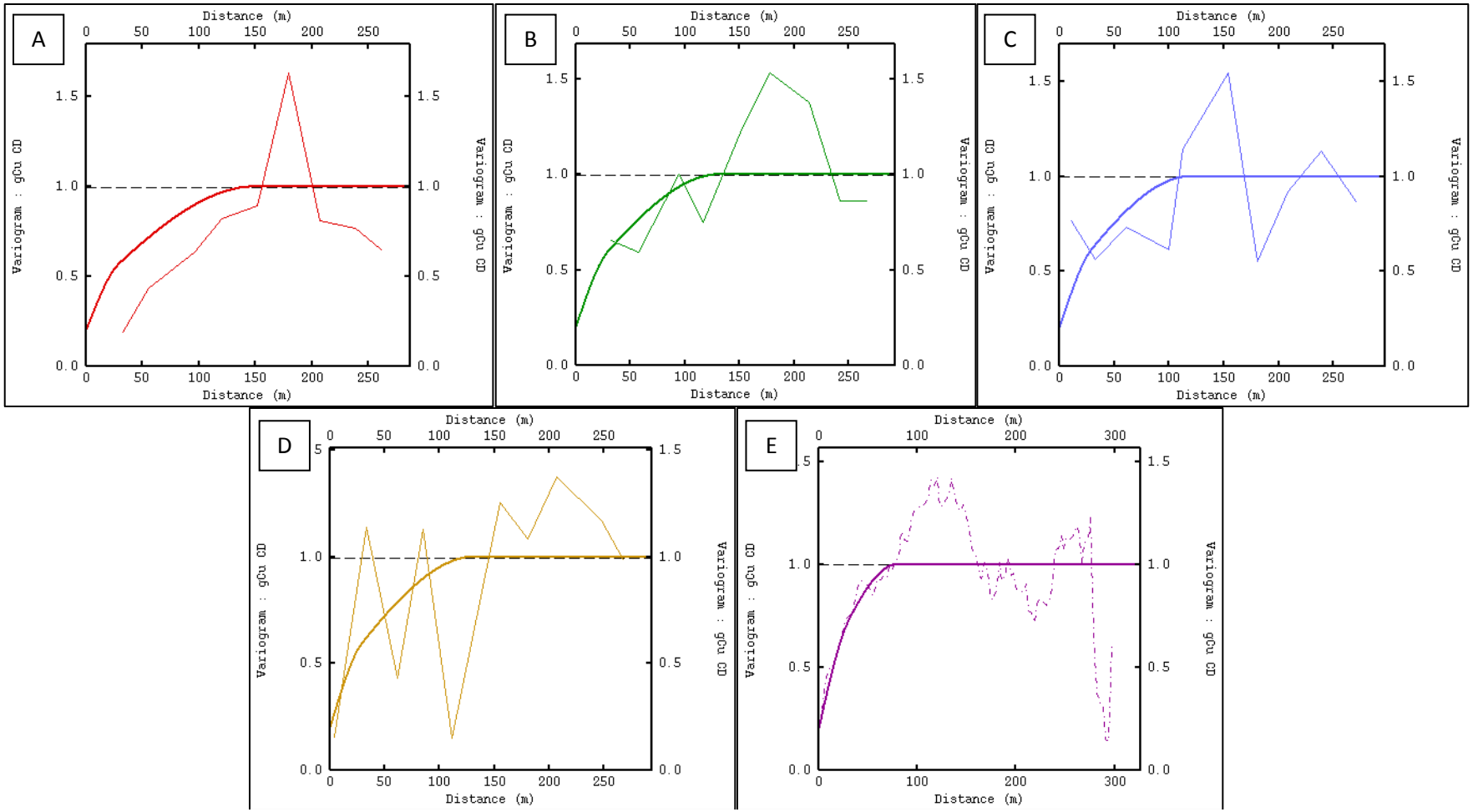

Figure 48. CD experimental variograms with modeled variograms for copper along various directions: A) 0°, B) 45°, C) 90°, D) 135° and E) D-90°

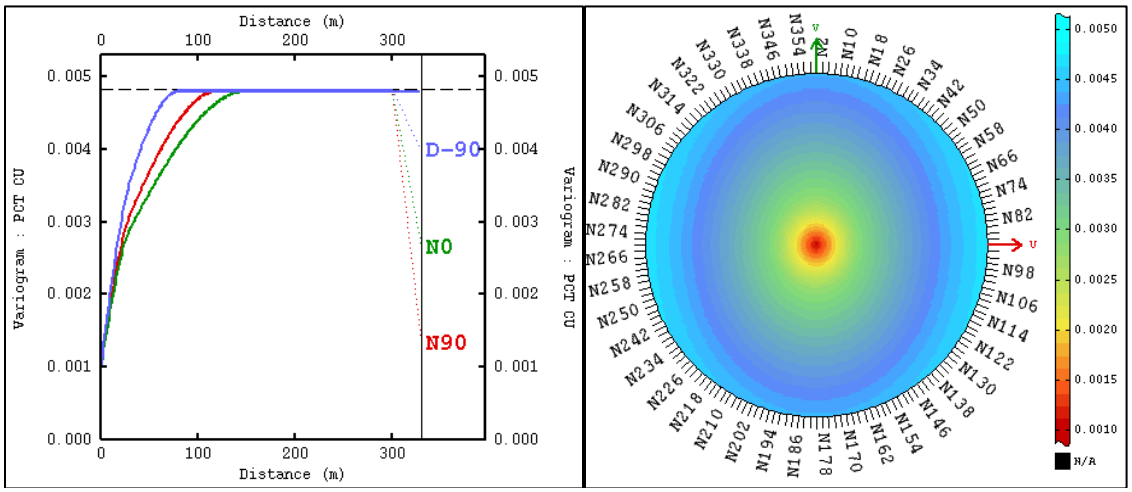

Figure 49. CD back-transformed variograms for copper

For the experimental variograms, the first data point for the N90 direction was not strictly modeled due to its impractical effect on the entire model and the low number of pairs that it represents. The back-transformed variograms have similar range on the first spherical structure. The N0 direction has the longest range on the second spherical structure while D-90 direction has notable short range, which makes the data directly above or below the block to have little effect on the estimate.

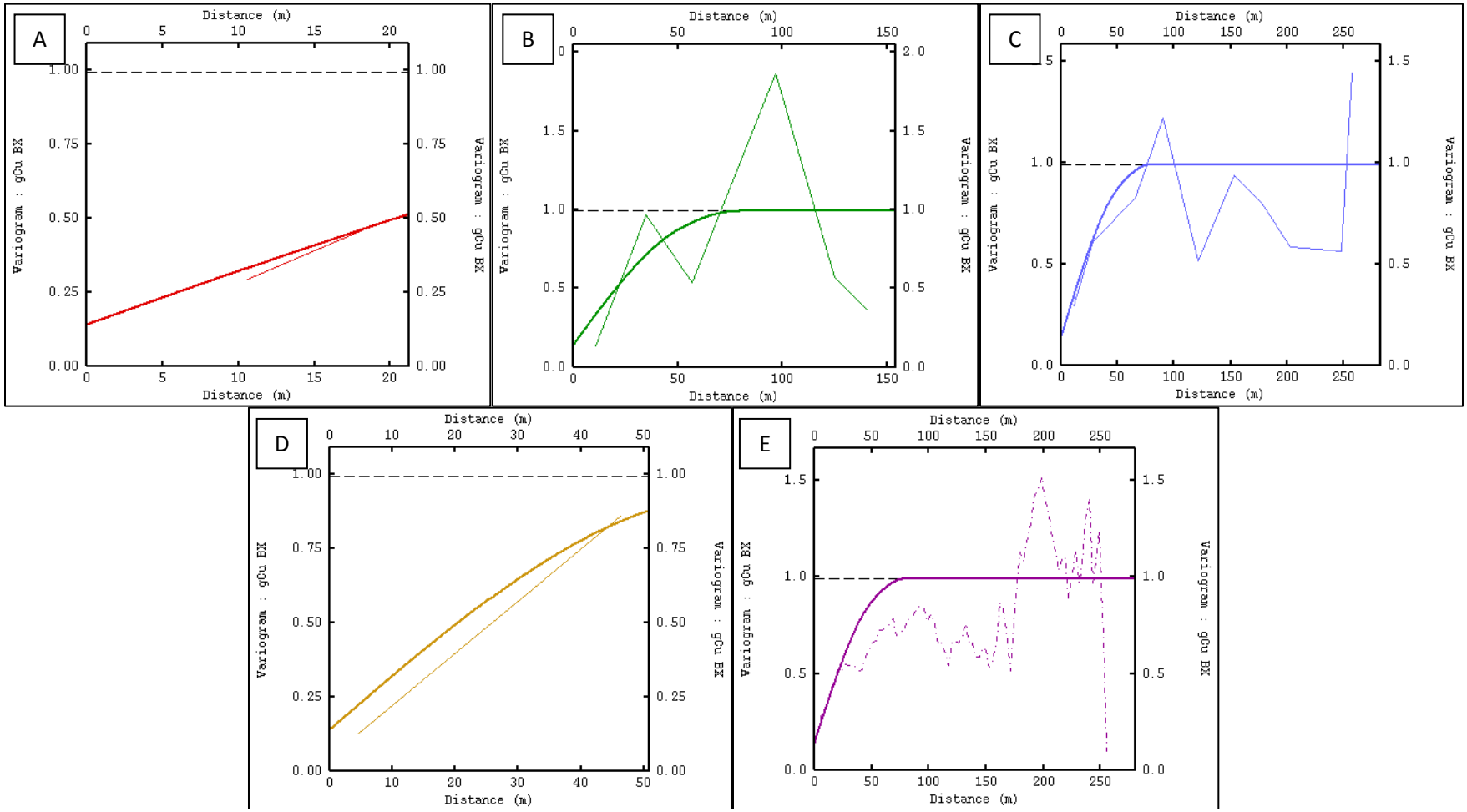

Figure 50. BX experimental variograms with modeled variograms for copper along various directions: A) 0°, B) 45°, C) 90°, D) 135° and E) D-90°

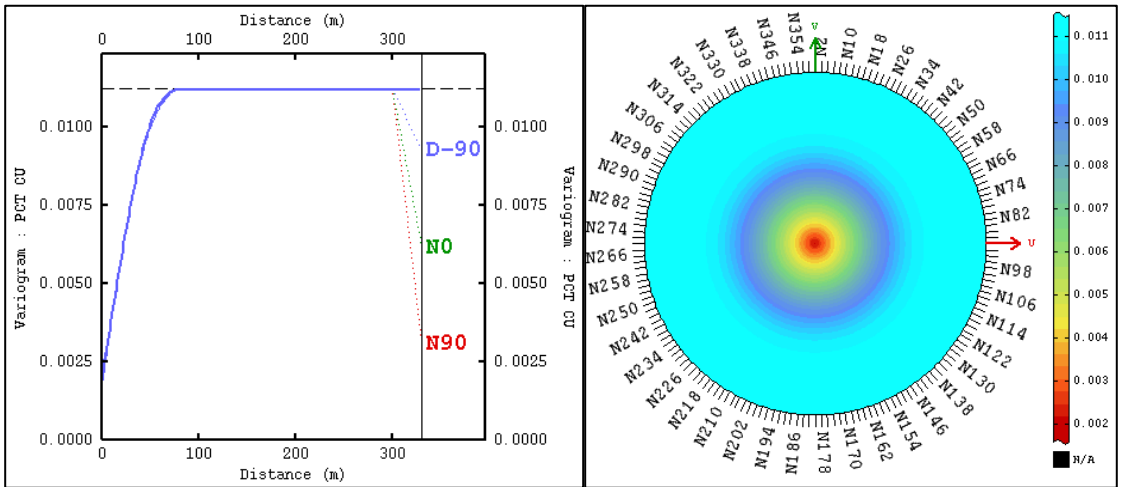

Figure 51. BX back-transformed variograms for copper

Unlike variograms for gold, experimental variograms for copper were modeled under directional condition, with no data points ignored in the modeling process. The back-transformed variograms exhibited isotropic behavior as shown by very similar ranges modeled. Very low nugget effect compared to the sill implies less smoothing in the kriging process.

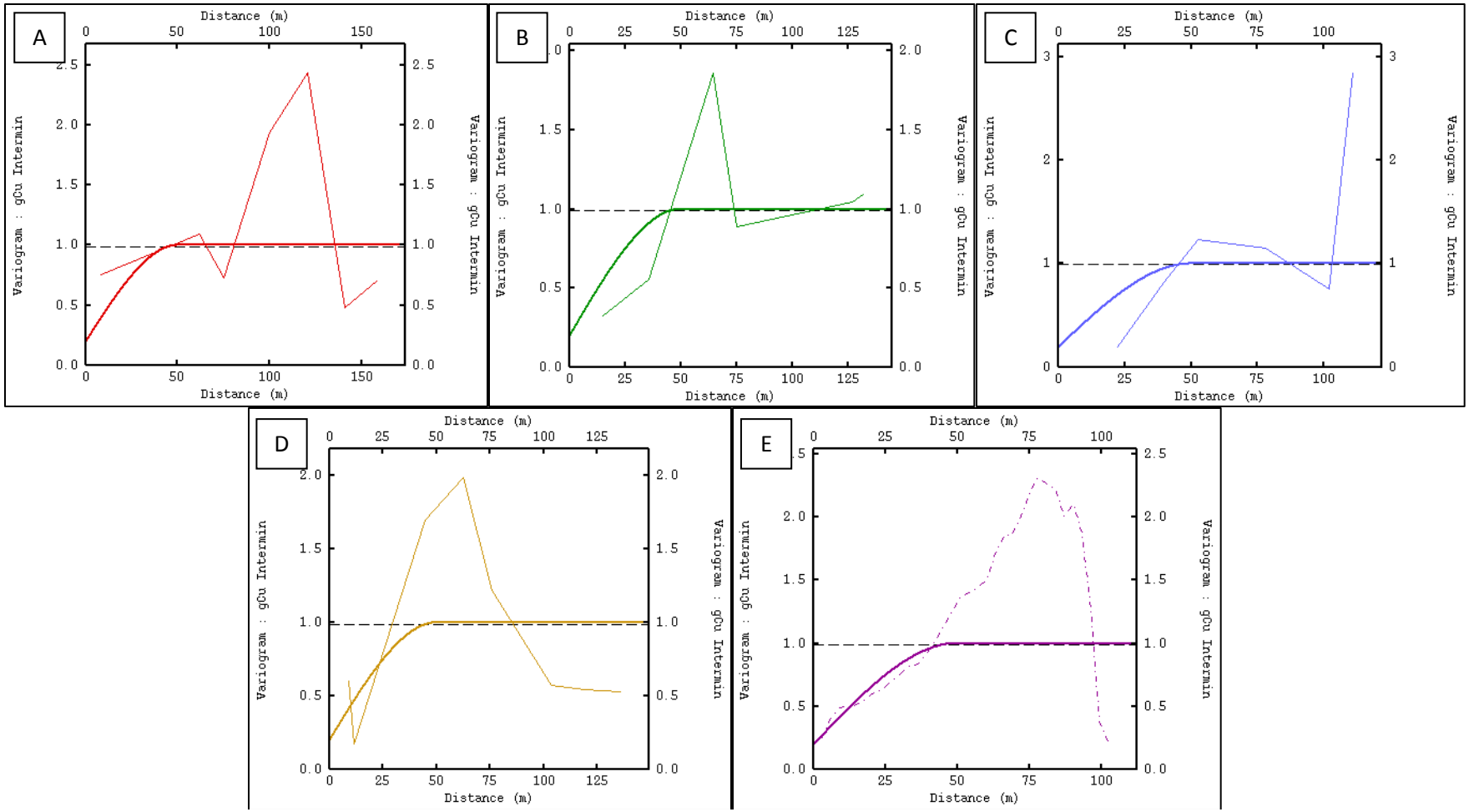

Figure 52. Inter Min experimental variograms with modeled variograms for copper along various directions: A) 0°, B) 45°, C) 90°, D) 135° and E) D-90°

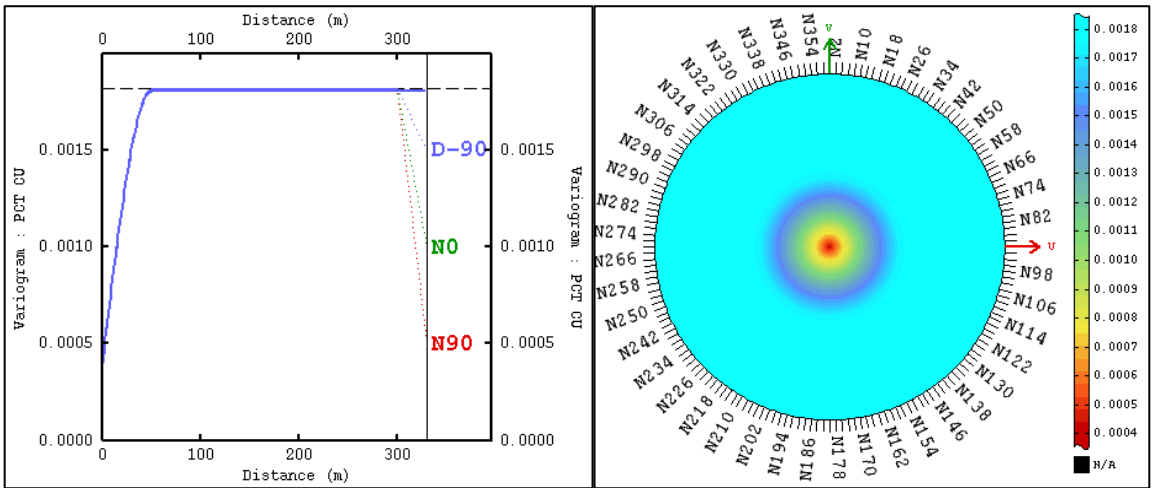

Figure 53. Inter Min back-transformed variograms for copper

For the experimental variograms, the first data point in the N135 direction was not strictly modeled due to its impractical effect on the entire model and the low number of pairs that it represents. The back-transformed variograms exhibited isotropic behavior as shown by amost similar ranges identified. The relatively high nugget effect compared to the sill implies greater smoothing effect in the kriging process.

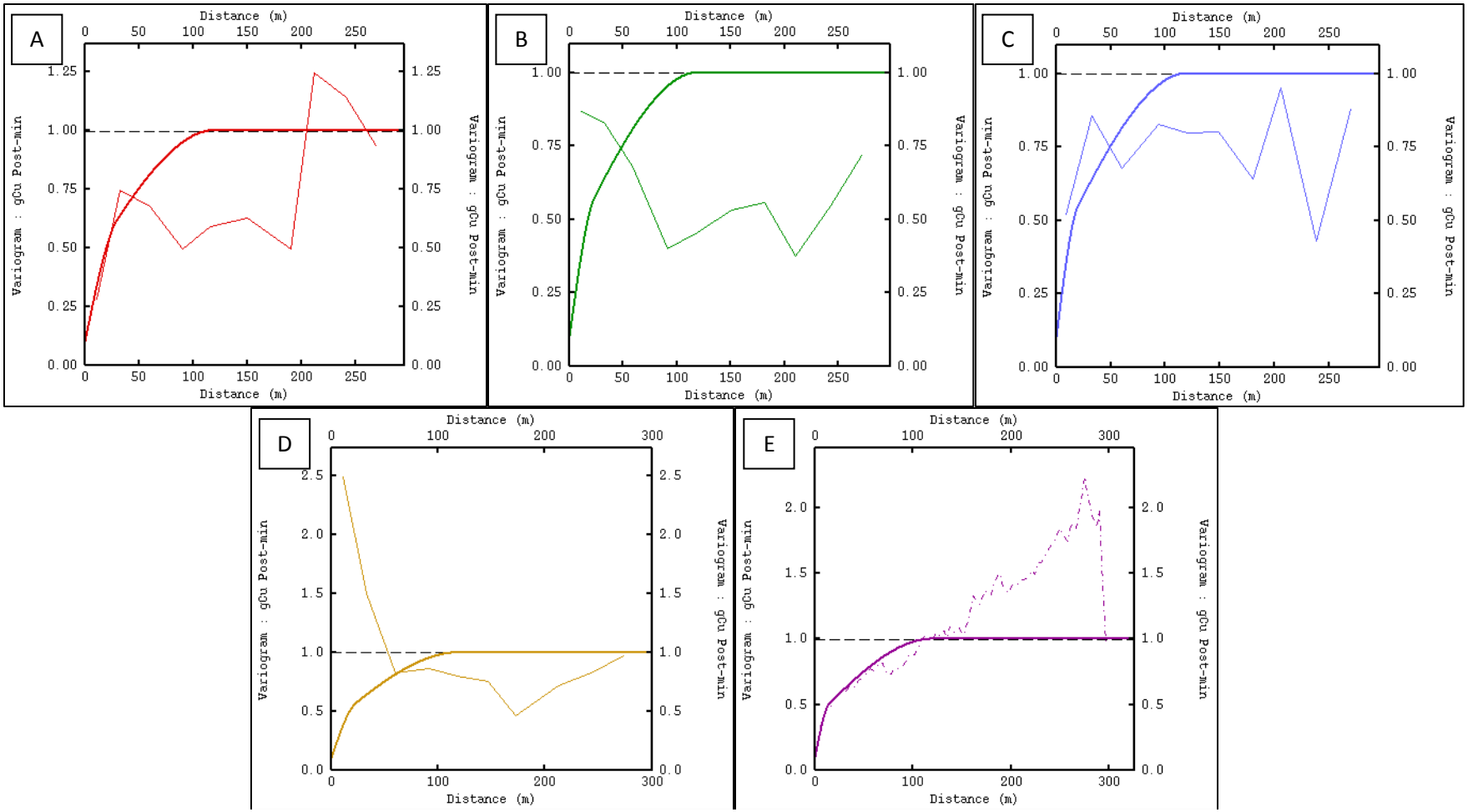

Figure 54. Post Min experimental variograms with modeled variograms for copper along various directions: A) 0°, B) 45°, C) 90°, D) 135° and E) D-90°

.

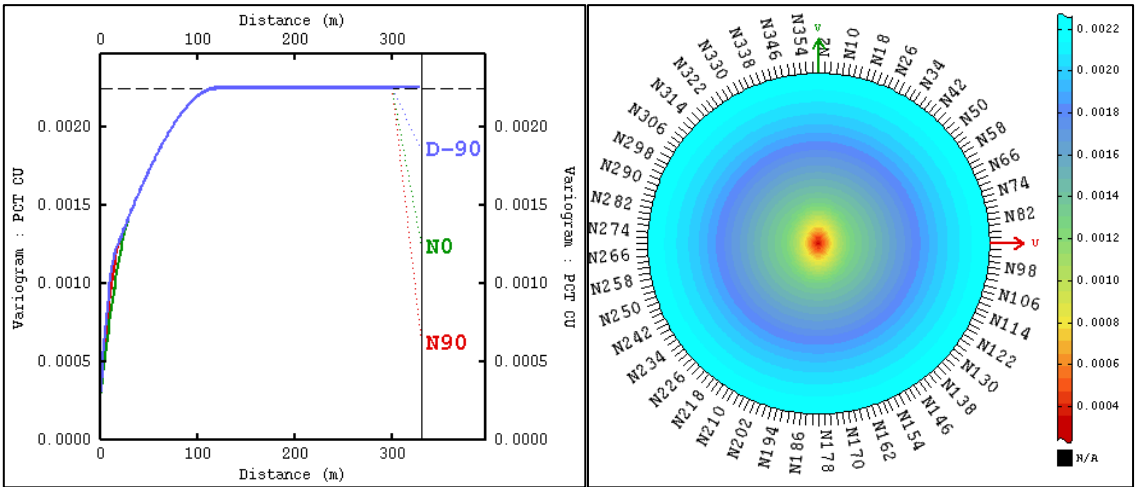

Figure 55. Post Min back-transformed variograms for copper

For the experimental variograms, the first data point for the N45 and N135 directions was not strictly modeled due to its impractical effect on the entire model and the low number of pairs that it represents. Very low nugget effect compared to the sill implies less smoothing in the kriging process. The back-transformed variograms exhibited isotropic behavior, with the N0 direction having slightly longer range on the first spherical structure.

10.7 Kriging

Ordinary Kriging (OK) was conducted independently on each domain. A total of two kriging runs per metal per domain have been done using varying kriging parameters. The appropriate variogram has been used with respect to the metal (gold and copper) and the domain to be kriged. Output was saved into separate block model files, which were later combined in the finalized block model.

10.7.1 Block model

A 30m by 30m by 10m block model was used in the kriging runs, which is similar to the nearby active Sto. Tomas II mine. The block details are presented in Table 14. The center of the origin block is at 33250 X, 14680 Y and 530 Z.

Table 14. Bumolo Block Attributes

Bumolo Block Attributes				
	From	**To**	**Size (m)**	**No. of blocks**
X	33250	34000	30	25
Y	14680	15310	30	21
Z	530	1480	10	95

10.7.2 Specific gravity

The specific gravity of drill cores was measured using water immersion test. Nearest-neighbor interpolation was then done independently for each domain. To check for the validity of the density estimates, on-screen visual inspection of drill hole composite to block data and mean value comparisons of composites to blocks (Table 15) were done. As expected of the nearest neighbor methodology, there was almost no smoothing of the

specific gravity variable. Overall, the reproduction of the average density values is acceptable as mean values were exactly similar.

Table 15. Bumolo Density Statistics

Bumolo Density Statistics		
	Drill hole	Blocks
Number of samples	3240	21098
Minimum value	2.33	2.33
Maximum value	3.45	3.45
Mean	**2.64**	**2.66**
Standard Deviation	0.09	0.10
Variance	0.01	0.01
Coefficient of variation	0.03	0.04

10.7.3 Kriging methodology

The same methodology was followed per metal per domain. First, the block model was flagged based on the domains shown earlier to determine which specific blocks are inside the domain to be kriged. Blocks flagged under multiple domains (i.e. along contact zones) were flagged under the domain that occupied the greatest space inside the block. Inputs in each run included composited grade values and back-transformed variograms, while outputs were stored in each block as estimated grade and standard deviation of estimate.

Table 16 shows that two kriging runs were performed per metal per domain. The first run ensures that interpolated blocks with sufficient data were estimated. Sufficient data refers to data points correlated to the target block as defined by the full ranges of the variograms. The second run is a catch-all run to make sure that all mineralized blocks have estimated grade value. Restriction was applied to the second run limiting the grade to no higher than the mean of the domain. After each run, successfully kriged blocks were flagged so that they are no longer included in the next run.

Kriging parameters common to all two runs are those that do not restrict the data selected to estimate a block. These include the number of data points ranging from three to fifteen and optimum samples of five per line. Top cuts were based on the histogram of each metal for points farther than 30m from the block to be estimated. Lastly, each block was divided into a grid of smaller blocks, 5 nodes along the x axis, 5 nodes along the y axis and 4 nodes along the z axis for block estimation purposes.

Table 16. Kriging Parameters for Bumolo

Bumolo Kriging Parameters (Search pass 1-2)										
Domain	Host		CD		BX		Inter Min		Post Min	
Element	Au	Cu	Au	Cu	Au	Cu	Au	Cu	Au	Cu
Rotation (°)	45	0	45	0	0	0	45	0	0	0
U-axis search (m)	160-1000	160-1000	155-1000	120-1000	100-1000	80-1000	40-1000	50-1000	105-1000	120-1000
V-axis search (m)	90-1000	160-1000	200-1000	150-1000	100-1000	80-1000	30-1000	50-1000	160-1000	120-1000
W-axis search (m)	150-1000	130-1000	95-1000	80-1000	100-1000	80-1000	45-1000	50-1000	115-1000	120-1000
Min. composites	3-1		3-1		3-1		3-1		3-1	
Max. composites	16-16		15-15		15-15		15-15		15-15	
Optimum per line	5-5		5-5		5-5		5-5		5-5	
Top cut value	0.07		0.16		0.23		-	-	-	-
Distance (m)	30		30		30		-	-	-	-
No. of angular sectors	2-1	2-1	4-1	3-1	3-1	3-1	3-1	3-1	3-1	3-1
Max. no. of consecutive empty sector	0-0	0-0	1-0	1-0	1-0	1-0	1-0	1-0	1-0	1-0
Discretization	5x5x4									
Search type	Ellipse									

10.7.4 Final block model

All the individual block models were combined to create a final block model. All kriging outputs except standard deviation were migrated into the finalized block model. For blocks belonging to more than one domain, the kriging outputs were weighted based on the proportion of the block to the respective domains.

10.7.5 Mineralized blocks

The basis for classifying blocks as mineralized or not mineralized depends on the domain. All blocks inside a domain flagged for estimation were considered mineralized. Grade estimates have been assigned to all domains using the methodology mentioned above.

10.7.6 Classification

All estimated blocks were classified under the maiden Inferred Resource category. At this early point of resource definition drilling activity, the current Bumolo geological and/or grade continuity was assessed to be limited in establishing a robust and confident interpretation. More detailed exploration through closely-spaced drilling aims to upgrade the resource to Indicated category.

10.8 Resource Estimate

At a copper equivalent cut-off of 0.274%, Bumolo Project contains total maiden Inferred resource of 21.7 MT at grades of 0.20% Cu and 0.30 g/t Au. This tonnage and grade translate to in-situ contained metals of 95.7 million pounds of Cu and 0.21 million ounces of Au (Table 15). Copper equivalent cut-off of 0.274% was chosen as this showed similar average metal grades with the active Padcal mine. Copper equivalent calculations derived by Padcal Mine for Bumolo are: %CuEq = %Cu + (0.693*g/t Au) based on Padcal mine's estimated prices of US$2.35/lb for copper and US$1,145/oz for gold, and metal recoveries of 82% for copper and 80% for gold based on average results from Padcal mine operations as of October 2015.

10.8.1 Validation

Validation of gold and copper estimates was done through:

- Visual comparison of drill hole composite grades to block grade estimates;
- Mean grade comparisons of composites to blocks per estimation domain; and
- 'Swath plot' grade comparisons of composites against block estimates per estimation domain.

Uncut grades were retained throughout the estimates both in the composited drillhole data and estimates block models.

10.8.2 Visual inspection

On-screen validation process involved visual comparison of (input) drill hole composite grades to (output) estimated block grades for the Bumolo deposit. Block grades generally conformed as expected with the composited drillhole data as higher grade blocks found in areas of high grade composites and low grade blocks in areas bounded by low grade composites. Extrapolations were deemed acceptable as they are mostly supported by nearby drill data points.

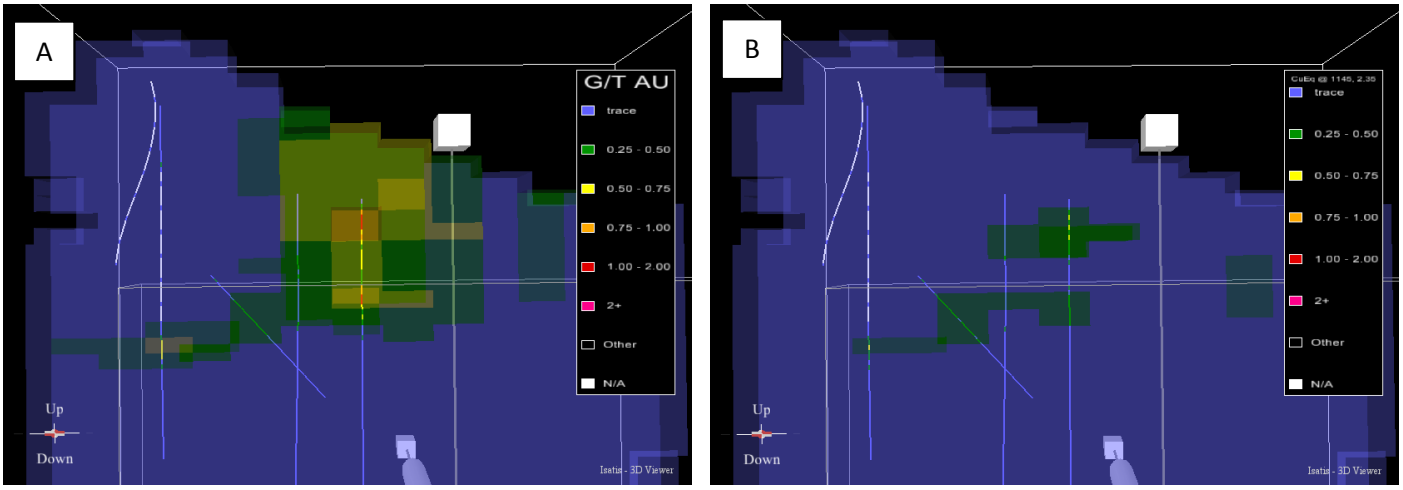

Figure 56. Cross-sectional view along N 14830 (looking North, 30m corridor) showing Bumolo blocks and drill lines for A) gold and B) copper.

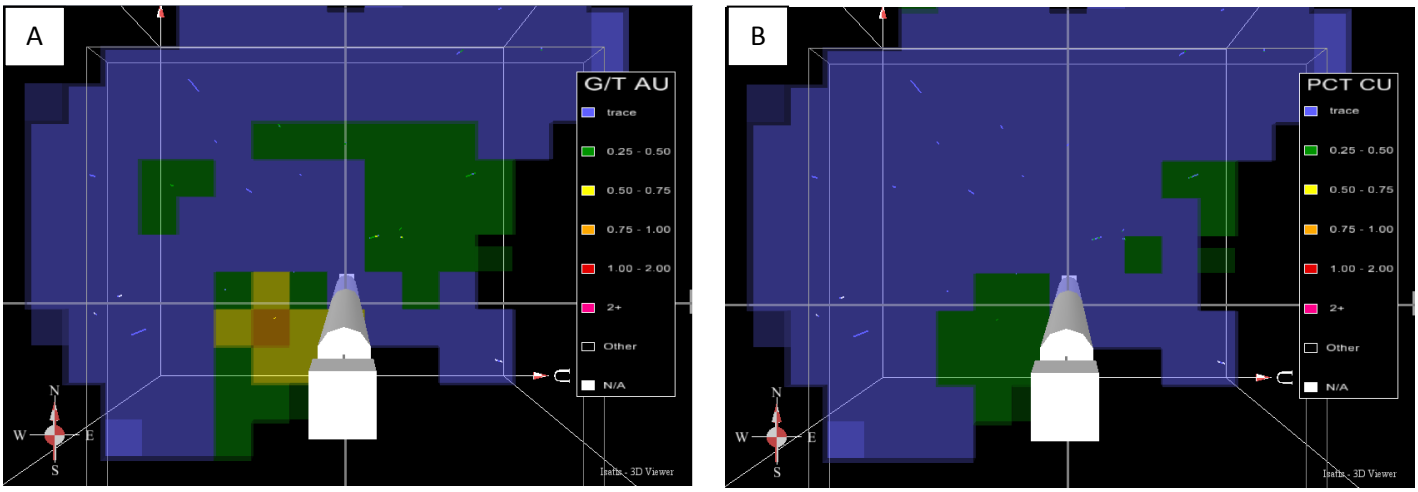

Figure 57. Plan view along 1230 RL (looking North, 10 meter corridor) showing Bumolo blocks and drill lines for A) gold and B) copper.

10.8.3 Statistical comparison per domain

Comparison of mean grades of estimated blocks against 3-meter composite data in each domain was done for both metals to confirm (or not) if there are interpolation errors such as incorrect sample selection for estimation of individual domains. Results are shown in Tables 17-18.

Table 17. Statistical comparison of Bumolo drillholes vs. blocks for gold per domain

Bumolo Statistical Comparison by Lithologic Domains						
g/t Au						
	Composites			Blocks		
Domain	No. of samples	**Mean**	Standard Deviation	No. of samples	**Mean**	Standard Deviation
Host	571	**0.07**	0.12	21098	**0.06**	0.05
CD	639	**0.16**	0.14	3859	**0.12**	0.08
BX	281	**0.23**	0.23	459	**0.20**	0.12
Inter Min	248	**0.09**	0.06	419	**0.12**	0.08
Post Min	816	**0.07**	0.06	4886	**0.06**	0.04
Total	3053	**0.10**	0.13	27396	**0.07**	0.06

Table 18. Statistical comparison of Bumolo drillholes vs. blocks for copper per domain

Bumolo Statistical Comparison by Lithologic Domains						
% Cu						
	Composites			Blocks		
Domain	No. of samples	**Mean**	Standard Deviation	No. of samples	**Mean**	Standard Deviation
Host	571	**0.06**	0.05	21098	**0.06**	0.03
CD	639	**0.12**	0.07	3859	**0.10**	0.05
BX	281	**0.18**	0.11	459	**0.16**	0.07
Inter Min	248	**0.08**	0.04	419	**0.10**	0.04
Post Min	816	**0.07**	0.05	4886	**0.06**	0.03
Total	3053	**0.09**	0.07	27396	**0.06**	0.04

Results show close mean grade values for drillhole composites and blocks. There is also slight smoothing effect as expected of the estimation method employed and un-preferential drilling followed for the entire deposit. Overall, these are acceptable as they confirm the overall methodology done during the resource estimation.

10.8.4 Trend analysis

Moving-window mean 'swath plots' were prepared by averaging the block grades and the composite data in panels of 50 meters, then plotting the results. The difference between the average block and composite grade and the location of the composite data relative to the extent of the block model was also included for assessment of the reproduction of grade trends by the estimation. Swath plots were produced for all kriged variables (copper and gold) for all estimation domains. The estimates should have a close relationship to the drill hole composite data used for estimation. The plots are useful for assessing average grade conformance, and also in detecting any obvious interpolation issues. The relationship between model and sample panel average grades was assessed graphically to allow some evaluation of the smoothing effect of the performed interpolation and further, to highlight areas with poor reproduction of mean grades compared to the composited drillhole data.

10.8.4.1 Trend Analysis Across Northing

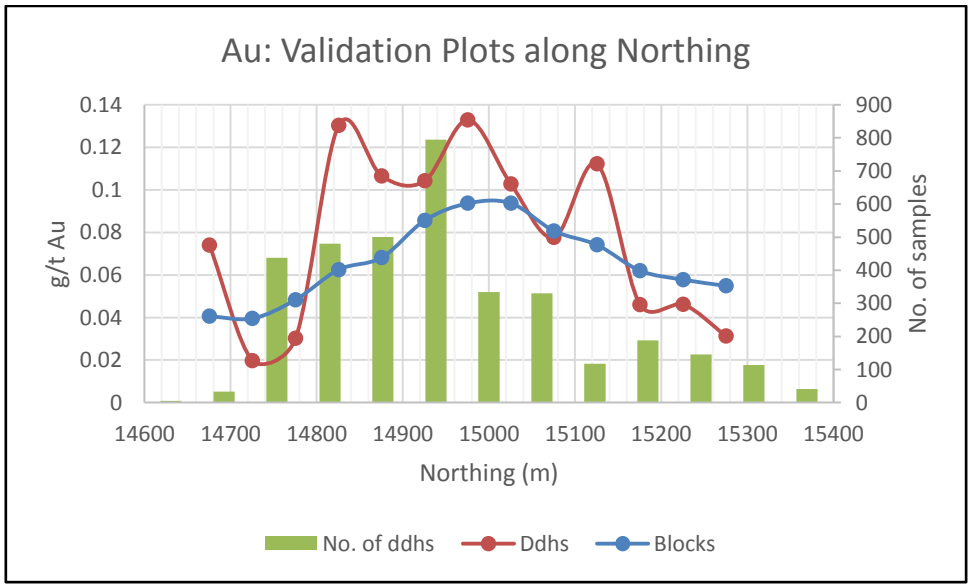

Figure 58. Swath plot for gold across Northing

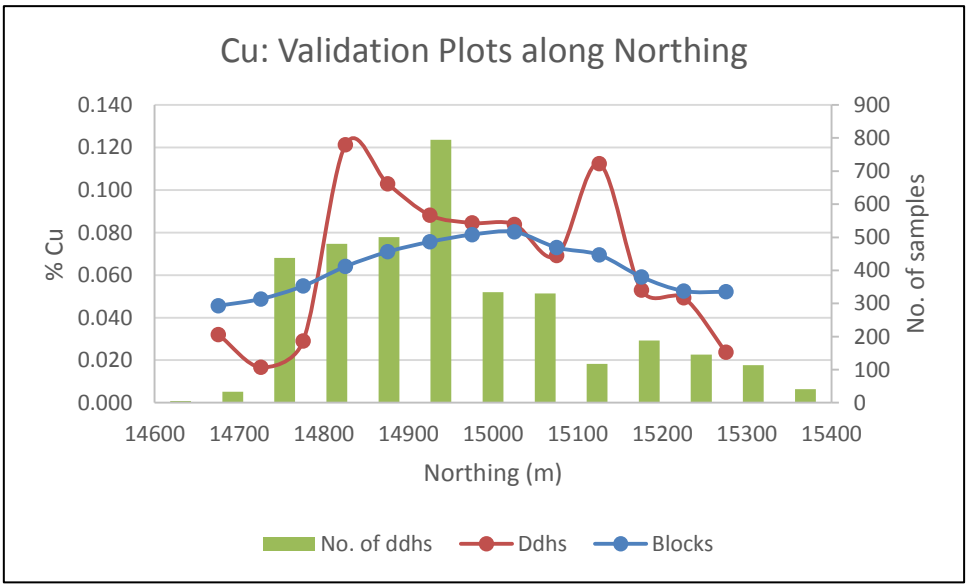

Figure 59. Swath plot for copper across Northing

Each node on Figures 58-59 represents 50 meters in the deposit from the southernmost tip going north. Block grade estimates are smoothed as expected and do not diverge significantly from data point grades, except for N 14800 despite significant drill data available. Both gold and copper grades of block estimates are consistently lower except for the outermost tips, where there are significantly lower drill hole data to deal with. These areas are recommended for future drilling to improve the number of data points and arrive at more acceptable blocks estimates.

10.8.4.2 Trend Analysis across Easting

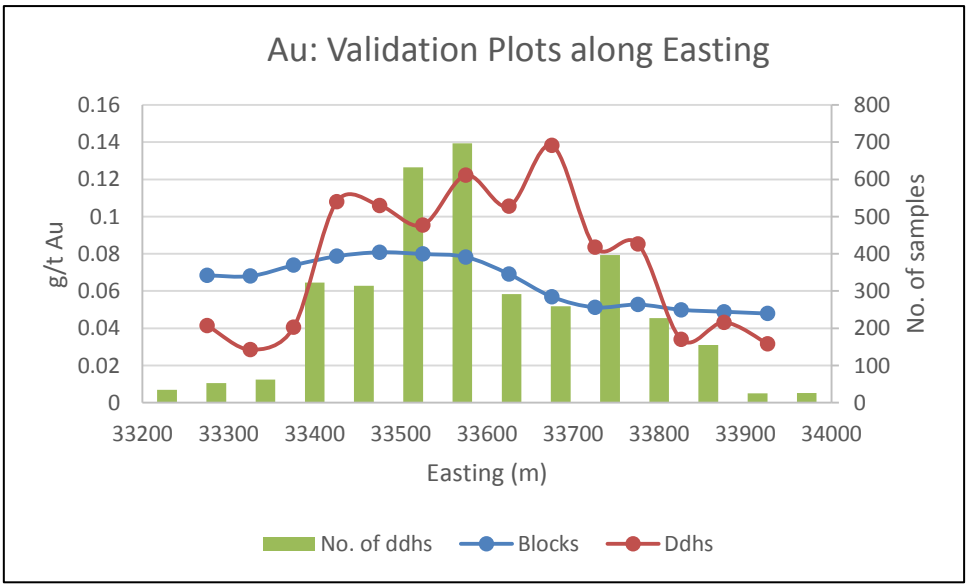

Figure 60. Swath plot for gold across Easting

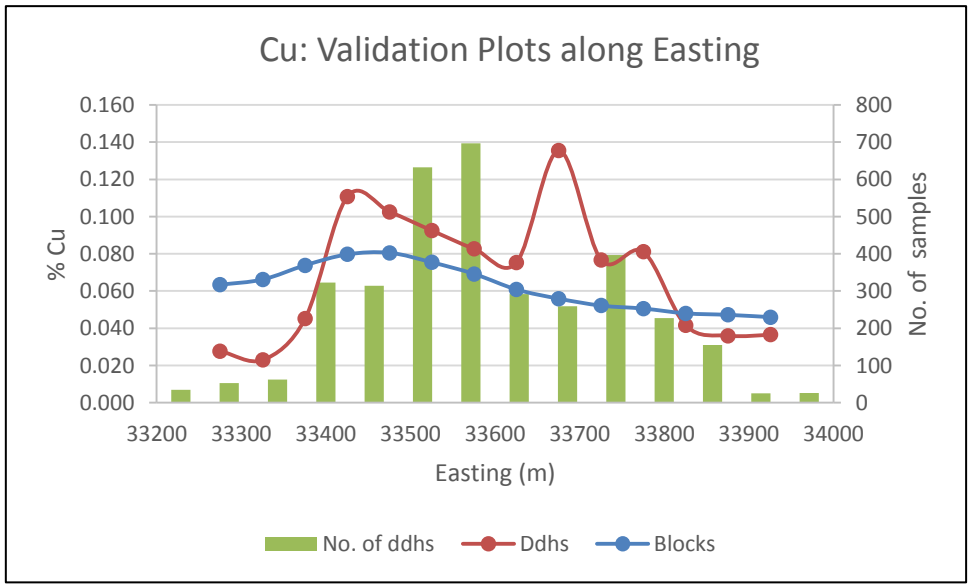

Figure 61. Swath plot for copper across Easting

Each node on Figures 60-61 represents 50 meters in the deposit from the westernmost tip going east. Block grade estimates are smoothed as expected and do not diverge significantly from data point grades, except for N 33400 and N 33700 although significant drill points are available. However, the blocks represented by the leftmost node are in question. This gives us an area for future drilling to improve the number of data points and corresponding block estimates.

10.8.4.3 Trend Analysis across Elevation

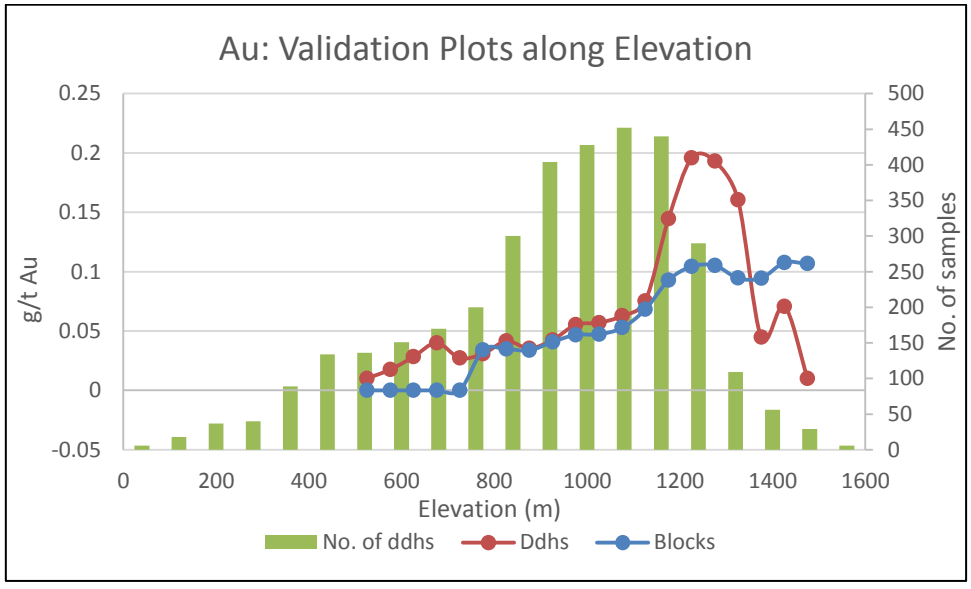

Figure 62. Swath plot for gold across Elevation

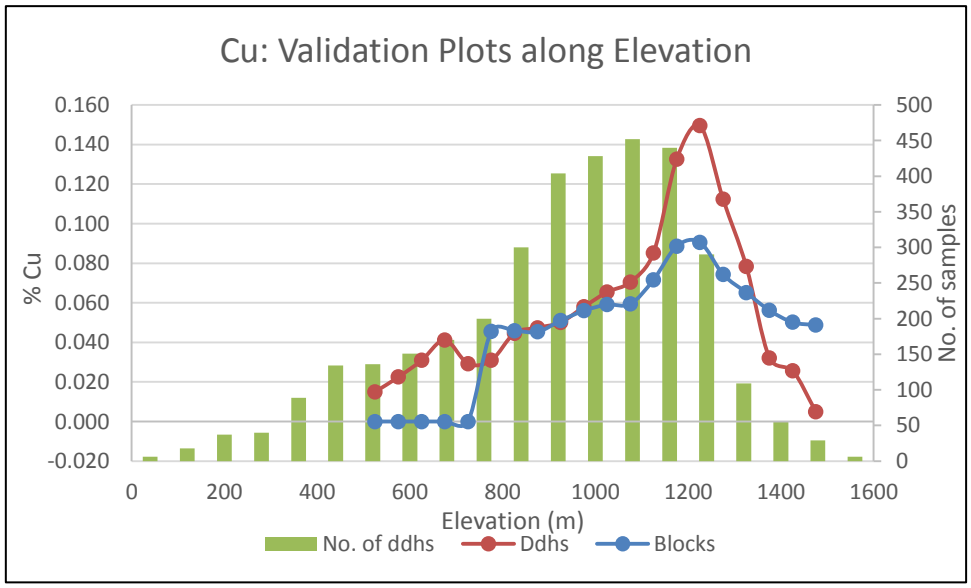

Figure 63. Swath plot for copper across Elevation

Each node on Figures 62-63 represents 50 meters in the deposit from the lowest elevation going towards the surface. Block grade estimates are smoothed as expected and do not diverge significantly from data point grades except for a sudden dip in block grades at ~750m downwards and higher grades at ~1350m upwards. This gives us areas for future drilling to improve the number of data points and corresponding block estimates.

11 SUMMARY AND CONCLUSIONS

The following summary is effectively a re-statement of the Executive Summary of the report.

The Bumolo Project exploration program is professionally managed and the database is acceptable for use in mineral resource estimation. Preliminary but robust geological and resource domains of the Bumolo deposit are defined and found suitable for the maiden MRE. There is continuity for both the copper and gold grades within the established domains with low nugget effects and large ranges. The QA-QC programs and core logging procedures follow the best industry practice and generally exceed commonly accepted standards. The copper and gold grades are estimated using Ordinary Kriging interpolation method as the mineralization is relatively homogenous. The Competent Person believes that the methodology used in the MRE is appropriate and that the result will have accuracy suitable for the intended mining method.

The assaying of samples commissioned to two laboratories with initial assay run conducted in Philex' Padcal Assay Laboratory and a parallel run submitted to Intertek Testing Services, Inc. (Intertek) in Manila also increased the confidence in the integrity of the results reported. Both laboratories assaying protocols are to industry standard. Results of the laboratory QA/QC sample insertions are generally within acceptable limits.

The maiden Bumolo MRE is supported by drilling data and initial geological information interpreted by Philex geologists as of February 2016. The current drillhole spacing for assayed holes which varies from around 80 by 80 meters and locally closer in central portions to around 125 by 125 meters in peripheral zones also warrants the mineral resource classification to Inferred Resources. Further

drilling and advanced geological studies such as geotechnical, mineragraphic and metallurgical studies are however, needed to support project feasibility.

12 CERTIFICATE OF AUTHOR

Certificate of the author who prepared this Technical Report is presented below.

PHILEX MINING CORPORATION

CERTIFICATION

Noel C. Oliveros
#27 Brixton St., Pasig City 1600
+632 6311381
+639989727249
ncoliveros@philexmining.com.ph

I, Noel C. Oliveros, do hereby certify that:

1. I am currently employed as the Exploration Division Manager of Philex Mining Corporation (Philex).
2. I am a graduate of the University of the Philippines with a B.S. Degree in Geology, 1985.
3. I am a registered Geologist, Philippine Regulatory Commission, with PRC License No. 1285.
4. I am an accredited "Competent Person" (CP) of the Geological Society of the Philippines, in accordance with the Philippine Mineral Reporting Code (PMRC), with accreditation No. Geology CP 07-08-07, in regard to reporting exploration results and mineral resources.
5. I am currently head of the Resource Management Division of Philex that covers the Sto.Tomas II and Bumolo porphyry Cu-Au deposits of Philex.
6. I have read the definition of "Competent Person" set out in PMRC and certify that by reason of my education and relevant experience, I fulfill the requirements to be a "Competent Person" for the purposes of PMRC.
7. I am responsible for the preparation of the "Technical Report on the Bumolo Porphyry Copper-Gold Deposit in Tuba, Benguet, Philippines" dated February 2016 relating to the exploration and mineral resource estimation of the Bumolo deposit.
8. I am responsible for the preparation of the annual disclosures of the Mineral Resource statements of the Sto. Tomas II porphyry copper-gold deposit of the Padcal Mine of Philex.
9. I have read the PMRC, and the Technical Report has been prepared in compliance with the rules and guidelines set forth in the PMRC.
10. I have more than ten (10) years relevant experience in the deposit type and mineralization style of the mineral resources evaluated.
11. I have worked as a geologist for 31 years and as resource estimator for 16 years.
12. I consent to the filing of the Technical Report with the Philippine Stocks exchange and publication by them.

Dated this 10th day of February, 2016

Noel C. Oliveros

REFERENCES

Aurelio, M., and Peña, R. E., 2004, Geology and mineral resources of the Philippines: Revised edition, Volume 1, DENR-MGB.

Hollings, P., Cooke, D. R., Waters, P. J., and Cousens, B., 2011a, Igneous Geochemistry of Mineralized Rocks of the Baguio District, Philippines: Implications for Tectonic Evolution and the Genesis of Porphyry-Style Mineralization: Economic Geology, v. 106, no. 8, p. 1317-1333.

Hollings, P., Wolfe, R., Cooke, D. R., and Waters, P. J., 2011b, Geochemistry of tertiary igneous rocks of northern Luzon, Philippines: Evidence for a back-arc setting for alkalic porphyry copper-gold deposits and a case for slab roll-back?: Economic Geology, v. 106, no. 8, p. 1257-1277.

Pubellier, M., Monnier, C., Maury, R., and Tamayo, R., 2004, Plate kinematics, origin and tectonic emplacement of supra-subduction ophiolites in SE Asia: Tectonophysics, v. 392, no. 1-4, p. 9-36.

Waters, P.J., Cooke, D.R., Gonzales, R.I. and Phillips, D. 2011, Porphyry and Epithermal Deposits and 40Ar/39Ar Geochronology of the Baguio District, Philippines: Society of Economic Geologists, v106, pp. 1335–1363